JOHN DAY RIVER BASIN TMDL

APPENDIX A:
TEMPERATURE MODEL CALIBRATION REPORT

Final
November 2010

THIS DOCUMENT IS SUPPLEMENTAL TO THE JOHN DAY RIVER TEMPERATURE TMDL

State of Oregon
Department of Environmental Quality

Prepared by:

Julia Crown, Oregon Department of Environmental Quality

Table of Contents

Figures

Tables

1. INTRODUCTION

This Appendix is a temperature assessment of the John Day River Basin (**Figure A-1**), focusing on the John Day River, North Fork John Day River & Middle Fork John Day River, as well as a generalized assessment of thermal objectives for perennial and intermittent tributaries throughout the basin, for the purpose of establishing a Total Maximum Daily Load (TMDL) of instream heat to implement the Oregon water quality standard for temperature. **Chapter 2** of the associated document is the TMDL policy expression and will rely on the information in this Appendix.

Figure A-1. John Day River Basin and subbasins

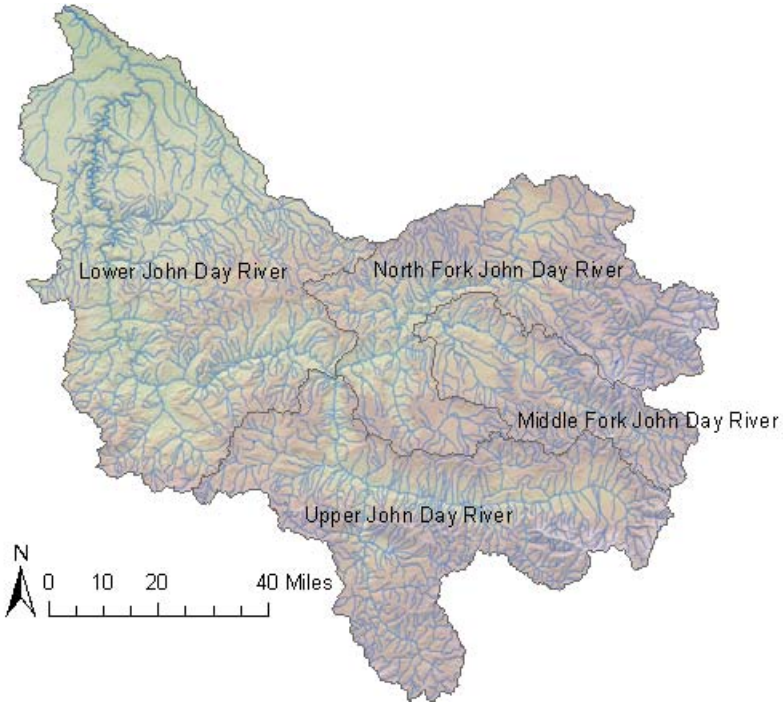

Many parameters effect stream temperature. The parameters can be grouped as near-stream vegetation and land cover, channel morphology, hydrology, and meteorology; including wind speed, humidity and air temperature. Many of these stream parameters are interrelated (i.e., the condition of one may influence one or more of the other parameters). These parameters effect stream heat transfer processes and stream mass transfer processes to varying degrees. The analytical techniques employed to develop this temperature TMDL are designed to consider all of the parameters that effect stream temperature.

Many parameters exhibit considerable spatial variability. For example, channel width measurements can vary greatly over small stream lengths. Some parameters exhibit diurnal and seasonal temporal variability. The current analytical approach developed for subbasin scale stream temperature assessment relies on ground level and remotely sensed spatial data. Techniques employed in this effort are statistical and deterministic modeling of hydrologic and thermal processes. Specifically, DEQ developed the Heat Source model to account for variables that influence stream heating. The model simulates 1-dimensional (longitudinal) temperature gradients over a user-specified time interval, typically at resolutions of 0.05-1.0 kilometer and 1.0 hour. The relevant heat transfer processes are identified in **Figure A-2**. Further explanation of stream thermal controls and the Heat Source model can be found in the Heat Source manual *Analytical Methods for Dynamic Open Channel Heat and Mass Transfer: Methodology for the Heat Source Model Version 7.0* (Boyd & Kasper 2003a). For further details, the DEQ website (Water Quality Division, TMDL Program) houses numerous examples of TMDLs in which

stream heating processes and Heat Source applications are discussed in detail – e.g., recent temperature TMDLs include the Rogue and Umpqua River Basins west of the Cascades and the Willow and Middle Columbia Hood (Miles Creeks) watersheds east of the Cascades.

Figure A-2. These parameters, along with latitude, elevation, humidity, air temperature, and wind speed, relate to stream temperature and are accounted for in this analytical framework

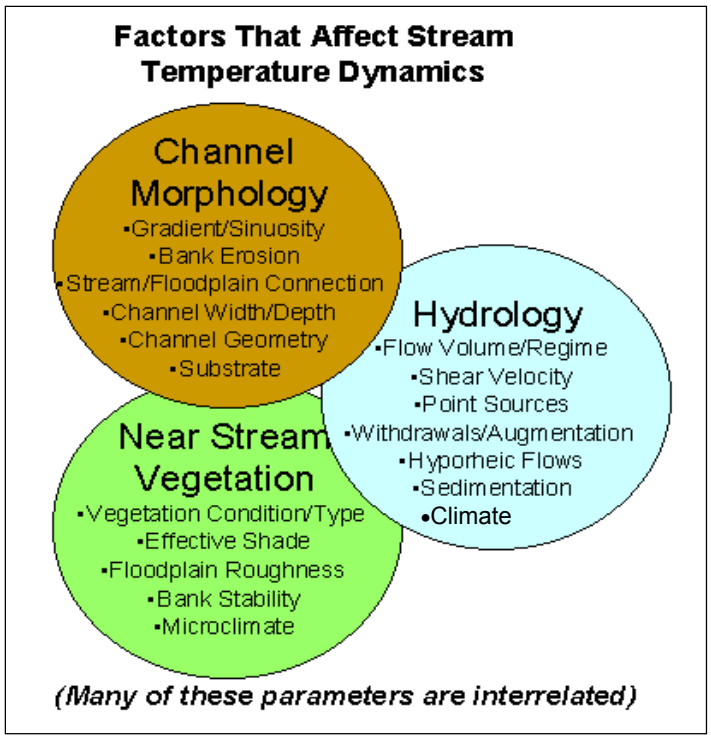

Using the Heat Source model and other analytical techniques, DEQ simulated conditions reflecting minimized anthropogenic (human-caused) warming. ***These simulations show that in the absence of quantifiable human disturbance, numeric biologically-based water quality standard temperature criteria are seasonally exceeded in much of the modeled channels.*** In such circumstances, the Oregon water quality standard targets a best estimate of natural condition, insofar as stream temperature is concerned. Accounting for the amount of human-related temperature increase is therefore central to the analysis. The pollutant is heat. The TMDL assesses the anthropogenic contributions of nonpoint source solar radiation heat loading that results from decreased levels of stream surface shade, which are caused by near stream land cover disturbance or removal and channel morphology changes. Another anthropogenic source of stream warming considered in this analysis is reduction in stream flow and geomorphic channel changes to hydraulics. The Oregon Department of Environmental Quality maintains a database for point source information. This database was used to identify potential point sources within the John Day River Basin. The individually and generally permitted point sources in the John Day River Basin are not expected to be a significant source of heat (for further discussion please refer to **Chapter 2.1** of this document).

Natural thermal potential (NTP, ***OAR 340-041-0002***) is a key term in the Oregon temperature TMDL context. In rule, *NTP* is defined as "the determination of the thermal profile of a water body using best available methods of analysis and the best available information on the site-potential riparian vegetation, stream geomorphology, stream flows, and other measures to reflect natural conditions." For the purpose of this assessment, **NTP near-stream land cover** (a.k.a. "potential vegetation") is defined as: *that vegetation which has the potential to grow and reproduce on a site, given climate, elevation and soil properties, and natural hydrologic and geomorphic processes*. **NTP channel morphology** *is the more*

stable configuration that would occur with less human disturbance. **NTP flow** is the volumetric flow of water that reflects natural conditions. "Natural" flows are estimates based on removing the assumed anthropogenic impacts on the current flow regimes. NTP does not assume management or land use are limiting factors. **NTP is the design condition used for TMDL analysis.** NTP is not necessarily an estimate of pre-settlement conditions. Although it is important to consider historic land cover patterns, channel conditions and hydrology, data are often scarce and many areas have been altered to the point that the historic condition is no longer attainable given irreversible changes.

For this TMDL, the Department has simulated stream temperature for the major rivers of the Basin: the John Day River mainstem, the Middle Fork of the John Day River and the North Fork of the John Day River (**Figure A-3**). Model coverages are spatially continuous including most of the length of each river, as follows:

- The mainstem from Tumwater falls near the mouth to the USFS Trout Farm Campground above Prairie City
- The North Fork from its mouth to Baldy Creek in the upper North Fork John Day Wilderness
- The Middle Fork from its mouth to roughly one kilometer above Clear Creek near Austin Junction

Figure A-3. Stream temperature simulation spatial extent

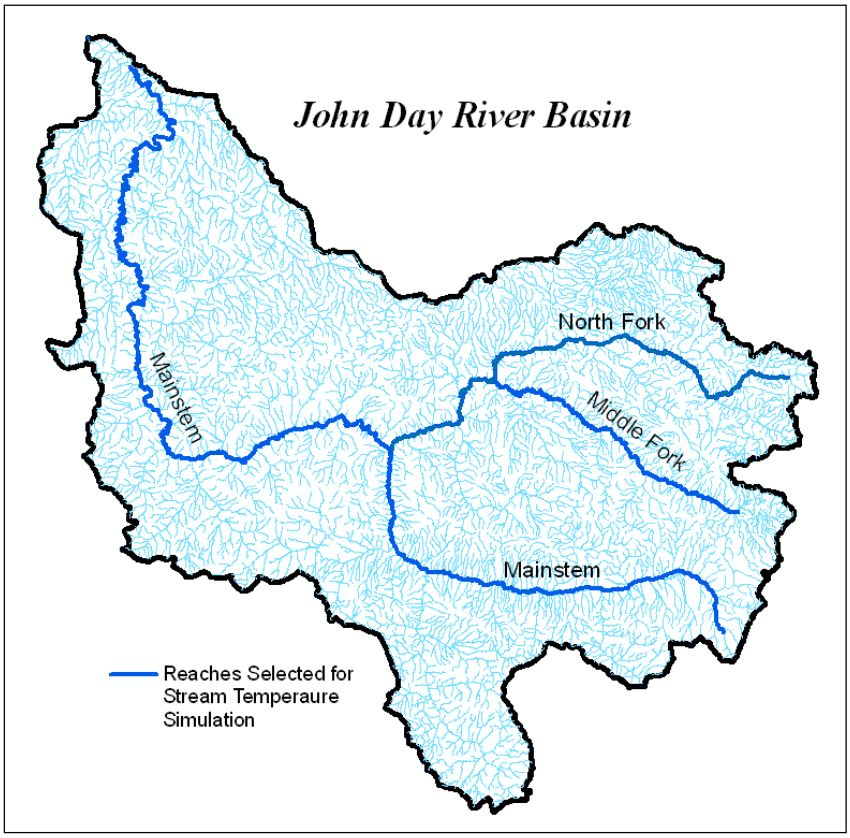

Each river was simulated separately. The North and Middle Fork models were calibrated for part of calendar year 2002, while the mainstem model simulated part of 2004, which were the years when data were collected specifically for temperature TMDL modeling. The temporal coverage of the temperature simulations is as follows:

- **The mainstem: 7/1/2004 – 9/1/2004**
- **The North Fork: 6/15/2002 – 9/1/2002**
- **The Middle Fork: 4/1/2002 – 10/31/2002**

1.1 Analysis Limitations

It should be acknowledged that there are limitations to this effort:

The scale of this effort is large, with obvious challenges in capturing spatial variability instream and landscape data. Available spatial data sets for vegetation and channel morphology are coarse, while derived data sets are limited to aerial photo resolution and human error.

Data are insufficient to describe high-resolution instream flow conditions, making validation of derived mass balances difficult.

The water quality issues are complex and interrelated. The state of the science is still evolving in the context of comprehensive landscape scaled water quality analysis. For example, quantification techniques for microclimates that occur in near stream areas are not developed and available to this effort. Regardless, recent studies indicate that forested microclimates play an important, yet variable, role in moderating air temperature, humidity fluctuations and wind speeds.

Quantification techniques for estimating potential subsurface inflows/returns and behavior within substrate are not employed in this analysis. While analytical techniques exist for describing subsurface/stream interactions, it is beyond the scope of this effort with regard to data availability, technical rigor and resource allocations.

Land use patterns vary throughout the drainage from heavily impacted areas to areas with little human impacts. However, it is extremely difficult to find large areas without some level of either current or past human impacts.

The development of natural thermal potential stream temperatures is based on stated assumptions within this document. Limitations to stated assumptions are presented where appropriate. It should be acknowledged that as better information is developed, these assumptions will be refined.

Current analysis is focused on a defined critical condition. This usually occurs in late July or early August when stream flows are low, radiant heating rates are high and ambient conditions are warm. However, there are several other important time periods where data and analysis are less explicit. For example, spawning periods have not received such a robust consideration.

Current analytical methods fail to capture some upland, atmospheric and hydrologic processes. At a landscape scale, these exclusions can lead to errors in analytical outputs. For example, methods do not currently exist to simulate riparian microclimates at a landscape scale. In some cases, there is not a scientific consensus related to riparian, channel morphology and hydrologic potential conditions. This is especially true when confronted with highly disturbed sites, meadows and marshes, potential hyporheic/subsurface flows, and sites that have been altered to a state where potential conditions produce an environment that is not beneficial to stream thermal conditions (such as a dike).

The following items affect model uncertainty:

Riparian vegetation was mapped from aerial photographs and placed within general height categories. For example, trees identified as “Large Conifers” were assigned a single height of 125 feet throughout a single watershed, when in reality, “Large Conifer” heights may range between 110 and 140 feet. It is not possible to assign actual heights to each tree mapped using aerial photographs. These general height categories became Heat Source inputs and are one source of modeling imprecision.

Current riparian vegetation densities were estimated based on aerial photograph analysis. Potential vegetation used single density values for each ecoregion and vegetation type. Actual vegetation community densities are variable and this variability is not accounted for in the simulations.

The actual position of the sun within the sky can only be predicted with an uncertainty of 10-15%. The sun's position is important when determining a stream's effective shade. Solar position is another source of modeling imprecision.

Heat Source assumes that the wetted stream is flowing directly down the center of the active channel, and effective shade calculations are based upon that assumption. In reality, a stream migrates across the active channel. This is another source of modeling imprecision.

Microclimates often develop around streams. Humidity, air temperature, and wind depend on factors such as elevation, vegetation, terrain, etc. Stream temperatures are affected by microclimates, which are another source of modeling imprecision. Further, climate is generalized from weather stations typically located away from the model corridors.

Existing air temperature and relative humidity were assigned to each simulation from various weather stations in the basin. Natural variations in air temperature and relative humidity along the stream may not be accounted for in the simulations. For example, temperatures may change as the landscape changes over short distances along the stream. These are similar to the microclimates created by vegetation cover.

Groundwater exchanges and hyporheic flows are difficult to measure and are not rigorously accounted for within stream temperature modeling. In addition, natural stream conditions generally include more groundwater connection, wetland areas, and hyporheic interactions prior to anthropogenic disturbances. These conditions are not included in the Natural Thermal Potential (NTP) scenarios. Stream restoration may increase groundwater connectivity, which could reduce the NTP temperatures.

Increased channel complexity and more coarse woody debris are not accounted for in the NTP simulations. Including these factors may result in cooler NTP temperatures.

For this TMDL, the model inputs (vegetation, channel morphology, etc.) are averaged for each 50-meter segment, which means that the simulation may not account for some of the real world variability. For example, isolated pools or riffles within a 50 meter reach will not be included as unique features.

Heat Source simulations were performed for a finite model period spanning a summer during one year, which was intended to represent a critical condition for aquatic life. Stream temperatures will react differently to effective shade under other flow regimes and climactic conditions in different years.

Estimates of flow were used to create the existing flow inputs to the modeled streams. Withdrawals were estimated for the current condition as well. As described subsequently in this Appendix, these estimates are based on thermal infrared aerial data, drainage area correlations, the OWRD points of diversion database, and instream flow measurements, and other methods.

Stream velocities and depths were calculated by Heat Source for the "natural" flow conditions based on measured channel dimensions and substrate composition. These estimated velocities and depths for the "natural" flows have error associated with them since they have not been verified through field measurements.

Stream elevations and gradients were sampled and calculated from 10-meter digital elevation models (DEMs). DEMs have a certain level of imprecision (roughly ± 1-m) associated with them and may be a source of uncertainty in the simulation results.

In this TMDL process, there are a number of necessary decisions which are based on information with a certain amount of uncertainty: determination of impairment, model calibration acceptance, model scenario acceptance and allocations. For each of these four decision points, the uncertainty is handled differently.

The determination of impairment is based on a comparison of data with the water quality standard. The comparison of data with a numeric standard is relatively straight forward, however comparison of data to

a ‘natural conditions’ based standard has more uncertainty because ‘natural condition’ cannot be observed and is based on estimates. DEQ accounts for this uncertainty by trying to minimize the likelihood of a Type II error (where the actual condition is impaired but analysis shows the system is not impaired).

The determination that a model is representing a system (i.e. acceptance of a calibrated model) is based on comparison of model results with observed data, using statistics and graphical comparison. The uncertainty related to model scenarios is evaluated using a sensitivity analysis. Lastly, the uncertainty related to allocations is accounted for in the Margin of Safety.

All important stream parameters that can be accurately quantified are included in the analysis, and all complex simulation efforts include assumptions and limitations. In the context of understanding stream temperature dynamics, these areas of limitations should be the focus for future studies.

2. AVAILABLE DATA

2.1 Ground Level Data

Overview

Several ground level data collection efforts have been completed in the John Day River Basin, in order to inform the Heat Source models and calculate the TMDL. Specifically, this stream temperature analysis relied on the following data types: continuous temperature data, flow volume (gage data and instream measurements), topographic surveys, vegetation surveys, channel morphology surveys, and effective shade measurements.

The following parties are credited for collecting the data used in the John Day River Basin Temperature TMDL:
Confederated Tribes of the Umatilla Indian Reservation
Confederated Tribes of the Warm Springs Indian Reservation
Monument Soil and Water Conservation District
The Nature Conservancy
Oregon Department of Fish and Wildlife
Oregon Department of Environmental Quality
Oregon Department of Geology and Mineral Industries
Oregon State University
Oregon Water Resources Department
Western Regional Climate Center
Wheeler Soil and Water Conservation District
Umatilla National Forest
US Bureau of Land Management
US Bureau of Reclamation
US Environmental Protection Agency
US Forest Service (Umatilla, Ochoco, Malheur and Wallowa-Whitman National Forests)
US Geological Survey

Continuous Temperature Data

Continuous temperature data were used in this analysis to:

Calibrate stream emissivity for thermal infrared radiometry (TIR),
Calculate temperature statistics and assess the temporal component of stream temperature,
Calibrate temporal temperature simulations.

Continuous temperature data were collected during several efforts and by groups at various locations throughout the basin, during several years. The data were complied in a database maintained by NOAA's Integrated Status and Effectiveness Monitoring Project. The continuous data measurements usually spanned several summertime months. Measurements were collected using temperature data logging devices, such as thermistors[1]. Data from these devices have widely varying levels of quality assurance for precision and accuracy. Where reported, DEQ data of quality levels A and B were utilized. Where not, diel patterns were screened for anomalies typically associated with air exposure or clock error. **Figure A-4** displays continuous temperature data monitoring locations for the years 2002 and 2004 (The data are available from DEQ upon request.).

Figure A-4. Continuous stream temperature measurement locations for 2002 & 2004

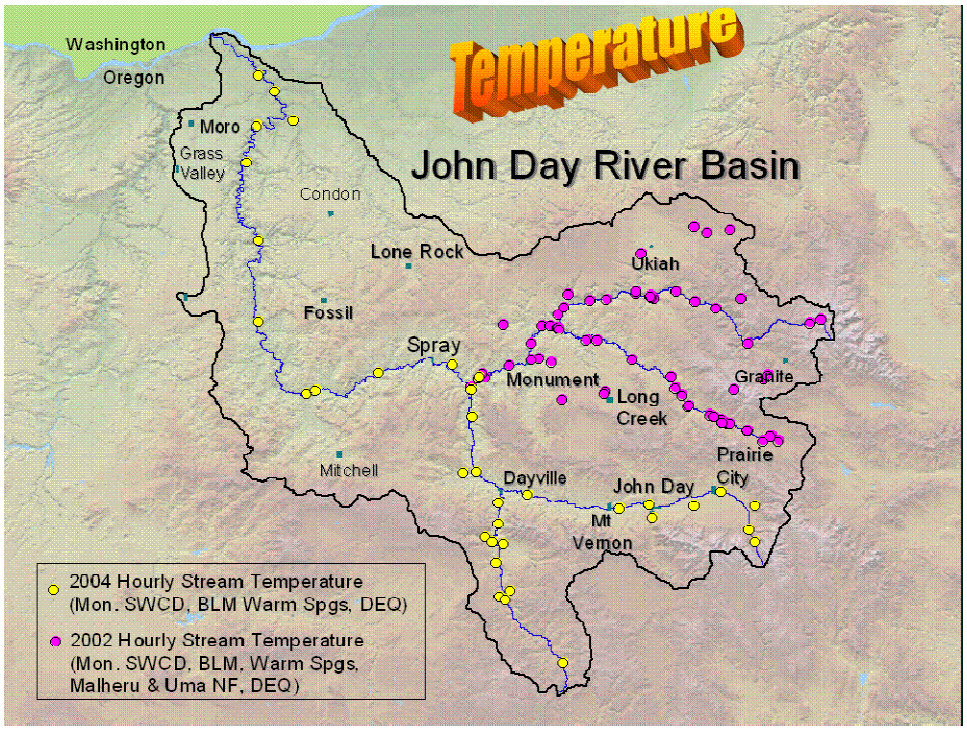

Flow Volume – Gage Data and Instream Measurements

Flow data of varying amounts and quality were collected throughout the basin (**Figure A-5**). Continuous flow measurements were available at USGS and OWRD gage sites. In addition, instantaneous flow volume data were collected at several sites during the critical stream temperature period in 2002 and 2004. Where applicable, these measurements were used to develop flow mass balances for the streams that were modeled for temperature (stream flow data are available upon request from DEQ).

[1] Thermistors are small electronic devices that are used to record half-hourly or hourly stream temperature at one location for a specified period of time.

Figure A-5. Available instream flow measurement and gage locations (2002 and/or 2004)

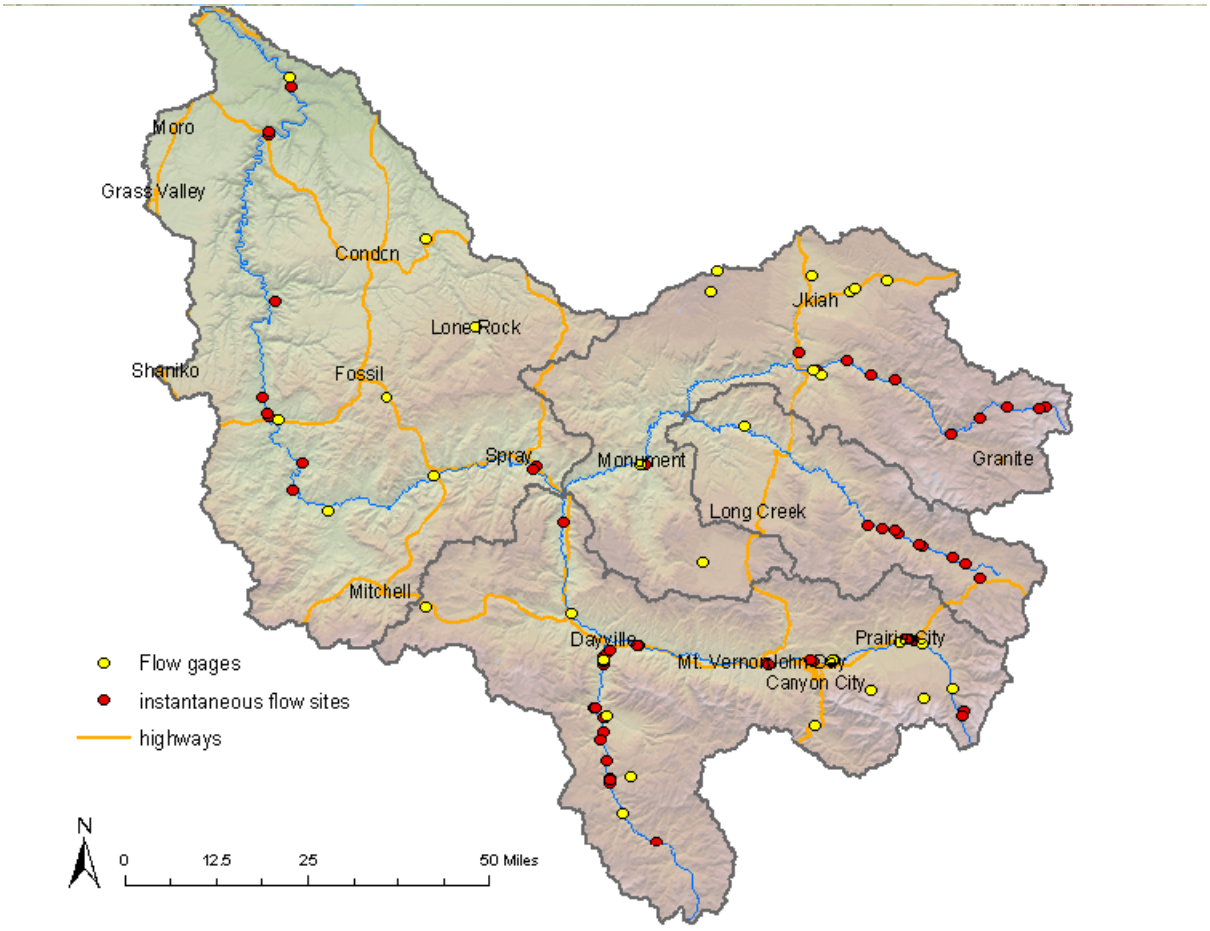

Channel Morphology and Vegetation

Channel morphology assessment relates to the bankfull stage of river flow. **Bankfull stage** is formally defined as the stream level that "*corresponds to the discharge at which channel maintenance is most effective, that is, the discharge at which moving sediment, forming or removing bars, forming or changing bends and meanders, and generally doing work that results in the average morphologic characteristics of channels*" (Dunne and Leopold, 1978). Research on bankfull discharge for North American streams has resulted in general agreement that the annual series bankfull discharge recurrence intervals are approximately equal to a 1.5 year event (Dury et al., 1963; Leopold et al., 1964; Hickin, 1968; Dunne and Leopold, 1978; Leopold, 1994). In other words, stream channels are built and maintained by relatively high flows, on a nearly annual basis. This has been verified for the John Day Basin (Castro and Jackson, 2001).

Through much of the John Day River Basin, stream channel modifications have occurred through various human influences. This is particularly evident in the agricultural and urban lowlands. Disturbance of upland and riparian vegetation, along with increased erosion, bank soil disturbance, stream re-location, stream straightening and diking are common. These alterations generally lead to channel widening or down-cutting followed by widening. Increased width and reduced shade lead to increased solar heating. Further, straightening and incision lead to decreased hyporheic cooling as well as channel disequilibrium.

In 2004, DEQ-led teams collected ground level stream morphologic data at several locations in the John Day River Basin (**Figure A-6** and **Figure A-7**). Stream survey data focuses on vegetation classification

and measurements, channel morphology measurements, and effective shade measurements. Transects were surveyed using a laser level. Substrate was measured based on modification of the Wolman (1954) pebble count method. A modified Rosgen Level II Inventory (Rosgen 1996) was applied to assess channel cross-sectional geometry and substrate composition. Riparian vegetation was assessed through the collection of the following types of field data:

- Solar pathfinder™ measurements of the vegetative horizon expressed as daily solar energy
- Field identification of shade producing vegetation species
- Vegetation height measurement using a digital range-finder

Figure A-6. Ground level Channel Morphology measurement locations for 2004

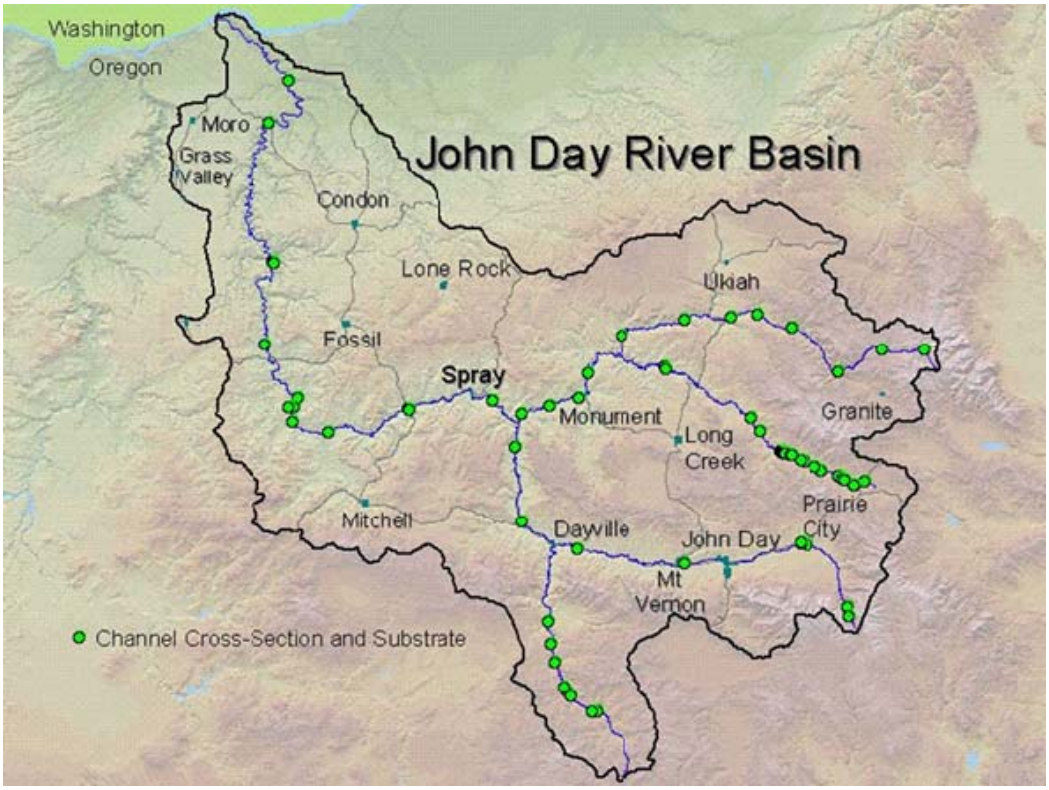

Figure A-7. Ground level vegetation assessment locations for 2004

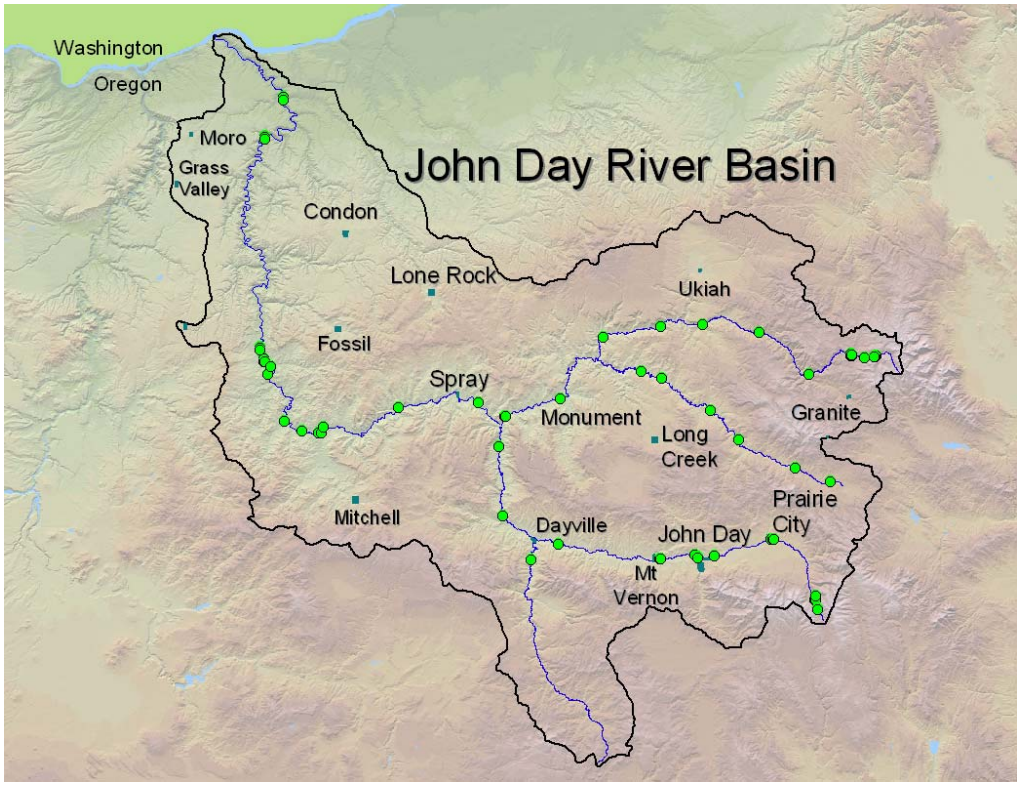

Meteorological Data

Hourly air temperature, wind speed, humidity and solar radiation (used to calculate cloudiness) measurements were retrieved from nearby weather station records. Each model reach used data from the weather station that best represented the local conditions. Weather sources with available data are shown in **Figure A-8**. The weather station data are from various organizations/databases: MesoWest, Remote Automated Weather Stations (Desert Research Institute RAWS – Western Regional Climate Center) and US Bureau of Reclamation Agrimet. Solar radiation was only available from the Agrimet sites at Goldendale and Prairie City. Temperature loggers were deployed for air temperature, by DEQ along the mainstem at McDonald Ferry, Clarno, Clyde Holliday and Trout Farm (all summer 2004), shown below. In 2004, air temperatures were collected by the Monument Soil and Water Conservation District at Kimberly on the mainstem and by the Nature Conservancy at Dunstan Preserve on the Middle Fork. Some adjustments were applied to meteorological data, because the weather stations are generally infrequent and more representative of uplands than stream corridors. These are discussed in the river-specific sections later in this Appendix.

Figure A-8. Available meteorological Data Sites for 2002 & 2004

2.2 GIS and Remotely Sensed Data

Overview

A wealth of spatial data has been developed for the John Day River Basin. The stream temperature TMDL relies extensively on GIS and remotely sensed data. Water quality issues in the John Day River Basin are interrelated, complex and spread over hundreds of square miles. The TMDL analysis strives to capture these complexities using the highest resolution spatial data available. Some of the GIS data used to develop the John Day River Basin Temperature TMDL are listed in **Table A-1** along with the application for which it was used.

Table A-1. Spatial Data and Application

Spatial Data	Application
10-Meter Digital Elevation Models (DEM)	Measure Stream Elevation and Gradient Measure Topographic Shade Angles
Aerial Imagery – Digital Orthophoto Quads	Map Vegetation Map Channel Morphology Map Roads, Development, Structures
Thermal Infrared Radiometry (TIR) Stream Temperature Data	Measure Surface Temperatures Develop Longitudinal Temperature Profiles Identify Subsurface Hydrology, Groundwater Inflow, Springs
Water Rights Information System (WRIS) and Points of Diversion (POD) Data	Map locations and estimate quantities of water withdrawals
Light Detection and Ranging (LiDAR) data	Measure vegetation heights Measure channel wetted widths

10-Meter Digital Elevation Model (DEM)

A digital elevation model (DEM) consists of digital information that provides a uniform matrix of terrain elevation values (**Figure A-9**). It provides basic quantitative data for deriving terrain elevation, slope, and topographic information. The 10-meter DEM contains a land surface elevation value for each 10-meter square. The U.S. Geological Survey, as part of the National Mapping Program, produces these digital cartographic/geographic data files. The DEMs were produced in 1999 and are available through the Oregon Geospatial Data Clearinghouse (OGDC). The data are available for the entire Basin.

Figure A-9. The 10-meter DEM, hill-shaded for contrast (Zoom at confluence of Middle Fork & North Fork John Day Rivers)

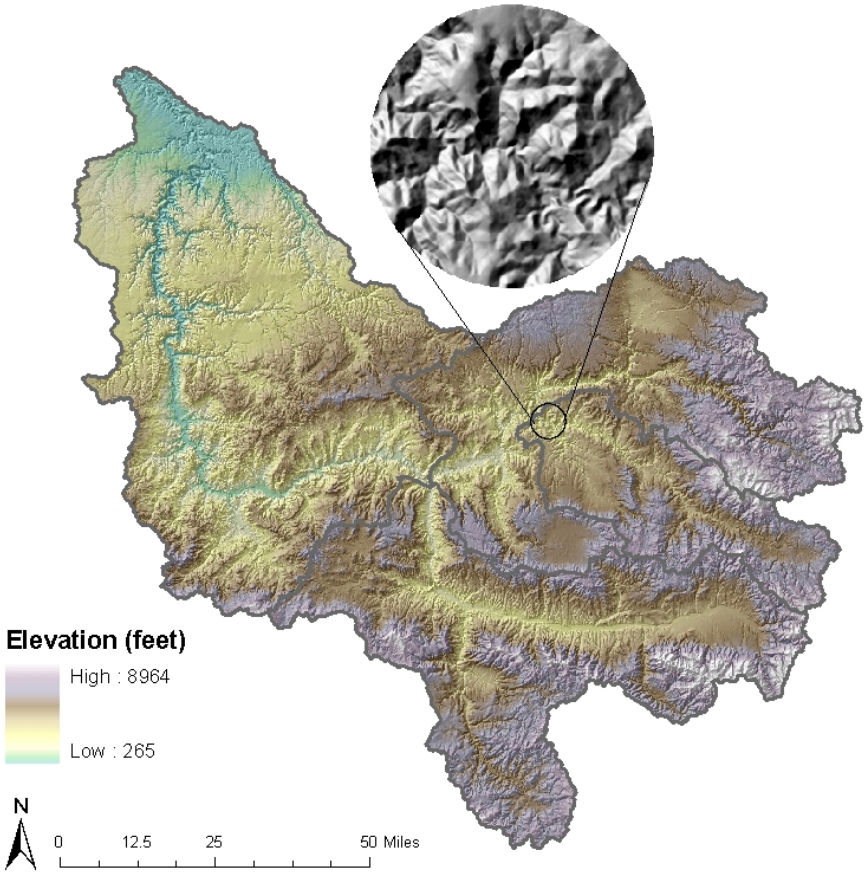

Aerial Imagery – Digital Orthophoto Quads

Aerial imagery was used to:

Map stream features such as stream position, channel edges and wetted channel edges,
Map near stream vegetation,
Map instream structures such as dams, weirs, unmapped diversions/withdrawals, etc.

A digital orthophoto quad (DOQ) is a digital image of an aerial photograph in which displacements caused by the camera distortion and projection have been removed. In addition, DOQs are projected in map coordinates combining the image characteristics of a photograph with the geometric qualities of a map. Color DOQs are available for the entire of the John Day River Basin and may be downloaded from http://www.oregonexplorer.info/imagery. Where available, the John Day Basin TMDL utilized NAIP versions with higher resolution (National Agriculture Imagery Program - half-meter pixel resolution, red-green-blue, uncompressed). Other reference sources were utilized to confirm vegetation characteristics, as described in the following sections.

WRIS and POD Data – Water Withdrawal Mapping

WRIS and POD Data were used to:

Map stream diversions/withdrawals,
Associate an estimated flow rate to each diversion/withdrawal.

The Oregon Water Resources Department (OWRD) maintains the Water Rights Information System (WRIS). WRIS is a database used to monitor information related to water rights. A separate OWRD database tracks points of diversion (POD). DEQ linked these two databases to map the locations of diversions, rates of water use and types of water use in the John Day River basin (**Figure A-10**). Interviews with and information from the local Water Master further informed the water withdrawal scenarios. Consumptive use was estimated using these data and incorporated in mass balance flow profiles for the simulated streams.

Figure A-10. Mapped points of diversion in the John Day River Basin derived from the WRIS and POD databases (Oregon Water Resources Department)

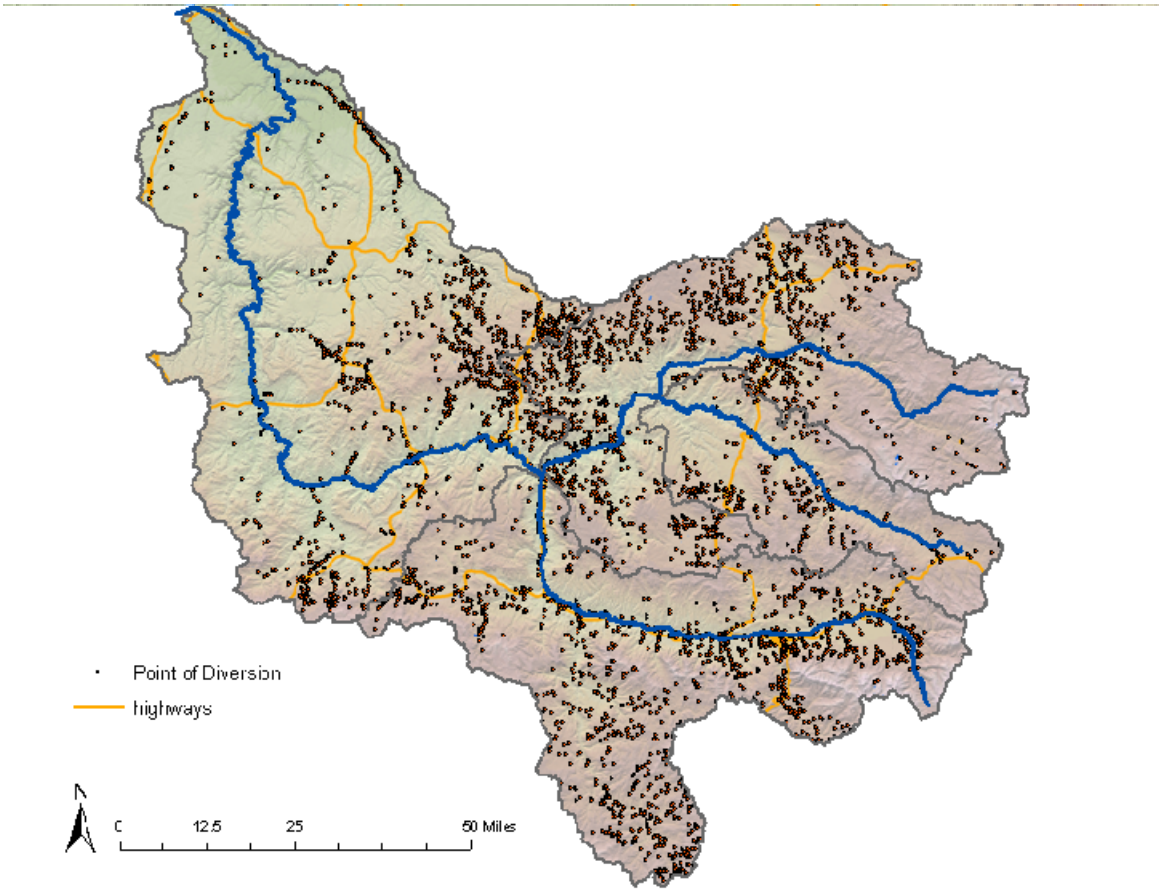

Thermal Infrared Radiometry (TIR) Temperature Data

TIR temperature data were used to:

Develop continuous spatial temperature data sets,
Calculate longitudinal heating profile/gradients,
Visually observe complex distributions of stream temperatures at a large landscape scale,
Map/Identify significant thermal features,
Develop flow mass balances,
Validate simulated stream temperatures.

TIR imagery measures the temperature of the outermost portions of the bodies/objects in the image (i.e., ground, riparian vegetation, and stream). The bodies of interest are opaque to longer wavelengths and there is little, if any, penetration of the bodies.

TIR data was gathered through a sensor mounted on a helicopter that collected digital data directly to an on-board computer at a rate that insured the imagery maintained a continuous image overlap of at least 40%. The TIR detected emitted radiation at wavelengths from 8-12 microns (long-wave) and recorded the level of emitted radiation as a digital image across the full 12-bit dynamic range of the sensor. Each image pixel contained a measured value that was directly converted to a temperature. Each thermal image has a spatial resolution of less than one-half meter/pixel. Visible video sensor captured the same field-of-view as the TIR sensor. GPS time was encoded on the imagery.

Data collection was timed to capture maximum daily stream temperatures, which typically occur between 14:00 and 18:00 hours. The helicopter was flown longitudinally over the center of the stream channel with the sensors in a vertical (or near vertical) position. In general, the flight altitude was selected so that the stream channel occupied approximately 20-40% of the image frame. A minimum altitude of approximately 300 meters was used both for maneuverability and for safety reasons. If the stream split into two channels that could not be covered in the sensor's field of view, the survey was conducted over the larger of the two channels.

Instream temperature data loggers (Onset Stowaways or VEMCOs) were distributed in each subbasin prior to the survey to ground truth the radiant temperatures measured by the TIR. TIR data can be viewed as GIS point coverages or TIR imagery.

Direct observation of spatial temperature patterns and thermal gradients is a powerful application of TIR derived stream temperature data. Thermally significant areas can be identified in a longitudinal stream temperature profile and related directly to specific sources (i.e., water withdrawal, tributary confluence, vegetation patterns, etc.). Areas with stream water mixing with subsurface flows (i.e., hyporheic and inflows) are apparent and often dramatic in TIR data. Thermal changes captured with TIR data can be quantified as a specific change in stream temperature or a stream temperature gradient that results in a temperature change over a specified distance.

John Day River Basin TIR Data

TIR data was collected for different parts of the John Day River Basin during 1998, 2002 & 2004 by Watershed Sciences, Inc. Longitudinal river temperatures were sampled using thermal infrared radiometry (TIR) in separate flights for each river segment (**Figure A-11**). Temperature data sampled from the TIR imagery revealed spatial patterns that are variable due to localized stream heating, tributary mixing, and groundwater influences.

Thermal stratification was identified in TIR imagery and by comparison with the instream temperature loggers. For example, the imagery may reveal a sudden cooling at a riffle or downstream of an instream structure, where water was rather stagnant or deep just upstream.

TIR-derived longitudinal stream temperature profiles are presented in **Section 3**. Each year's John Day Basin TIR survey report is available for download at the Oregon DEQ website (Watershed Sciences, Inc., 1998, 2002 and 2004). The TIR survey reports contain detailed flight information, results discussions, sample imagery, and longitudinal temperature profiles. (Actual TIR data is available upon request from DEQ. Viewing the TIR data requires ArcView with Spatial Analyst.)

Figure A-11. TIR flight paths in the John Day Basin.

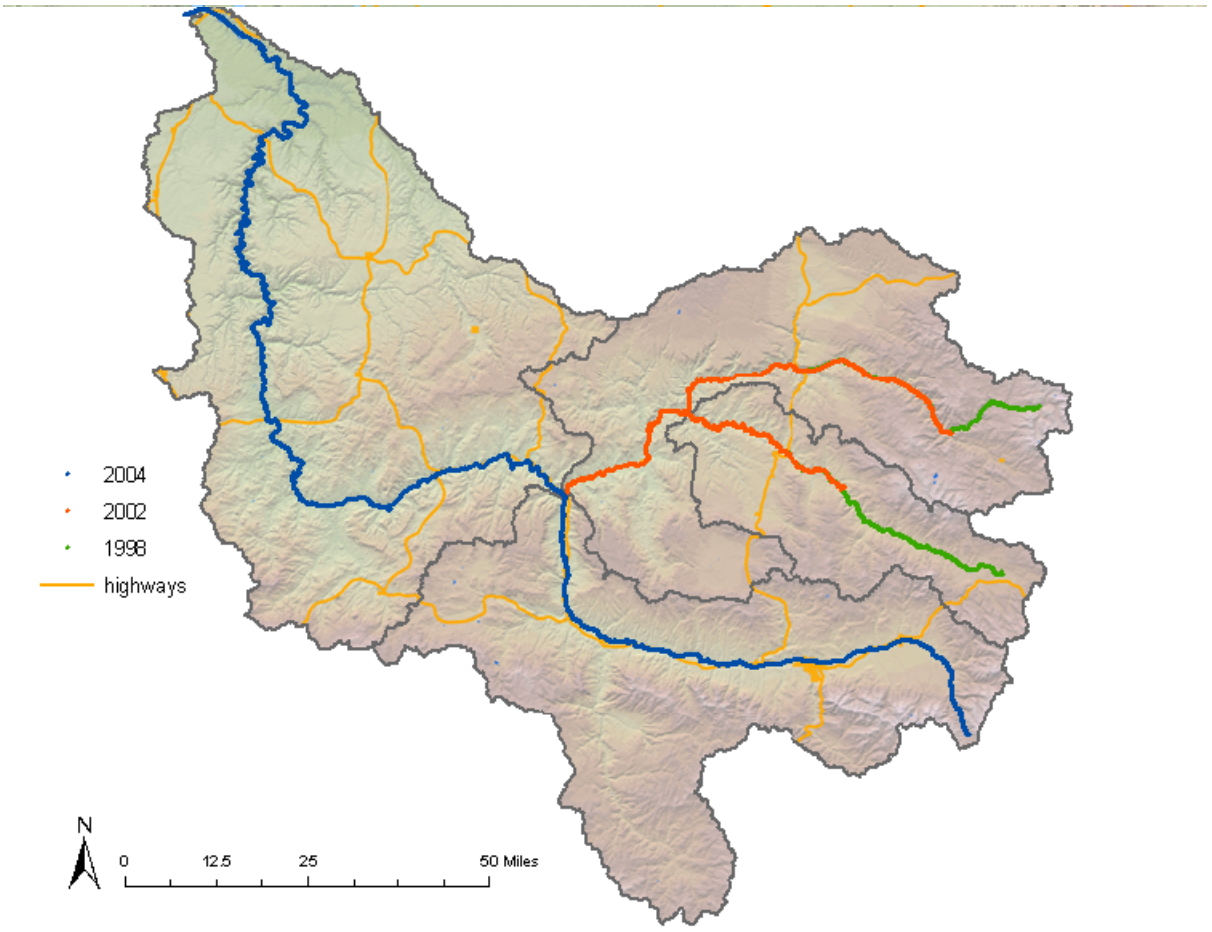

Light Detection and Ranging (LiDAR) Data

LiDAR is a remote sensing technique allowing the collection of large amounts of high quality data at a high density. A low flying plane emits a light beam at the target terrain. A sensor mounted on the plane receives and measures the intensity and timing of the reflected light. Using these data, the morphology of the river can be more accurately represented.

John Day River Basin LiDAR Data

Watershed Sciences, Inc. collected Light Detection and Ranging (LiDAR) data from October 5-7, 2006 for the Puget Sound LiDAR Consortium. The survey areas cover the floodplains of Desolation Creek from the mouth to Bruin Creek; the Middle Fork John Day River from just upstream of Big Creek to Summit Creek; and the John Day River from Prairie City to just above Dans Creek. The study areas total ~9,149 acres (**Figure A-12**).

Figure A-12. Full extent of LiDAR Study Areas in the John Day Basin: Desolation Creek, Middle Fork John Day, and John Day River, totaling 9,149 acres

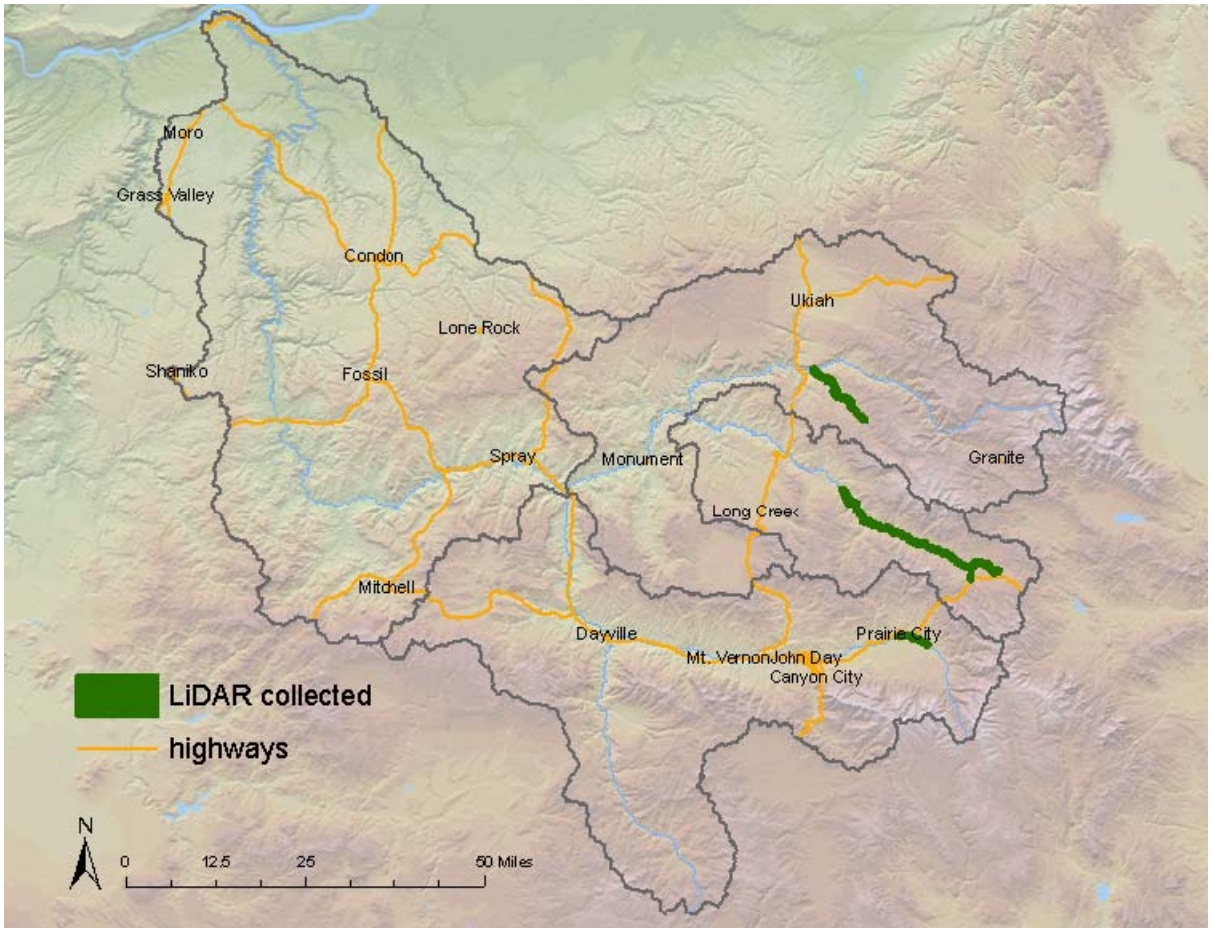

Laser points were collected over the study area using a Leica ALS50 Phase II LiDAR laser system set to acquire points at an average density of ≥8 points per square meter. Full overlap (i.e., ≥50% side-lap) ensured complete coverage and minimized laser shadows created by buildings and tree canopies. A real-time kinematic (RTK) survey was conducted throughout the study area for quality assurance purposes. The accuracy of the LiDAR data is described as standard deviations of divergence (sigma ~ σ) from RTK ground survey points and root mean square error (RMSE) which considers bias (upward or downward).

For the Desolation Creek, Middle Fork John Day River, and John Day River study areas, the data have an RMSE of 0.069 meters, a 1-sigma absolute deviation of 0.069 meters and a 2-sigma absolute deviation of 0.138 meters. Deliverables include point data in ASCII and *.las v.1.1 format, 1- meter resolution laser intensity images, 1-meter resolution bare ground model ESRI GRIDs, and 1-meter resolution Highest Hit vegetation model ESRI GRIDs for the entire study area. All data are delivered in Universal Transverse Mercator (UTM) Zone 11, in the NAD83/NAVD88 datum (Geoid 03).

For further information, DEQ maintains copies of contactor reports detailing remote sensing surveys. These are available upon request.

2.3 Derived Data and Model Inputs

Overview

Several landscape scale GIS data sets were sampled to derive spatial stream data. The following sub-sections detail the methodologies, results, resolution and accuracy for each derived data type. Sampling density was user-defined and generally matched any GIS data resolution and accuracy. The data sets, sampling methods, and derived data sets are documented in more detail in the individual model sections. The sampled parameters used in the stream temperature analysis were:

- Stream Position and Aspect
- Stream Elevation and Gradient
- Maximum Topographic Shade Angles (East, South, West)
- Channel Width
- Vegetation
- Wetted Widths

Most of these parameters were derived using TTools (Boyd & Kasper, 2003b). TTools is a set of ArcView GIS tools that are designed to automatically sample spatial data sets and assemble an input database for Heat Source modeling. TTools documentation is included as part of the Heat Source documentation "*Analytical Methods for Dynamic Open Channel Heat and Mass Transfer: Methodology for Heat Source Model Version 7.0*" (Boyd & Kasper, 2003a) and can be found at www.deq.state.or.us/WQ/TMDLs/tools.htm. In addition to these GIS-derived landscape parameters, other inputs to the model were also derived from a variety of data sources and scales. These include:

- Constant values that applies to the whole model corridor
  - Wind function coefficients
  - Deep alluvium temperature
- Parameters that vary by model node
  - Channel bottom width
  - Channel angle z
  - Manning's n
  - Sediment thermal conductivity
  - Sediment thermal diffusivity
  - Sediment/hyporheic zone thickness
  - Percent hyporheic exchange
  - Porosity)
- Parameters that apply to tributary inputs
  - Flow
  - Temperature

Stream Position, Aspect, Stream Elevation, Gradient, Shade Angles

A stream position (center) line is digitized using orthoimagery and segmented into equidistant nodes (for model data input; nodes are spaced 50 meters apart). Stream elevation is sampled from 10-m digital elevation model files and gradient is calculated from the DEM elevation and stream position (**Figure A-13**). Topographic shade angles are measured via the same DEM and stream position data file. Topographic shade is assessed with near (bank) and far (hills, valley wall) field reference. Land cover base elevation is developed by simultaneous sampling of the DEM and the land cover position polygon codes as described later in this Appendix.

Channel Width and Gradient Assessment

As noted above, effective shade, stream surface area, wetted perimeter, stream depth and stream hydraulics are all sensitive to channel width. Channel width is dependent on gradient, channel materials, discharge and other controls. Accurate measurement of channel width and gradient across the stream

network, coupled with other derived and ground level data, provides for channel morphology simulation. The steps for conducting channel width assessment are listed below.

Step 1. Stream channel edges were digitized from DOQs at a 1:5,000 or less map scale. These channel boundaries establish the channel width, which is defined for purposes of the TMDL, as the width between shade-producing near-stream vegetation. Where near-stream vegetation is absent, the near-stream boundary is used, defined as downcut stream banks or where the near-stream zone is unsuitable for vegetation growth due to external factors (i.e., roads, railways, buildings, etc.).
Step 2. Channel widths were sampled at each stream data node using TTools[2]. The sampling algorithm measured the channel width in the transverse direction relative to the stream aspect.
Step 3. Compared sampled channel width and ground level measurements. TTools sampled channel widths were then compared to ground level measurements for verification purposes.

Figure A-13. Digitized channel centerline, right bank, and left bank

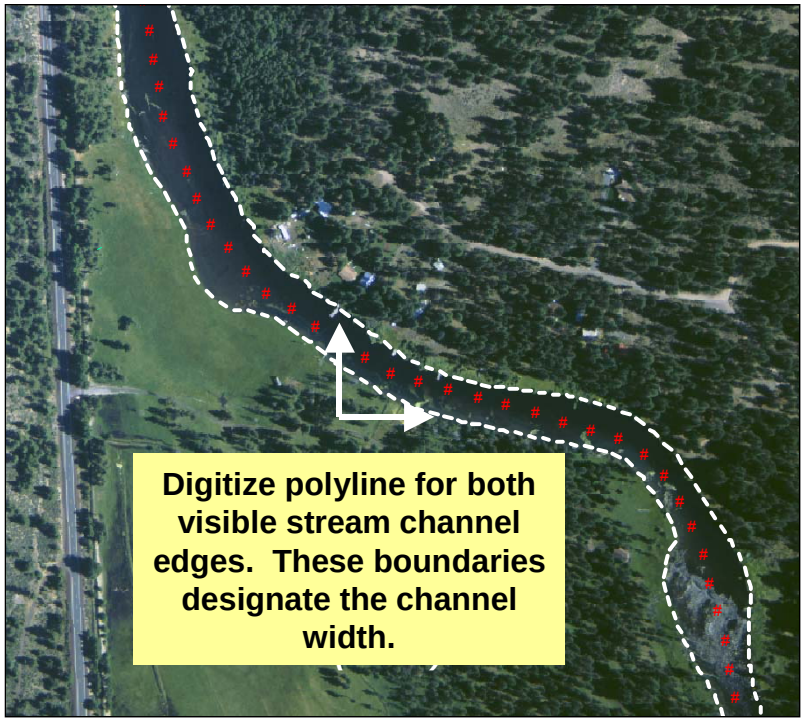

In places where there is sufficient LiDAR data (Middle Fork John Day River), the channel wetted widths can be determined by identifying and isolating the continuous areas with no vegetation. The general steps for deriving channel wetted widths are described below. Some steps are illustrated in **Figure A-14**.

1. Of the modeled reaches in the subbasin, only the upper 45.6 km of the Middle Fork John Day River were surveyed with LiDAR techniques. The LiDAR data grids describe the "highest hit" and "bare earth" elevations recorded at each point.
2. Subtracting the "bare earth" elevation from the "highest hit" elevation calculates the vegetation height at each point on the grid.

[2] A GIS tool developed by Oregon DEQ for automatically sampling spatial data sets and creating a Heat Source input database (Boyd, Kasper, 2003).

3. The LiDAR data grids also describe the relative "intensity" of the reflected light at each point. The range of intensities that represent water can be determined by visual inspection and then isolated.
4. Those points on the grid that have no vegetation (vegetation height of zero) and are within the range of intensity representative of water were selected and isolated. These points are commonly indistinguishable from roads.
5. The digitized stream center line, from the TTools process, generally overlaps with the LiDAR-isolated water. After buffering the center line nodes, most of the road segments identified in the previous step were excluded. The remaining non-water points were manually excluded. In addition, dams or breaks in the continuous channel corridor were manually reconnected by adding a very thin artificial water channel.
6. When the continuous channel corridor was finalized, the channel wetted width was calculated at each TTools node using the TTools routine.
7. These high density channel wetted widths were graphically compared to the wetted widths predicted by the HeatSource model. These sampled measurements are less reliable than direct measurements, so they were only used for model validation and calibration. Also, we used the LiDAR data as a validation tool to visually estimate the performance of the model, but we did not calculate statistics. While aware of the imprecision of the data, the LiDAR data were assumed to be accurate enough to use for visual comparison.

Figure A-14. Illustrations from selected steps for deriving channel wetted widths from LiDAR.

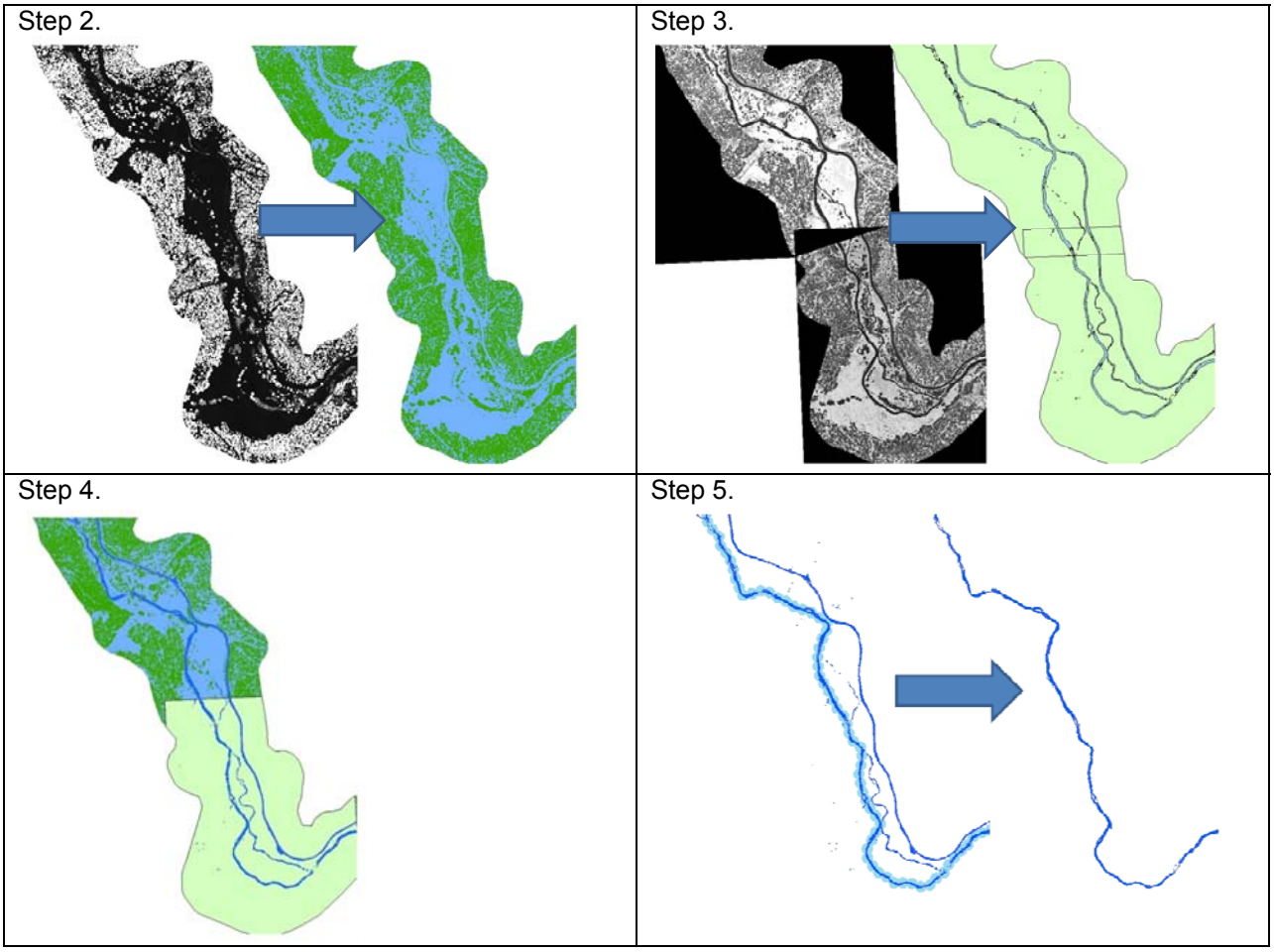

Vegetation

The role of vegetation in maintaining a healthy stream condition and water quality is well documented and accepted in scientific literature (Beschta et al. 1987). Vegetation impacts the stream and the surrounding environment in the following ways:

- Vegetation plays an important role in regulating radiant heat in stream thermodynamic regimes.
- Channel morphology is often highly influenced by vegetation type and condition by affecting flood plain and instream roughness, contributing coarse woody debris, and influencing sedimentation, stream substrate compositions and stream bank stability.
- Vegetation creates a thermal microclimate that generally maintains cooler air temperatures, higher relative humidity and lower wind speeds along stream corridors.
- Riparian and instream nutrient cycles are affected by vegetation.

With the recognition that vegetation is an important parameter in influencing water quality, DEQ made the development of vegetation data sets in the John Day River Basin a high priority. Riparian vegetation was assessed through field assessment and remote sensing for the model reaches (**Figure A-15**). Variable vegetation conditions in the John Day River Basin require a higher resolution than currently available GIS data sources. To meet this need, DEQ has mapped vegetation using Digital Orthophoto Quads (DOQs) at a 1:5,000 map scale. Vegetation features were mapped 300 feet in the transverse direction from channel edge. Vegetation data was developed by DEQ in successive steps.

Step 1. Vegetation polygons and stream polylines were digitized from DOQs. All digitized polygons were drawn to capture visually like vegetation features. All digitized line work was completed at a 1:5,000 map scale or less.

Step 2. Basic vegetation types were categorized and assigned to individual polygons. The vegetation categories used in this effort were aggregate vegetation groups, such as: conifers, hardwoods, shrubs, etc. An attribute code was assigned to each polygon as described below.

Step 3. Automated sampling was conducted on classified vegetation spatial data sets in 2-dimensions using TTools. Every 50 meters along the stream (i.e., in the longitudinal direction), the vegetation was sampled 4 times radially away from the channel center in seven directions, at a radial sample spacing that was optimized for channel width range along the model corridor. This resulted in 560 measurements of vegetation per every kilometer of stream.

Figure A-15. Streams where near stream vegetation and channel morphology were digitized from digital orthophoto quads.

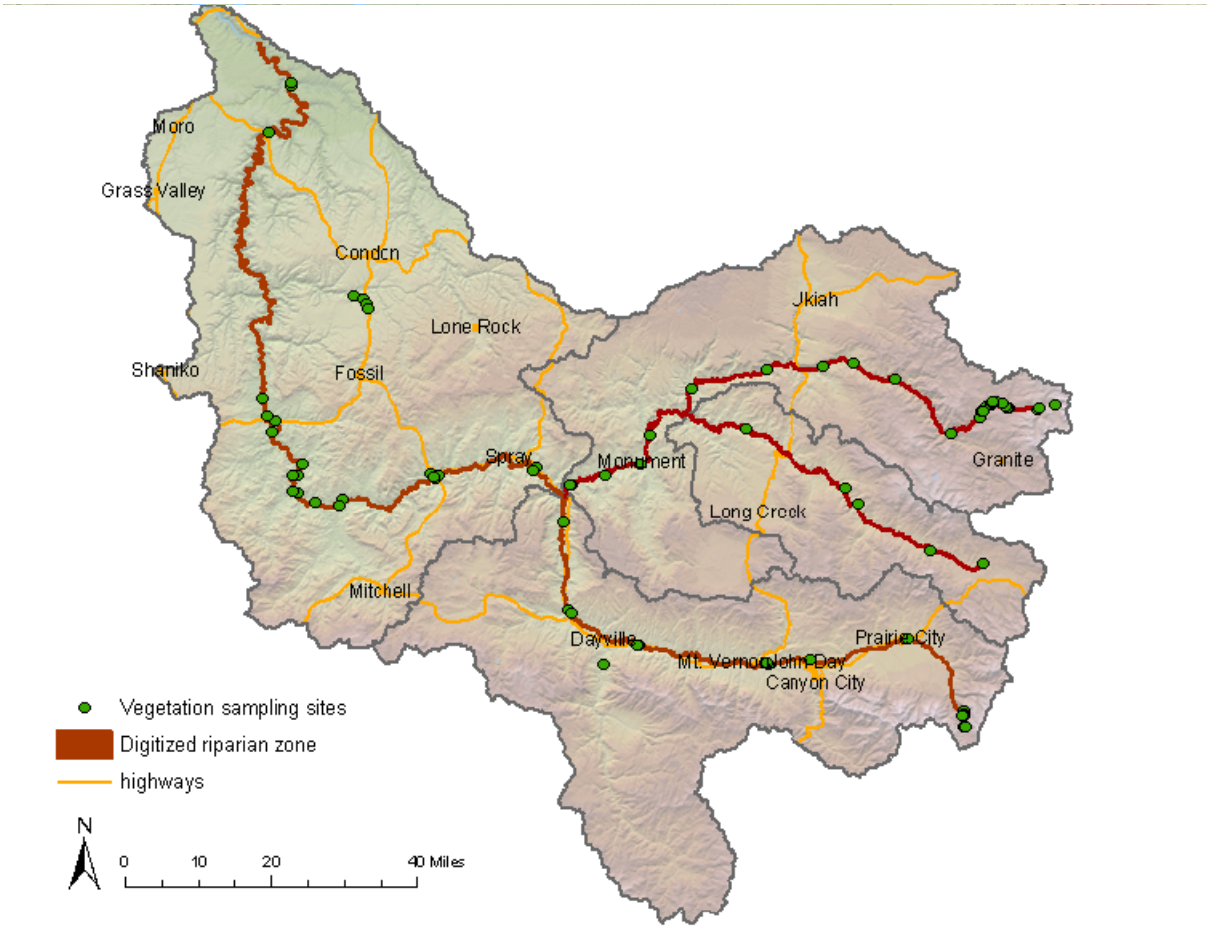

Figure A-16 summarizes the steps followed for vegetation classification. More detailed information can be found in *Analytical Methods for Dynamic Open Channel Heat and Mass Transfer: Methodology for Heat Source Model Version 7.0* (Boyd & Kasper, 2003a), which can be downloaded from the DEQ website. (http://www.heatsource.info/).

Figure A-16. Steps for digitizing and classifying vegetation.

Example of Polygon Mapping of Vegetation from Aerial Color Imagery

(At this point only the line work is complete and no data is associated with the polygons.)

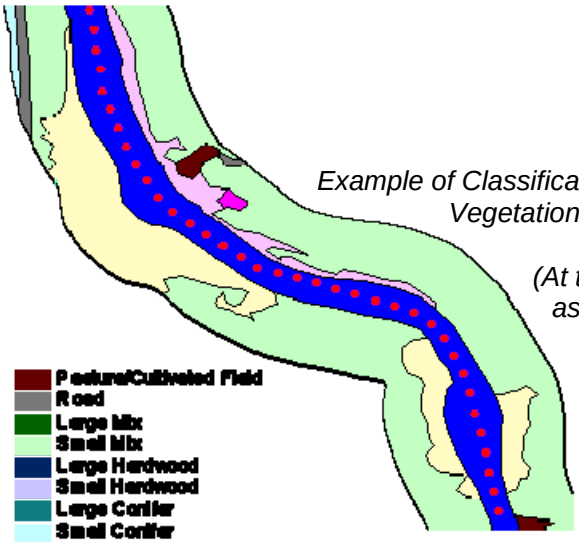

Example of Classification of the Vegetation Polygons Associating a Vegetation Type to Each of the Polygons

(At this point a vegetation type numeric code is associated with each polygon.)

Pasture/Cultivated Field
Road
Large Mix
Small Mix
Large Hardwood
Small Hardwood
Large Conifer
Small Conifer
Shrubs - Upland
Shrubs - Wetland
Grasses - Upland
Grasses - Wetland
Water
Developed - Residential
26% Distribution of Shrubs
76% Distribution of Shrubs

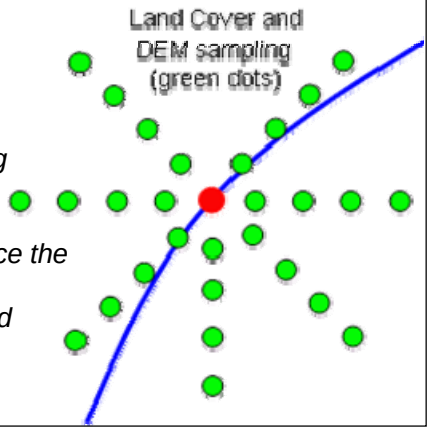

TTools radial sampling pattern for vegetation (sampling interval is user defined). Sampling occurs for every stream data node at four user-defined intervals every 45 degrees from north (North is not sampled since the sun does not shine from that direction in the northern hemisphere). A database of vegetation type in created for each stream data node.

Derivation of Attribute Codes

Within each digitized polygon described in Step 2 above, the vegetation was assigned an attribute code from four categories (**Table A-2** and **Table A-3**). The attribute codes are not case sensitive. The Middle Fork John Day coding scheme was slightly different from the mainstem and North Fork John Day Rivers, because greater detail was available via the upper Middle Fork LiDAR data. The combination of assigned attributes created a 4 digit code, which represented a land cover type, vegetation height and density (**Table A-4, Table A-5, and Table A-6**). Digital range finder height measurements, aerial photo shadow lengths and personal interviews were incorporated into the final determination of existing vegetation height for the model calibration. Aerial photography interpretation was aided by field identification conducted by DEQ and BLM, which included field measurements, species lists, and on-site comparison of vegetation stands with photos. As mentioned previously, LiDAR data, high resolution and infrared images from other agencies assisted as well, where available. Vegetation density was obtained from aerial photography and was expressed as the percentage of solar radiation passing through, and grouped in categories: 0-20, 20-40, 40-60, 60-80, 80-100.The attribute overhang was assigned afterward specific to model corridor and land cover type. The percentage of each code that was sampled by TTools in each model is shown in **Table A-4, Table A-5, and Table A-6**. Heat Source used these inputs to simulate existing vegetation scenarios.

Table A-2. Mainstem and North Fork John Day River land cover coding.

1st Digit Land Cover		2nd Digit Relative Elevation		3rd Digit Height (feet)		4th Digit Density (%)	
1	small shrubs and grasses, wetlands, crops, pasture, lawn	f	within post Euro-settlement floodplain	a	< 5 (2.5 avg.)	1	0-20
2	deciduous - general	u	upland - hill slope or ancient terrace above 'f'	b	5-20 (12.5 avg.)	2	20-40
3	large shrubs or brush willow			c	20-40 (30 avg.)	3	40-60
4	orchard			d	40-60 (50 avg.)	4	60-80
5	conifer			e	60-100 (80 avg.)	5	80-100
6	mixed deciduous/conifer			f	100-150 (125 avg.)		
A	water			g	> 150 (160 avg.)		
B	channel						
C	transportation corridor						
D	barren - natural						
E	barren - developed						
F	urban, residential, commercial or industrial development						

Note: shaded areas clearly represent anthropogenic influence

Note: for river, 'water' and 'channel' always receive 'f'

Table A-3. Middle Fork John Day River land cover coding.

1st 2 Digits Land Cover		3rd Digit Height (feet)		4th Digit Density (%)	
Vegetated		**General height and density**			
11	small shrubs and grasses, wetlands, crops, pasture, lawn	A	less than 1 (0.6 avg.)	1	0-20
15	deciduous and/or lg. shrubs	B	1-5 (3.0 avg.)	2	20-40
16	orchard	C	5-10 (7.5 avg.)	3	40-60
18	conifer	D	10-15 (12.5 avg.)	4	60-80
19	mixed deciduous/conifer	E	15-20 (17.5 avg.)	5	80-100
		F	20-30 (25 avg.)		
		G	30-40 (35 avg.)		
		H	40-50 (45 avg.)		
		I	50-60 (55 avg.)		
		J	60-70 (65 avg.)		
		K	70-90 (80 avg.)		
		L	90-110 (100 avg.)		
		M	110-130 (120 avg.)		
		N	130-160 (145 avg.)		
		O	160*190 (175 avg.)		
Other		**Specific assignments of height and density**			
30	water	0	0	0	0
35	channel	0	0	0	0
41	roadway - paved	0	0	0	0
42	roadway - not paved	0	0	0	0
43	railroad right-of-way	0	0	0	0
50	barren - natural	0	0	0	0
51	barren - developed	0	0	0	0
60	residential	0	0	0	0
61	urban	0	10	0	0
62	Industrial	0	20	0	0
80	misc anthropogenic shade producing structures	use general height and density codes above			

Note: shaded areas clearly represent anthropogenic influence

Table A-4. Mainstem John Day River vegetation code attributes and percent of model inputs.

Code	Height (m)	Density (0 - 1)	Overhang (m)	percent of input
1fA1	0.76	10%	0.0	3.19%
1fA2	0.76	30%	0.0	5.25%
1fA3	0.76	50%	0.0	16.07%
1fA4	0.76	70%	0.0	0.70%
1fA5	0.76	90%	0.0	0.04%
1uA1	0.76	10%	0.0	0.42%
1uA2	0.76	30%	0.0	12.39%
1uA3	0.76	50%	0.0	0.81%

1uA4	0.76	70%	0.0	0.00%
3fB1	3.81	10%	0.0	1.52%
3fB2	3.81	30%	0.0	0.92%
3fB3	3.81	50%	0.0	1.17%
3fB4	3.81	70%	0.0	0.82%
3fB5	3.81	90%	0.0	0.13%
3uB1	3.81	10%	0.0	0.65%
3uB2	3.81	30%	0.0	0.12%
3uB3	3.81	50%	0.0	0.02%
3uB4	3.81	70%	0.0	0.02%
3uB5	3.81	90%	0.0	0.01%
2fC1	9.14	10%	0.0	0.22%
2fC2	9.14	30%	0.0	0.18%
2fC3	9.14	50%	0.0	0.36%
2fC4	9.14	70%	0.0	0.29%
2fC5	9.14	90%	0.0	0.16%
2fD1	15.24	10%	0.5	0.03%
2fD2	15.24	30%	0.5	0.09%
2fD3	15.24	50%	0.5	0.33%
2fD4	15.24	70%	0.5	0.55%
2fD5	15.24	90%	0.5	0.32%
2fE1	24.38	10%	2.0	0.00%
2fE2	24.38	30%	2.0	0.04%
2fE3	24.38	50%	2.0	0.22%
2fE4	24.38	70%	2.0	0.70%
2fE5	24.38	90%	2.0	0.63%
2uC1	9.14	10%	0.0	0.00%
2uC2	9.14	30%	0.0	0.01%
2uC3	9.14	50%	0.0	0.01%
2uC4	9.14	70%	0.0	0.00%
2uC5	9.14	90%	0.0	0.00%
2uD4	15.24	70%	0.0	0.00%
2uD5	15.24	90%	0.0	0.01%
2uE3	24.38	50%	0.0	0.00%
2uE4	24.38	70%	0.0	0.00%
2uE5	24.38	90%	0.0	0.00%
5fB1	3.81	10%	0.0	0.13%
5fB2	3.81	30%	0.0	0.00%
5fB3	3.81	50%	0.0	0.00%
5fC1	9.14	10%	0.0	0.35%
5fC2	9.14	30%	0.0	0.17%
5fC3	9.14	50%	0.0	0.06%
5fC4	9.14	70%	0.0	0.03%
5fC5	9.14	90%	0.0	0.01%
5fD1	15.24	10%	0.5	0.03%
5fD2	15.24	30%	0.5	0.11%
5fD3	15.24	50%	0.5	0.06%

5fD4	15.24	70%	0.5	0.08%
5fD5	15.24	90%	0.5	0.01%
5fE1	24.38	10%	1.0	0.05%
5fE2	24.38	30%	1.0	0.03%
5fE3	24.38	50%	1.0	0.06%
5fE4	24.38	70%	1.0	0.18%
5fE5	24.38	90%	1.0	0.51%
5uB1	3.81	10%	0.0	0.63%
5uB2	3.81	30%	0.0	0.04%
5uB3	3.81	50%	0.0	0.00%
5uC1	9.14	10%	0.0	2.69%
5uC2	9.14	30%	0.0	0.94%
5uC3	9.14	50%	0.0	0.45%
5uC4	9.14	70%	0.0	0.02%
5uC5	9.14	90%	0.0	0.00%
5uD1	15.24	10%	0.0	0.14%
5uD2	15.24	30%	0.0	0.03%
5uD3	15.24	50%	0.0	0.02%
5uD4	15.24	70%	0.0	0.01%
5uD5	15.24	90%	0.0	0.00%
5uE1	24.38	10%	0.0	0.02%
5uE3	24.38	50%	0.0	0.05%
5uE4	24.38	70%	0.0	0.04%
5uE5	24.38	90%	0.0	0.00%
6fC1	9.14	10%	0.0	0.08%
6fC2	9.14	30%	0.0	0.09%
6fC3	9.14	50%	0.0	0.07%
6fC4	9.14	70%	0.0	0.05%
6fC5	9.14	90%	0.0	0.02%
6fD1	15.24	10%	0.5	0.01%
6fD2	15.24	30%	0.5	0.06%
6fD3	15.24	50%	0.5	0.07%
6fD4	15.24	70%	0.5	0.04%
6fD5	15.24	90%	0.5	0.05%
6fE1	24.38	10%	1.5	0.01%
6fE2	24.38	30%	1.5	0.01%
6fE3	24.38	50%	1.5	0.05%
6fE4	24.38	70%	1.5	0.02%
6fE5	24.38	90%	1.5	0.01%
6uC1	9.14	10%	0.0	0.02%
6uC2	9.14	30%	0.0	0.03%
6uC3	9.14	50%	0.0	0.01%
6uC4	9.14	70%	0.0	0.00%
6uC5	9.14	90%	0.0	0.00%
6uD1	15.24	10%	0.0	0.00%
6uD2	15.24	30%	0.0	0.00%
6uD3	15.24	50%	0.0	0.00%

6uD4	15.24	70%	0.0	0.00%
6uE4	24.38	70%	0.0	0.00%
AfA1	0	0%	0.0	40.94%
AuA1	0	0%	0.0	0.00%
BfA1	0	0%	0.0	0.16%
DfA1	0	0%	0.0	0.01%
DuA1	0	0%	0.0	0.01%
EfA1	0	0%	0.0	0.75%
EuA1	0	0%	0.0	0.03%
CfA1	0	0%	0.0	0.66%
CuA1	0	0%	0.0	0.79%
FfA1	0.76	10%	0.0	0.15%
FfB1	3.81	10%	0.0	0.10%
FfB2	3.81	30%	0.0	0.01%
FfB3	3.81	50%	0.0	0.01%
FfB4	3.81	70%	0.0	0.01%
FfB5	3.81	90%	0.0	0.01%
FfC1	9.14	10%	0.0	0.04%
FfC2	9.14	30%	0.0	0.03%
FfC3	9.14	50%	0.0	0.12%
FfC4	9.14	70%	0.0	0.04%
FfC5	9.14	90%	0.0	0.02%
FfD3	15.24	50%	0.0	0.01%
FfD4	15.24	70%	0.0	0.00%
FfD5	15.24	90%	0.0	0.00%
FuA3	0.76	50%	0.0	0.02%
FuB1	3.81	10%	0.0	0.00%
FuB2	3.81	30%	0.0	0.00%
FuB3	3.81	50%	0.0	0.00%
FuB4	3.81	70%	0.0	0.00%
FuB5	3.81	90%	0.0	0.00%
FuC2	9.14	30%	0.0	0.00%
FuC3	9.14	50%	0.0	0.00%
FuC4	9.14	70%	0.0	0.00%
FuC5	9.14	90%	0.0	0.00%
FuD5	15.24	90%	0.0	0.00%
OfB1	3.81	10%	0.0	0.00%
OfB3	3.81	50%	0.0	0.00%
OfB4	3.81	70%	0.0	0.00%
OfC3	9.14	50%	0.0	0.02%
OfC4	9.14	70%	0.0	0.00%
OfD4	15.24	70%	0.0	0.00%

Table A-5. North Fork John Day River vegetation code attributes and percent of model inputs.

Code	Height (m)	Density (0 - 1)	Overhang (m)	Percent of input
1au4	0.76	70%	0.0	0.01%
1f13	0.76	50%	0.0	0.00%
1fa1	0.76	10%	0.0	0.31%
1fa2	0.76	30%	0.0	0.33%
1fa3	0.76	50%	0.0	8.12%
1fa4	0.76	70%	0.0	0.38%
1fa5	0.76	90%	0.0	0.13%
1fb1	3.81	10%	0.0	0.02%
1fc3	9.14	50%	0.0	0.02%
1ua1	0.76	10%	0.0	0.00%
1ua2	0.76	30%	0.0	0.20%
1ua3	0.76	50%	0.0	0.01%
1ua4	0.76	70%	0.0	0.03%
2f14	0.76	70%	1.0	0.00%
2fa1	0.76	10%	1.0	0.01%
2fa2	0.76	30%	1.0	0.08%
2fa3	0.76	50%	1.0	0.12%
2fa4	0.76	70%	1.0	0.10%
2fa5	0.76	90%	1.0	0.01%
2fb1	3.81	10%	1.0	0.03%
2fb2	3.81	30%	1.0	0.26%
2fb3	3.81	50%	1.0	0.61%
2fb4	3.81	70%	1.0	0.37%
2fb5	3.81	90%	1.0	0.23%
2fc2	9.14	30%	1.0	0.04%
2fc3	9.14	50%	1.0	0.11%
2fc4	9.14	70%	1.0	0.04%
2fc5	9.14	90%	1.0	0.03%
2fd3	15.24	50%	1.0	0.12%
2fd4	15.24	70%	1.0	0.07%
2fd5	15.24	90%	1.0	0.01%
2fe3	24.38	50%	1.0	0.06%
2fe5	24.38	90%	1.0	0.02%
2uc3	9.14	50%	1.0	0.01%
4fb4	3.81	70%	0.0	0.08%
4fb5	3.81	90%	0.0	0.11%
4fc4	9.14	70%	0.0	0.14%
4fc5	9.14	90%	0.0	0.00%
5cf2	38.10	30%	0.0	0.04%
5ef4	38.10	70%	0.0	0.13%
5fb1	3.81	10%	0.0	0.37%
5fb2	3.81	30%	0.0	0.26%
5fb3	3.81	50%	0.0	0.22%
5fb4	3.81	70%	0.0	0.54%
5fc1	9.14	10%	0.0	3.63%
5fc2	9.14	30%	0.0	1.84%
5fc3	9.14	50%	0.0	2.02%
5fc4	9.14	70%	0.0	0.96%
5fd1	15.24	10%	0.0	2.72%

5fd2	15.24	30%	0.0	2.13%
5fd3	15.24	50%	0.0	5.82%
5fd4	15.24	70%	0.0	4.23%
5fd5	15.24	90%	0.0	3.07%
5fe1	24.38	10%	0.0	0.91%
5fe2	24.38	30%	0.0	0.49%
5fe3	24.38	50%	0.0	1.90%
5fe4	24.38	70%	0.0	2.86%
5fe5	24.38	90%	0.0	1.38%
5ff1	38.10	10%	0.0	0.20%
5ff2	38.10	30%	0.0	0.00%
5ff3	38.10	50%	0.0	0.52%
5ff4	38.10	70%	0.0	1.18%
5ff5	38.10	90%	0.0	0.78%
5u21	3.81	10%	0.0	0.00%
5ub1	3.81	10%	0.0	0.29%
5ub2	3.81	30%	0.0	0.03%
5uc2	9.14	30%	0.0	0.16%
5ud3	15.24	50%	0.0	0.00%
6fa3	0.76	50%	0.0	0.00%
6fb1	3.81	10%	0.0	0.15%
6fb2	3.81	30%	0.0	0.23%
6fb3	3.81	50%	0.0	0.40%
6fb4	3.81	70%	0.0	0.38%
6fb5	3.81	90%	0.0	0.07%
6fc1	9.14	10%	0.0	0.22%
6fc2	9.14	30%	0.0	0.41%
6fc3	9.14	50%	0.0	0.63%
6fc4	9.14	70%	0.0	0.23%
6fc5	9.14	90%	0.0	0.05%
6fd2	15.24	30%	0.0	0.07%
6fd3	15.24	50%	0.0	0.11%
6fd4	15.24	70%	0.0	0.12%
6fd5	15.24	90%	0.0	0.16%
6fe2	24.38	30%	0.0	0.01%
6fe3	24.38	50%	0.0	0.01%
6fe4	24.38	70%	0.0	0.00%
6fe5	24.38	90%	0.0	0.34%
6ff3	38.10	50%	0.0	0.05%
6gb1	3.81	10%	0.0	0.14%
af	0.00	0%	0.0	40.50%
bf	0.00	0%	0.0	0.00%
cf	0.00	0%	0.0	1.54%
cu	0.00	0%	0.0	0.00%
df	0.00	0%	0.0	0.25%
du	0.00	0%	0.0	0.12%
ef	0.00	0%	0.0	0.35%
efb3	3.81	50%	0.0	0.03%
eub2	3.81	30%	0.0	0.00%
ffb2	3.81	30%	0.0	0.03%
ffb3	3.81	50%	0.0	0.01%
ffc2	9.14	30%	0.0	0.01%

ffc3	9.14	50%	0.0	0.04%
fuc2	9.14	30%	0.0	0.02%
gf14	0.76	70%	0.0	0.00%
gfa2	0.76	30%	0.0	0.17%
gfa3	0.76	50%	0.0	0.57%
gfa4	0.76	70%	0.0	1.46%
gfa5	0.76	90%	0.0	0.23%

Table A-6. Middle Fork John Day River vegetation code attributes and percent of model inputs.

Code	Height (m)	Density (0 - 1)	Overhang (m)	Percent of input
3000	0.00	0%	0.0	43.63%
4100	0.00	0%	0.0	4.22%
4200	0.00	0%	0.0	0.05%
11a3	0.18	50%	0.0	0.19%
11a4	0.18	70%	0.0	5.67%
11b1	0.91	10%	0.0	0.05%
11b2	0.91	30%	0.0	0.04%
11b3	0.91	50%	0.0	1.05%
11b4	0.91	70%	0.0	15.60%
11b5	0.91	90%	0.0	0.14%
11c1	2.29	10%	0.0	0.09%
11c2	2.29	30%	0.0	0.06%
11c3	2.29	50%	0.0	0.31%
11d2	3.81	30%	0.0	0.07%
15b2	0.91	30%	0.0	0.07%
15b3	0.91	50%	0.0	0.00%
15c1	2.29	10%	0.0	0.07%
15c2	2.29	30%	0.0	0.12%
15c3	2.29	50%	0.0	0.19%
15c4	2.29	70%	0.0	0.24%
15c5	2.29	90%	0.0	0.03%
15d1	3.81	10%	0.0	0.07%
15d2	3.81	30%	0.0	0.23%
15d3	3.81	50%	0.0	1.48%
15d4	3.81	70%	0.0	0.63%
15d5	3.81	90%	0.0	0.11%
15f1	7.62	10%	0.0	0.16%
15f2	7.62	30%	0.0	0.14%
15f3	7.62	50%	0.0	0.92%
15f4	7.62	70%	0.0	0.47%
15f5	7.62	90%	0.0	0.04%
15g1	10.67	10%	0.0	0.00%
15g2	10.67	30%	0.0	0.00%
15g3	10.67	50%	0.0	0.13%

15g4	10.67	70%	0.0	0.22%
15g5	10.67	90%	0.0	0.09%
15h1	13.72	10%	0.0	0.09%
15h2	13.72	30%	0.0	0.05%
15h3	13.72	50%	0.0	0.02%
15h4	13.72	70%	0.0	0.05%
15h5	13.72	90%	0.0	0.01%
15i2	16.76	30%	0.0	0.03%
15i3	16.76	50%	0.0	0.06%
15i4	16.76	70%	0.0	0.09%
15i5	16.76	90%	0.0	0.02%
15j2	19.81	30%	0.0	0.02%
15j3	19.81	50%	0.0	0.02%
15j4	19.81	70%	0.0	0.10%
15j5	19.81	90%	0.0	0.05%
15k3	24.38	50%	0.0	0.02%
15k4	24.38	70%	0.0	0.08%
15k5	24.38	90%	0.0	0.01%
15x1	5.33	10%	0.0	0.25%
15x2	5.33	30%	0.0	0.34%
15x3	5.33	50%	0.0	1.33%
15x4	5.33	70%	0.0	1.43%
15x5	5.33	90%	0.0	0.20%
18f1	7.62	10%	0.0	1.51%
18f2	7.62	30%	0.0	0.27%
18f3	7.62	50%	0.0	0.08%
18f4	7.62	70%	0.0	0.04%
18f5	7.62	90%	0.0	0.01%
18g1	10.67	10%	0.0	1.19%
18g2	10.67	30%	0.0	0.33%
18g3	10.67	50%	0.0	0.62%
18g4	10.67	70%	0.0	0.07%
18g5	10.67	90%	0.0	0.00%
18h1	13.72	10%	0.0	0.46%
18h2	13.72	30%	0.0	0.52%
18h3	13.72	50%	0.0	0.46%
18h4	13.72	70%	0.0	0.07%
18h5	13.72	90%	0.0	0.01%
18i1	16.76	10%	0.0	0.09%
18i2	16.76	30%	0.0	0.89%
18i3	16.76	50%	0.0	0.73%
18i4	16.76	70%	0.0	0.02%
18i5	16.76	90%	0.0	0.06%
18j1	19.81	10%	0.0	0.54%

18j2	19.81	30%	0.0	0.38%
18j3	19.81	50%	0.0	0.60%
18j4	19.81	70%	0.0	0.40%
18j5	19.81	90%	0.0	0.13%
18k1	24.38	10%	0.0	0.25%
18k2	24.38	30%	0.0	0.39%
18k3	24.38	50%	0.0	0.85%
18k4	24.38	70%	0.0	0.52%
18k5	24.38	90%	0.0	0.11%
18l1	30.48	10%	0.0	0.31%
18l2	30.48	30%	0.0	0.20%
18l3	30.48	50%	0.0	0.55%
18l4	30.48	70%	0.0	1.16%
18l5	30.48	90%	0.0	0.00%
18m2	36.58	30%	0.0	0.20%
18m3	36.58	50%	0.0	0.44%
18m4	36.58	70%	0.0	0.77%
18m5	36.58	90%	0.0	0.05%
18n2	44.20	30%	0.0	0.04%
18n4	44.20	70%	0.0	0.02%
18o4	53.34	70%	0.0	0.31%
18x1	5.33	10%	0.0	0.13%
18x2	5.33	30%	0.0	0.03%
18x3	5.33	50%	0.0	0.04%
18x4	5.33	70%	0.0	0.01%
19d2	3.81	30%	0.0	0.00%
19d3	3.81	50%	0.0	0.00%
19d4	3.81	70%	0.0	0.02%
19f1	7.62	10%	0.0	0.10%
19f2	7.62	30%	0.0	0.28%
19f3	7.62	50%	0.0	0.59%
19f4	7.62	70%	0.0	0.14%
19g2	10.67	30%	0.0	0.12%
19g3	10.67	50%	0.0	0.33%
19g4	10.67	70%	0.0	0.10%
19h2	13.72	30%	0.0	0.02%
19h3	13.72	50%	0.0	0.11%
19h4	13.72	70%	0.0	0.04%
19i2	16.76	30%	0.0	0.26%
19i3	16.76	50%	0.0	0.23%
19i4	16.76	70%	0.0	0.05%
19j1	19.81	10%	0.0	0.05%
19j3	19.81	50%	0.0	0.06%
19j4	19.81	70%	0.0	0.04%

19k3	24.38	50%	0.0	0.10%
19k4	24.38	70%	0.0	0.00%
19l4	30.48	70%	0.0	0.02%
19x1	5.33	10%	0.0	0.11%
19x2	5.33	30%	0.0	0.07%
19x3	5.33	50%	0.0	0.24%
19x4	5.33	70%	0.0	0.14%

Additional Derived Model Inputs

For many parameters, default values from the Heat Source model were used for the John Day models. These parameters include: wind function coefficients, sediment thermal conductivity, sediment thermal diffusivity, sediment/hyporheic zone thickness and porosity. Non-spatially or temporally varying coefficients used in the models are presented in **Table A-7**.

Table A-7. Model coefficients for non-spatially varying parameters

Parameter name (units)	Value
Wind Function, coefficient a	1.51×10^{-9}
Wind Function, coefficient b	1.60×10^{-9}
Sediment Thermal Conductivity (W/m/*C)	1.57
Sediment Thermal Diffusivity (cm^2/sec)	0.0064
Sediment / hyporheic zone thickness (m)	1.00
Porosity (%)	42.5

Heat Source provides additional parameters that can be activated by the user. For example, the deep alluvium layer was activated for all three models described in this Appendix. The routines to incorporate interactions between the deep alluvium, substrate characteristics and hyporheic exchange are described in the Heat Source manual (Boyd & Kasper 2003a). Other derived parameters varied spatially. These include: channel bottom width, channel angle z, Manning's n, and percent hyporheic exchange. The calculation of each of these parameters was not the same in each of the model corridors so the details of derivation are described in each of the model calibration sections. The use of different calculation methods was in part due to differences in modeling approaches by different modelers. Because there were no measured data for any of these parameters, these were often parameters that were manipulated during model calibration so that the model better reproduced measured instream temperatures.

The final type of derived data needed as model input is the flow and temperature associated with each tributary input. A general discussion of these inputs is described below, with further detail provided in each of the model calibration sections.

Hydrology Inputs

Both constant and time-variable mass transfers are incorporated into the model. Several methods were used to assess flow inputs (mass transfer) to John Day modeled streams, which are described in more detail in each of the following sections on model setup and calibration. For springs and seeps, TIR was the primary data source and the resultant flow computations are discussed below under 'Mass Balance Development.' For temporal arrays, methods include: (1) gage station data; (2) arrays from nearby gaged streams proportioned to (3) one-time flow measurements, (4) watershed area, (5) estimates based on OWRD Water Availability Basins (6) TIR-based mass balance values, and/or (7) data from other modeled streams. Typically, springs and seeps are considered constant and tributaries vary on daily and seasonal scales. The theory behind mass balance development is described below.

Mass Balance Development
TIR sampled stream temperature data were used to develop a flow mass balance, which were verified with ground level flow measurements, where available. Mass transfer areas (tributaries, springs, return flows, etc.) were identified for each stream. Several unmapped subsurface mass transfer areas were identified and the relative thermal and hydrologic impact to the stream system was quantified.

All stream temperature changes that result from mass transfer processes can be described mathematically using the following relationship:

$$T_{mix} = \frac{(Q_{up} \cdot T_{up}) + (Q_{in} \cdot T_{in})}{(Q_{mix})}$$

where,
Q_{up}: Stream flow rate upstream from mass transfer process
Q_{in}: Inflow volume or flow rate
Q_{mix}: Resulting volume or flow rate from mass transfer process ($Q_{up} + Q_{in}$)
T_{up}: Stream temperature directly upstream from mass transfer process
T_{in}: Temperature of inflow
T_{mix}: Resulting stream temperature from mass transfer process assuming complete mix

All water temperatures (i.e., T_{up}, T_{in} and T_{mix}) were provided by the TIR data. Provided that at least one instream flow rate is known the other flow rates can be calculated. This calculation provides a flow estimate at one point in time. The details of how this information was extrapolated to the rest of the model season is described in more detail under each model section.

Following are assumptions and limitations of the flow mass balance methodology:
Small mass transfer processes were not accounted for. Only mass transfer processes with measured flow rates or those that caused a quantifiable change in stream temperature in the receiving waters (identified by TIR data) could be included. *This assumption can lead to an under estimate of influent mass transfer processes.*
Ground level flow data is limited. Errors in the calculations of mass transfer can become cumulative and propagate in the methodology since validation can only be performed at sites with known flow rates. *These mass balance profiles should be considered estimates of a steady state flow condition*.
Water withdrawals were not directly quantified. Instead, water right data is obtained from the POD and WRIS OWRD databases. An assumption is made that these water rights are being used if water availability permits. *This assumption can lead to an over estimate of water withdrawals.*
Water withdrawals are assumed to occur only at OWRD mapped points of diversion sites. There may have been additional diversions occurring throughout the stream network. *This assumption can lead to an underestimate of water withdrawals and an under estimate of potential flow rates.*

Temperature Inputs

Where continuous temperature data sets were not available during the model year, temperatures of tributary inflows were estimated. Descriptions of the methods used varied by model and are provided in the following individual sections.

3. STREAM TEMPERATURE MODEL SETUP AND CALIBRATION

3.1 Overview

Heat Source version 8.0 was used to model stream temperatures in the John Day River Basin. For detailed information regarding Heat Source and the methodologies used, refer to "Analytical Methods for Dynamic Open Channel Heat and Mass Transfer: Methodology for Heat Source Model Version 7.0" (Boyd & Kasper, 2003a). Specifics for each of the modeled streams follow.

Spatial and Temporal Scale

The length of the defined finite difference and data input sampling rate was 50 meters. Prediction time steps and spatial scale were limited by stability considerations for the finite difference solution method. Simulations were performed for a total of 722.85 stream kilometers in the John Day River Basin (**Table A-8**).

Table A-8. Stream Temperature Simulation Periods and Extents

River/Stream	Simulation Period	Time Step (minutes)	Spatial Resolution (meters)	Model spin up (days)	Simulation Extent
Middle Fork John Day River	May 01 – Oct 31, 2002	0.5	200	5	112.95
North Fork John Day River	June 15 – Sept 01, 2002	0.5	100	10	179.2
John Day River	July 01 - Sept 01, 2004	1.0	1000	6	437.0
					Total Simulation Extent: 722.85 stream kilometers

Simulation Accuracy

Error statistics were calculated for each calibrated model. Below are the equations used for each type of error statistic.

Mean Error: $$ME = \frac{1}{n}\sum\left(X_{sim} - X_{obs}\right)$$

Mean Absolute Error: $$MAE = \frac{1}{n}\sum\left|X_{sim} - X_{obs}\right|$$

Root Mean Square Error: $$RMSE = \sqrt{\frac{1}{n}\sum\left(X_{sim} - X_{obs}\right)^2}$$

Nash-Sutcliffe efficiency coefficient: $$E = 1 - \frac{\sum\left(X_{sim} - X_{obs}\right)^2}{\sum\left(X_{sim} - \overline{X_{obs}}\right)^2}$$

where,

X_{sim} = the simulated temperature;

X_{obs} = the observed or measured temperature;

$\overline{X_{obs}}$ = the mean of the observed or measured temperatures;

n = the sample size.

Error statistics were calculated for both the spatial (TIR) and temporal (hourly instream measurements) temperatures (see specific stream discussions below).

Effective Shade

In addition to modeling stream temperatures, Heat Source was also used to model effective shade. The term 'shade' has been used in several contexts, including its components such as shade angle or shade density. **For purposes of this TMDL, effective shade is defined as the percent reduction of potential daily solar radiation load delivered to the water surface.** Heat Source simulates effective shade using factors that influence the stream surface, including the following:

Season/Time: Date/Time (Solar Altitude, Solar Azimuth)
Stream Morphology: Aspect, Channel Width, Incision
Geographic Position: Latitude, Longitude, Stream Elevation, Surrounding Topography
Vegetation: Vegetation Height, Width, Density

For detailed information, refer to "Analytical Methods for Dynamic Open Channel Heat and Mass Transfer: Methodology for Heat Source Model Version 7.0" (Boyd & Kasper, 2003a).

Effective shade was simulated along the stream at intervals determined by the model's distance step. Simulation periods included, at a minimum July and August. Effective shade simulations were performed for a total of 722.85 stream kilometers in the John Day River Basin (see **Chapter 2**: *The John Day River Basin Temperature TMDL*).

Effective shade simulation validation was conducted by comparing simulated results with ground level measured shade values. These data were compared to the predicted shade simulated by the model.

Total Daily Solar Heat Load Analysis

The total daily solar heat load is the cumulative solar heat received by a stream over one day during the critical period (i.e., July/August period). For the purposes of this analytical effort, the total daily solar heat load is the sum of the products of the daily solar heat flux and surface area of exposure for each stream reach (i.e., for each stream data node every 50 meters).

$$H_{solar} = \sum \left(\Phi_{solar} \cdot A_y \right) = \sum \left(\Phi_{solar} \cdot W_{wetted} \cdot dx \right)$$

Background levels of solar heat estimate the portion of the total daily solar heat load that occurs when anthropogenic nonpoint sources of heat are minimized. The total daily solar load is calculated for both the current condition (H_{solar}) and the potential condition ($H_{solar}^{Background}$). The anthropogenic nonpoint source total daily solar load is the difference between the total daily solar load and the background total daily solar load.

$$H_{solar}^{NPS} = H_{solar} - H_{solar}^{Background}$$

where,

A_y:	Stream surface area unique to each stream segment
Dx:	Stream segment length and distance step in the methodology
Φ_{solar}:	Solar heat flux for unique to each stream segment
H_{solar}:	Total daily solar heat load delivered to the stream
H_{solar}^{NPS}:	Portion of the total daily solar heat load delivered to the stream that originates from anthropogenic nonpoint sources of pollution
$H_{solar}^{Background}$:	Portion of the total daily solar heat load delivered to the stream that originates from background sources of pollution that are not affected by human activities
W_{wetted}:	Wetted width unique to each stream segment

The John Day River Basin Temperature TMDL displays the solar heat load contributions for each stream where temperature/hydrology was simulated. Longer and wider streams have the most solar heat load. In any case, anthropogenic nonpoint sources account for a fraction of the heat load in most streams simulated (i.e., much of the existing heat load is naturally occurring).

3.2 John Day River

The John Day River is a tributary to the Columbia River. The John Day River Basin comprises an area of 5,076,758 acres and is referenced by the 3rd field Hydrologic Unit Code (HUC) 170702. Instream temperature was simulated for 437.0 km of the John Day River from the Tumwater Falls to the Trout Farm Campground. The following documents the calibration methods and decisions and ultimately describes the model used in the John Day River TMDL.

Overview

Stream Name: John Day River
Model: Heat Source version 8.0.4
Beginning date: 7/1/04
Ending date: 9/1/2004
Time step: 1 minute
Distance step: 1000 m
Transverse sample rate: 23 m
"Deep alluvium" option on at 12 °C
Initial flush condition: 6 days
Extent: Tumwater Falls to Trout Farm Campground (437.0 km) (**Figure A-17**).

Figure A-17. Extent of the John Day River temperature model.

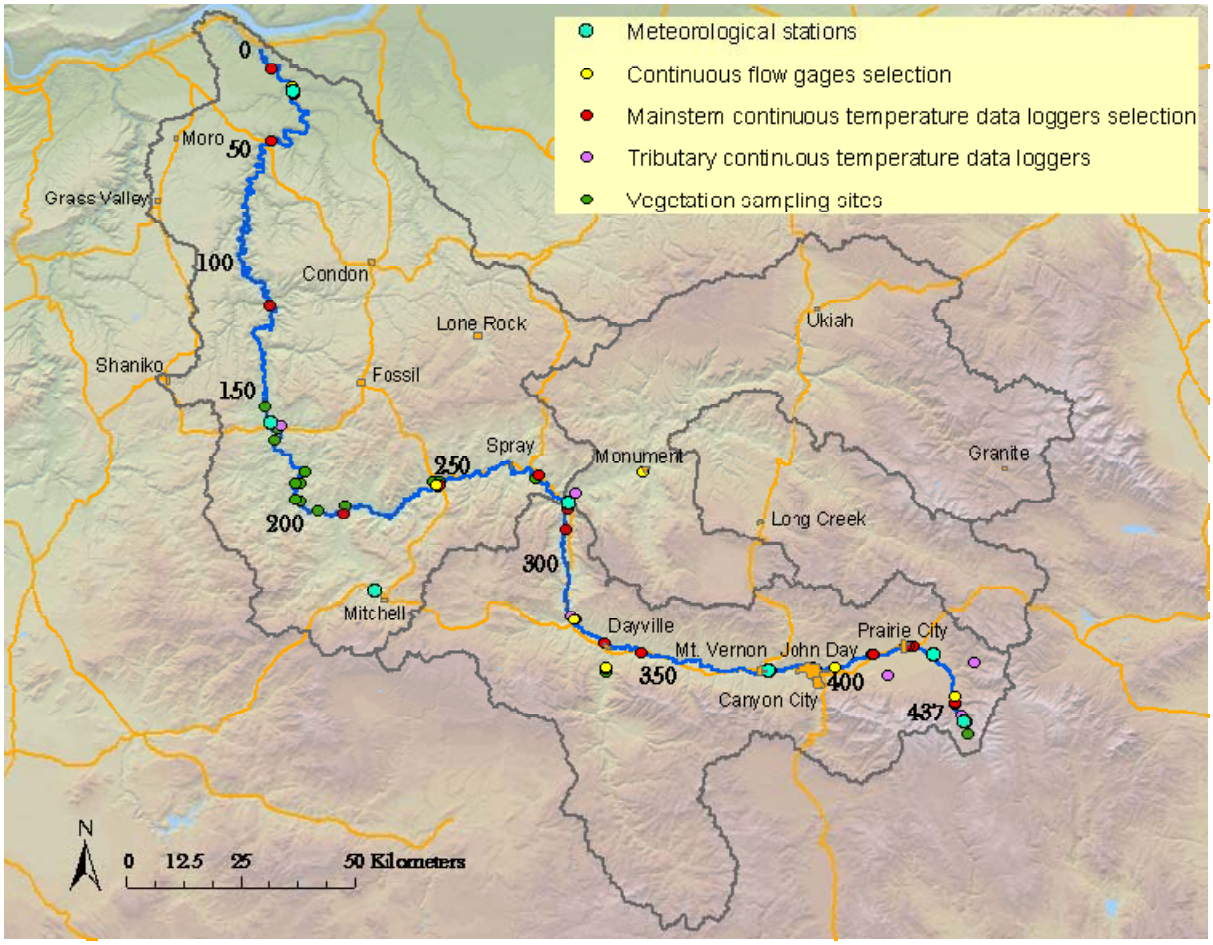

Reach Properties

Table A-9 identifies the sources of spatial GIS data used in the model. See **Section 2.3** for methodology. The elevation profile and reach gradient were determined using DEM files (**Figure A-18**). The reach gradient was averaged over the neighboring 7 reaches because overly steep gradients resulted from the coarse scale of the DEM leading to numeric instability in the hydraulic routines of the model. The bankfull channel widths were measured from DOQ images and verified by field measurements (**Figure A-19**). Additional aerial images were used as supplemental sources of information for both channel morphology and riparian vegetation mapping.

The bottom width and channel angle z values in the model were calculated based on data collected by DEQ in 2004 at 18 surveyed transects. Visually fitted trapezoids were developed for each transect from the field data, such that the trapezoid dimensions maintained the integrity of the channel cross-sectional area as well as possible. The trapezoid dimensions were compared to field data to determine the best correlations. Measured bankfull channel width and trapezoid bottom width had an excellent correlation (R^2=0.99) (**Figure A-20**). This relationship was used to determine bottom width model inputs using the bankfull channel width measured from the DOQs using TTools (**Figure A-21**). The relationship between measured bankfull width and trapezoid channel depth relationship (R^2=0.49) was used to calculate bottom depth using the bankfull channel width measured from the DOQs (**Figure A-22**). Channel angle z was then calculated for each TTools node using the relationship depicted in **Figure A-23** and represented by **Equation A-1**. **Figure A-24** shows the channel angle z values used after changes that were made to the channel model inputs during calibration. As the channel morphology changed, the temperature profile responded and better matched observed temperatures. In the John Day River mainstem model, the bottom widths were decreased from KM 320-416 and increased from KM 416-431. Channel angle z values were decreased from KM 314-419 and KM 434-436 and increased from KM 419-434.

Topographic shade angles used in the model are presented in **Figure A-25**. The average of the riparian feature heights and densities sampled at each node is presented in **Figure A-26** and **Figure A-27**. With a wide river, such as the John Day, the average height and densities include many non-vegetation features like water and gravel bars. Therefore, the average heights and densities do not necessary represent streamside vegetation. Using these inputs, the John Day River model's ability to simulate shade is shown in **Figure A-28**.

Manning's n and percent hyporheic exchange values were iteratively altered during calibration so that the model temperatures approximately reproduced measured temperatures (**Figure A-29**). Throughout the mainstem model, the percent of hyporheic exchange was determined by the calibration process. There were no measurements taken of percent hyporheic exchange downstream of the confluence with the North Fork John Day River. There is anecdotal evidence of active subsurface water flow from tributaries and throughout the river substrate, which may lead to moderate hyporheic exchanged rates. Model simulations showed that high Manning's n values were inconsistent with the amount of time it took for the bulk of the water in the North Fork to reach the John Day River gage at MacDonald Ferry, apparent in the storm hydrographs. The most downstream 10km appears to be influenced by pooling from the Columbia River (Watershed Sciences, 2004), represented by a relatively high Manning's n value. The Manning's n and percent hyporheic exchange values, with accompanying model parameters, represent the best resulting scenarios, with the available data.

Table A-9. Spatial Data and Application

Spatial Data	Data Source	Application
10-Meter Digital Elevation Models (DEM)	10-m DEM files provided by OGDC	Measure Stream Elevation and Gradient Measure Topographic Shade Angles
Aerial Imagery	Lower 350 km: 1-m compressed color Digital Orthophoto Quads - National Agriculture Imagery Program (NAIP) Upper 90 km: 0.5-m uncompressed color NAIP Additional sources: 3rd order geo-rectified images (USBR, 2003) 1-foot Near Infrared Imagery (NIR) –lower 240 km (Bureau of Land Management)	Map Vegetation Map Channel Morphology Measure Active Channel Widths Map Roads, Development, Structures
Thermal Infrared Radiometry (TIR) Stream Temperature Data	Watershed Sciences, LLC, 2004	Measure Surface Temperatures Develop Longitudinal Temperature Profiles Identify Subsurface Hydrology, Groundwater Inflow, Springs
LiDAR vegetation data	Watershed Sciences, LLC, 2006 (~9 km reach above Prairie City)	Verify vegetation heights

Figure A-18. Model setup channel elevation and gradient

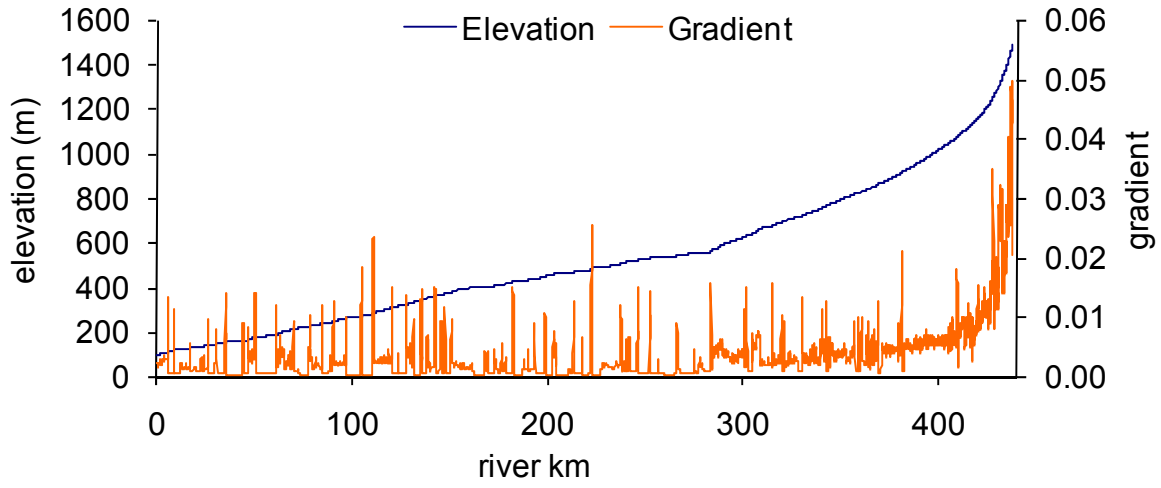

Figure A-19. TTools measurements for bankfull width used to calculate bottom width and channel angle z.

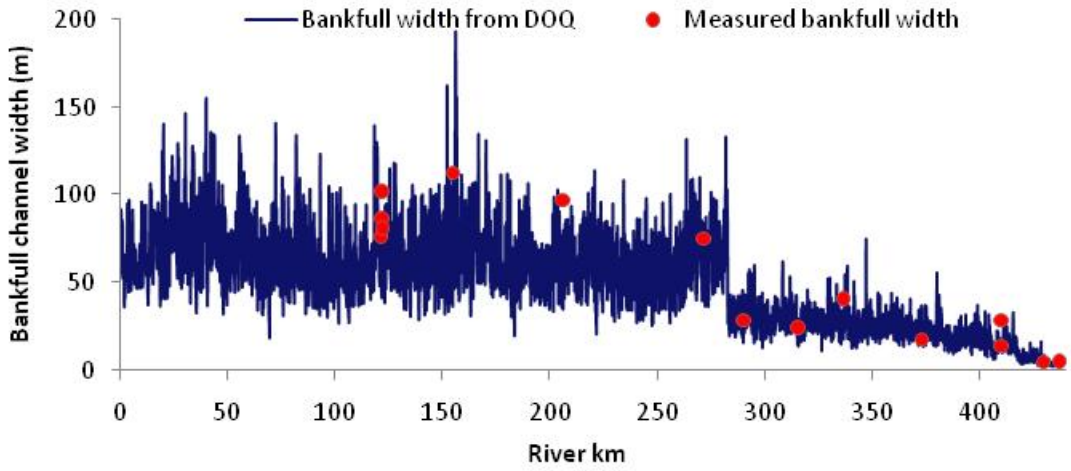

Figure A-20. Calculation of bottom width for model setup

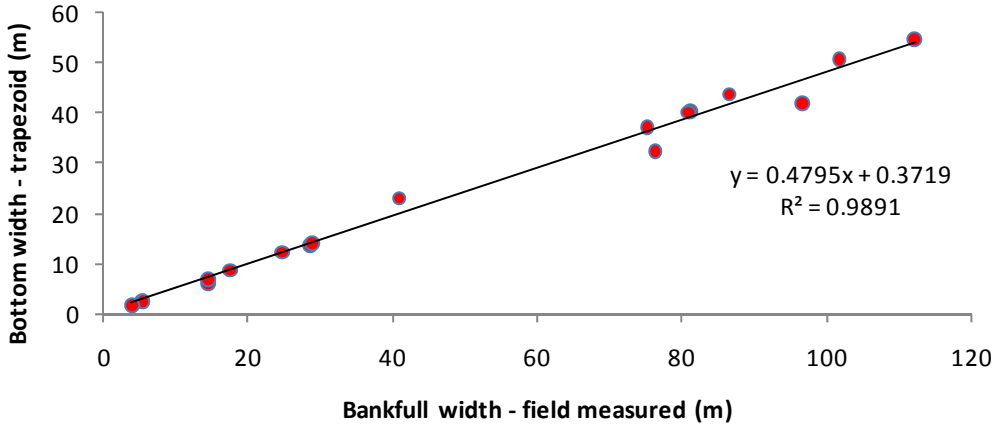

Figure A-21. Model setup for bottom width

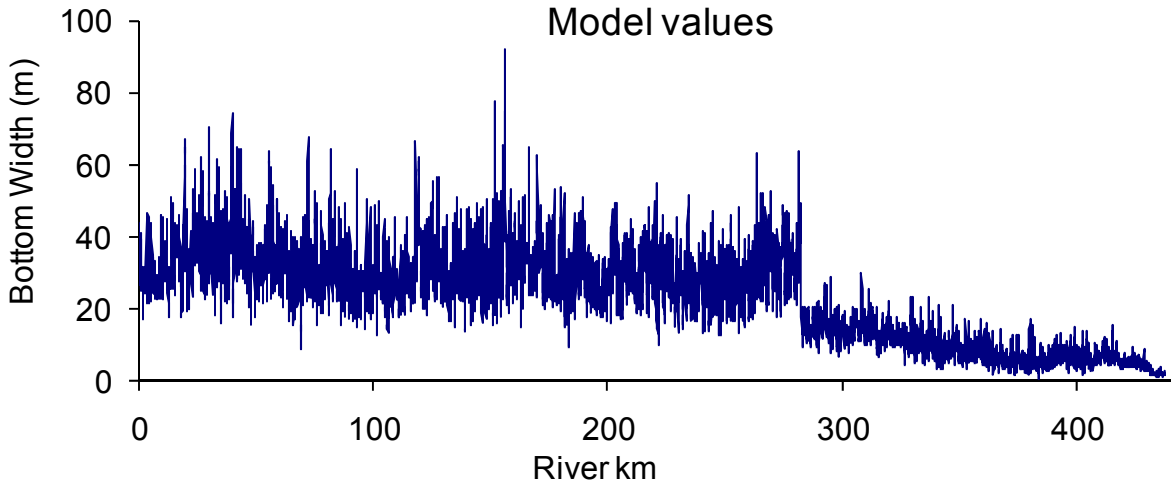

Figure A-22. Calculation of channel depth for model setup

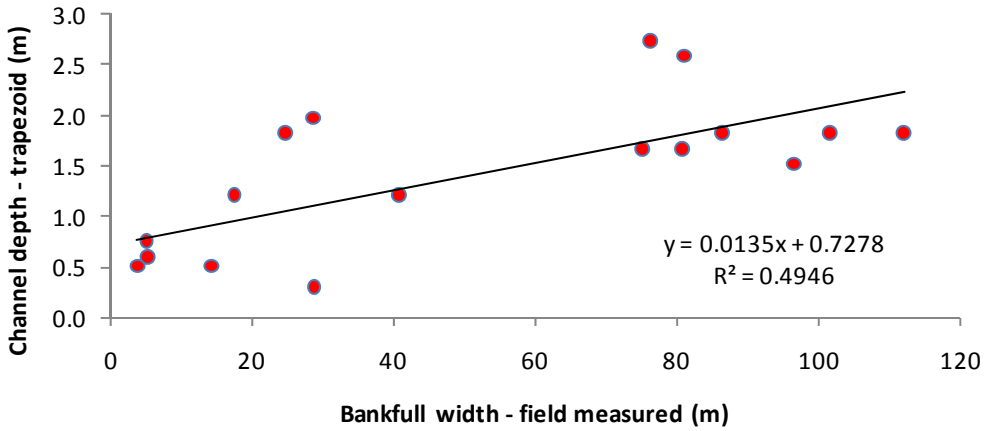

Figure A-23. Calculation of channel angle z for model setup

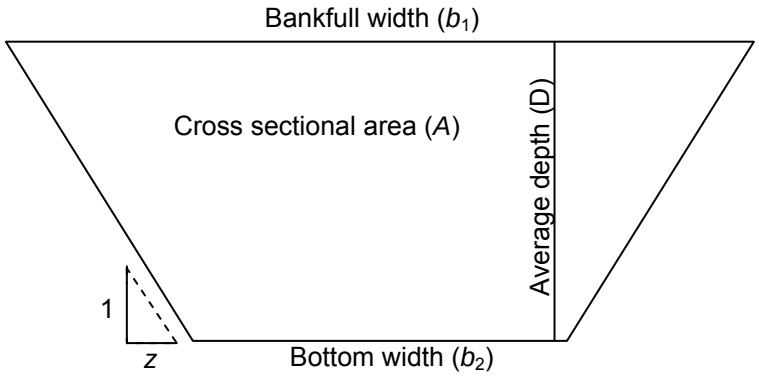

Equation A-1. $$z = \frac{b_1 - b_2}{2D}$$

Figure A-24. Model setup for channel angle z

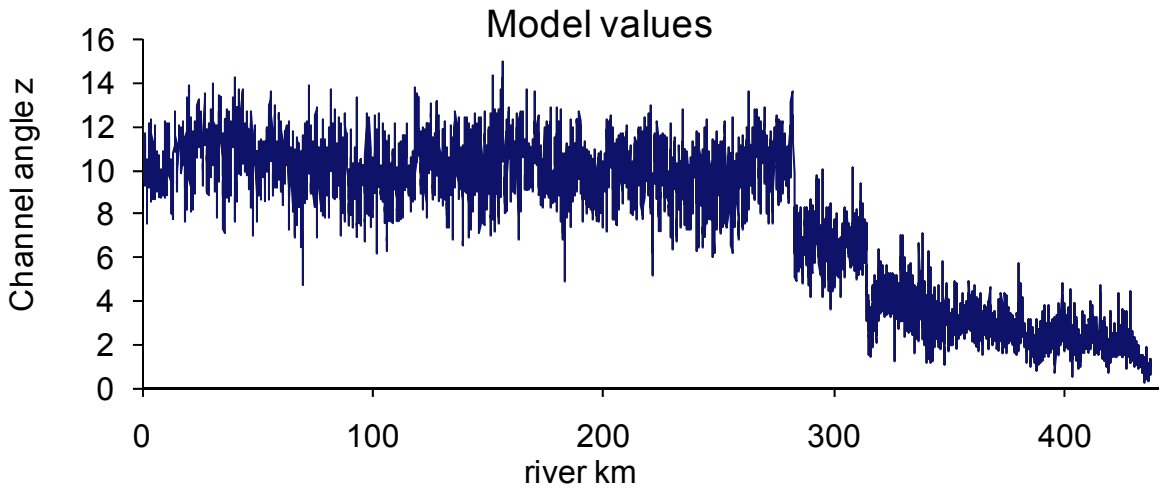

Figure A-25. Model setup for topographic shade angle

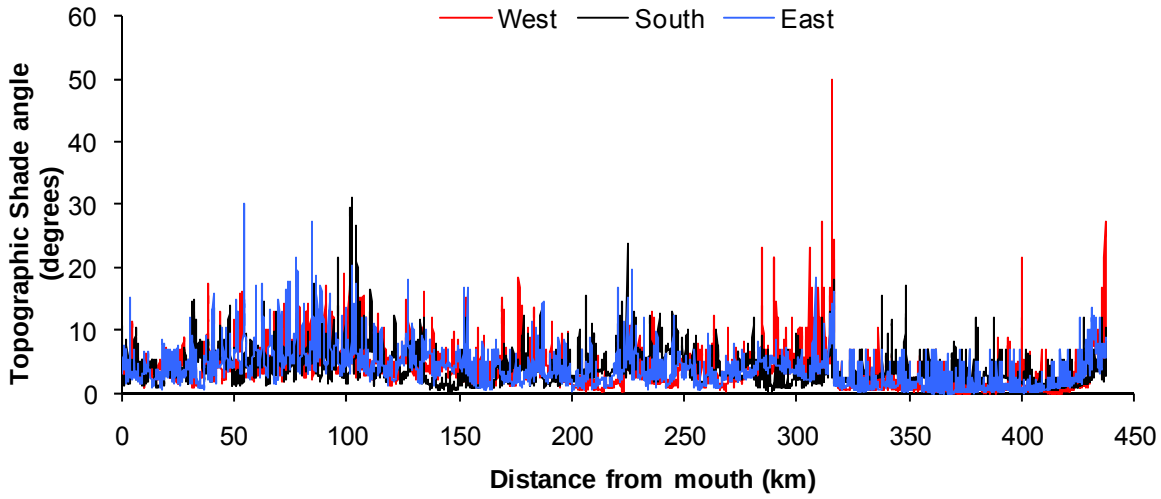

Figure A-26. Model setup for average height of streamside vegetation

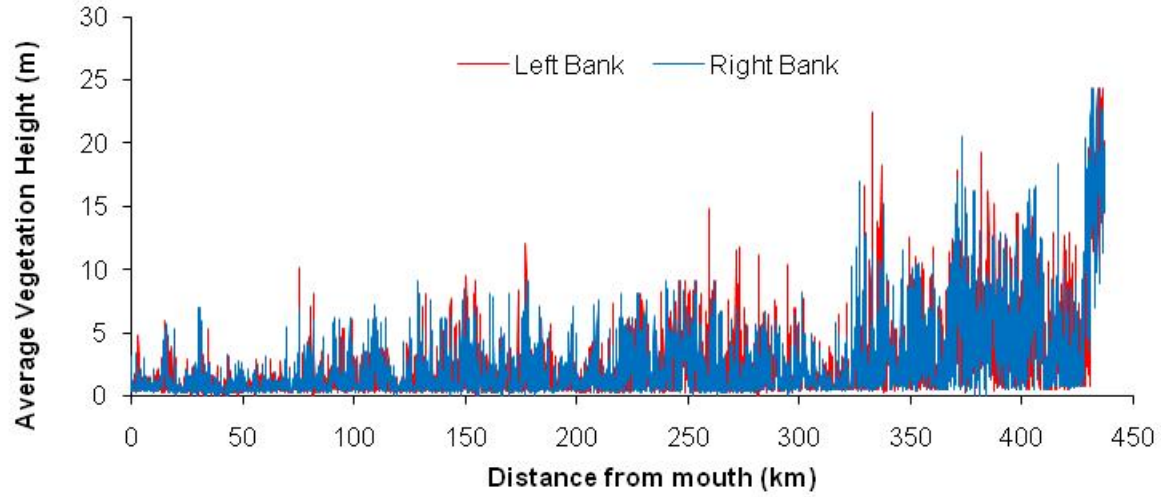

Figure A-27. Model setup for average density of streamside vegetation.

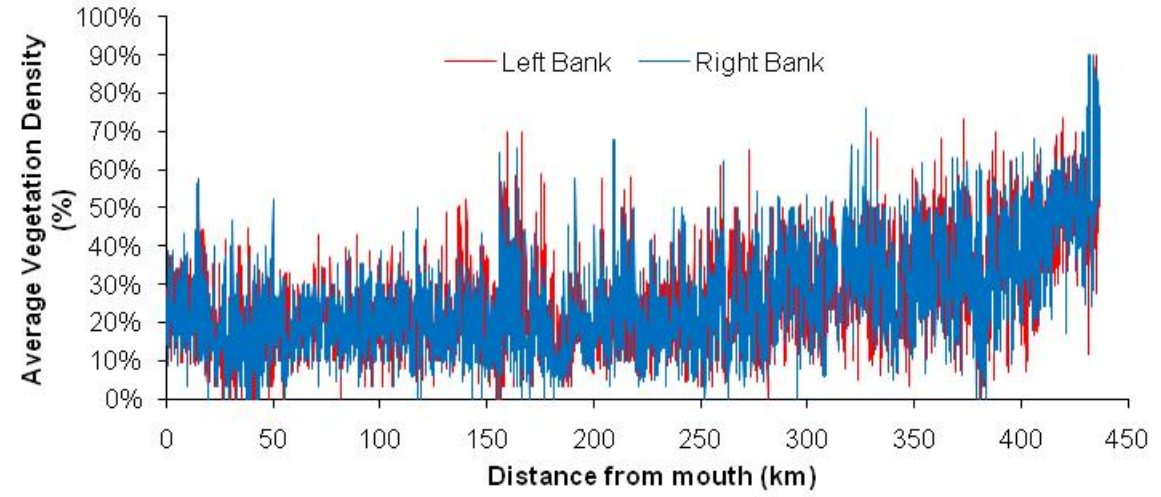

Figure A-28. Predicted shade on John Day River.

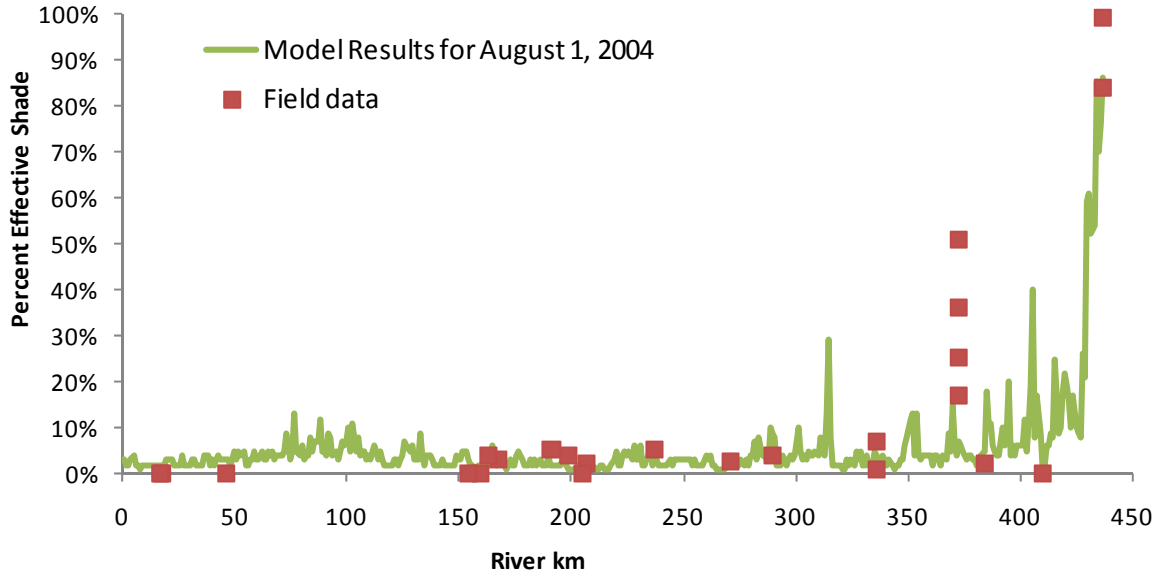

Figure A-29. Model setup for Manning's n and percent hyporheic exchange per 50 meter reach.

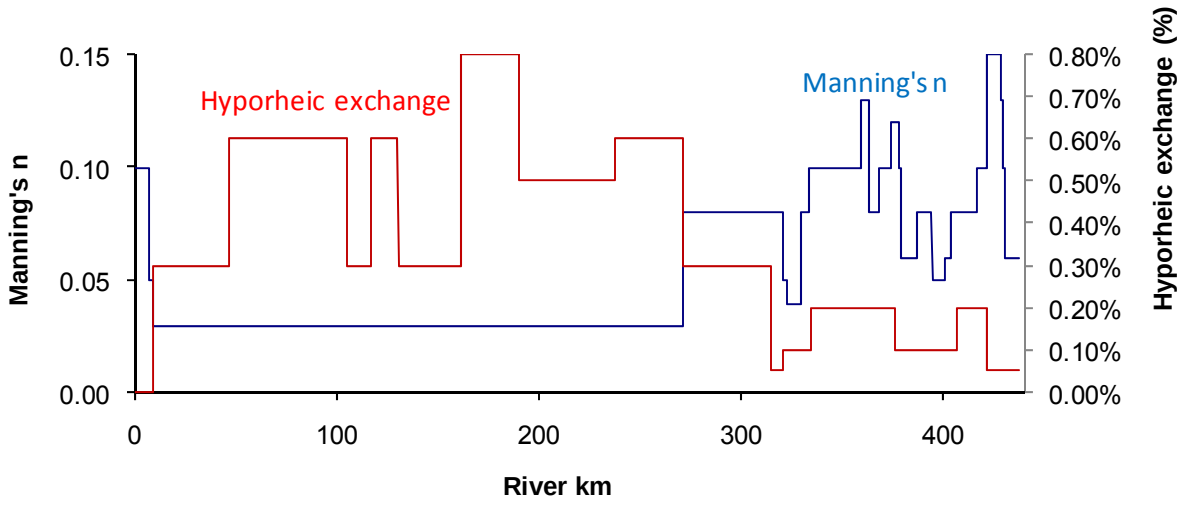

Meteorology

Meteorological data were collected at different stations in and near the basin (**Table A-10**, **Figure A-8**). The meteorological inputs varied by stream kilometer based on proximity to the weather station and are presented in **Table A-11**. Cloudiness was determined by calculating the deviation of measured solar radiation from theoretical maximum solar radiation on a rolling 24 hour average. Air temperature data were adjusted from the closest station to the continuous data node based on elevation and the dry adiabatic lapse rate of 9.8ºC/km, according to the following equation: adjustment for dry adiabatic lapse rate = $9.8*(Elev_{metstation} - Elev_{contnode})/1000$. Relative humidity from the nearest weather station was used without any modifications. Wind speed was used from the nearest weather station, although a multiplicative wind sheltering coefficient was applied to the wind speed during calibration. The meteorological observations are presented in **Figure A-30, a-f**.

Table A-10. Meteorological data sources

Site	Source	Elevation (m)	Meteorological Parameters
Trout Farm	DEQ	1484	Air temperature (measured data 7/22-8/31; adiabatic adjustment of -3.33 relative to Prairie City station prior to 7/22)
Prairie City	Agrimet	1144	Cloudiness, wind speed, relative humidity, air temperature
Clyde-Holliday	DEQ	873	Air temperature (measured data 7/22-8/31; adiabatic adjustment of +2.7 relative to Prairie City station prior to 7/22)
Mitchell	DRI-RAWS	778	Wind speed, relative humidity, air temperature
Kimberly	SWCD	561	Air temperature
Clarno	DEQ	393	Air temperature (measured data 7/12-8/31; adiabatic adjustment of +3.8 relative to Mitchell station prior to 7/12). It should be noted that the maximum temperature that could be read by this thermistor was 38.8ºC. There are several instances where air temperatures were probably above 38.8ºC.
McDonald Ferry	DEQ	124	Air temperature (measured data 7/8-8/31; adiabatic adjustment of +4.9 relative to Goldendale station prior to 7/8)
Goldendale	Agrimet	626	Cloudiness, wind speed, relative humidity, air temperature

Table A-11. Data inputs by river km

Range (river km)	Cloudiness	Air Temperature	Adiabatic Adjustment	Relative Humidity	Wind Speed	Wind sheltering coefficient
437.0-431.4	Prairie City	Trout Farm	1.5	Prairie City	Prairie City	0
431.4-421.1	Prairie City	Trout Farm	1.6	Prairie City	Prairie City	0
421.1-410.4	Prairie City	Prairie City	0.6	Prairie City	Prairie City	0
410.4-409.3	Prairie City	Prairie City	0.7	Prairie City	Prairie City	0
409.3-404.6	Prairie City	Prairie City	0.7	Prairie City	Prairie City	0
404.6-394.9	Prairie City	Prairie City	1.2	Prairie City	Prairie City	0
394.9-386.8	Prairie City	Prairie City	1.9	Prairie City	Prairie City	0.1
386.8-378.6	Prairie City	Prairie City	2.1	Prairie City	Prairie City	0.9
378.6-354.9	Prairie City	Clyde Holliday	0.0	Prairie City	Prairie City	0.9
354.9-331.0	Prairie City	Clyde Holliday	1.3	Prairie City	Prairie City	0.8
331.0-320.3	Prairie City	Clyde Holliday	1.6	Prairie City	Prairie City	0.8
320.3-302.6	Prairie City	Kimberly	-1.1	Mitchell	Mitchell	0.1
302.6-287.0	Prairie City	Kimberly	-0.3	Mitchell	Mitchell	0.1
287.0-277.7	Prairie City	Kimberly	0.0	Mitchell	Mitchell	0.1
277.7-254.6	Prairie City	Kimberly	0.2	Mitchell	Mitchell	0.1
254.6-221.8	Prairie City	Kimberly	0.6	Mitchell	Mitchell	0.1
221.8-182.9	Prairie City	Clarno	-0.7	Mitchell	Mitchell	0.1
182.9-140.0	Prairie City	Clarno	0.0	Mitchell	Mitchell	0.1
140.0-83.4	Prairie City	Clarno	0.9	Mitchell	Mitchell	0.1
83.4-27.0	Prairie City	McDonald Ferry	-0.3	Goldendale	Goldendale	0.5
27.0-0	Prairie City	McDonald Ferry	0.1	Goldendale	Goldendale	1.0

Figure A-30, a-f. Meteorology inputs for model setup

Figure A-30, a

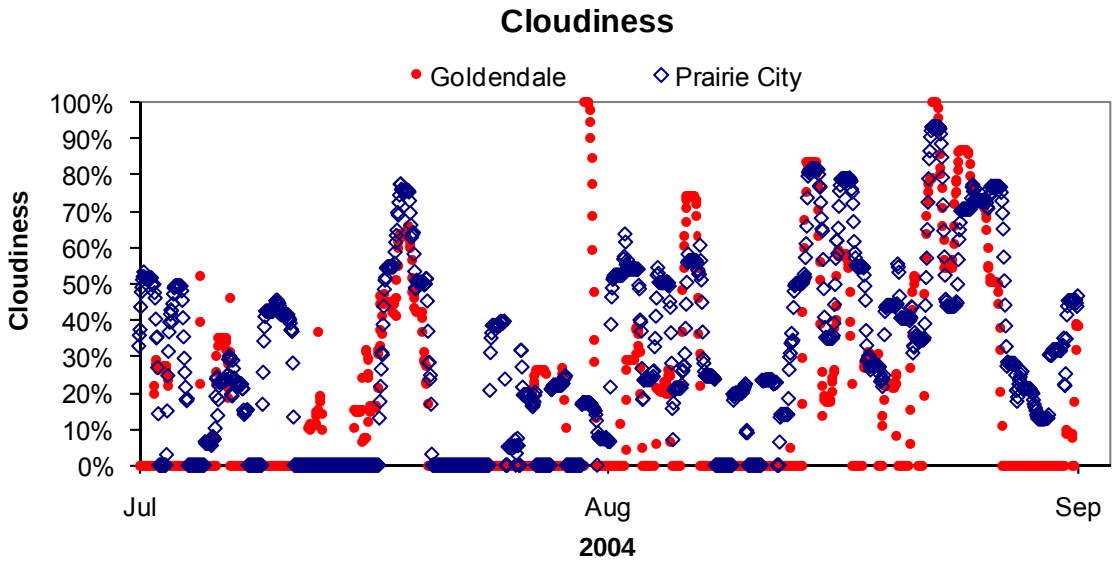

Figure A-30, b

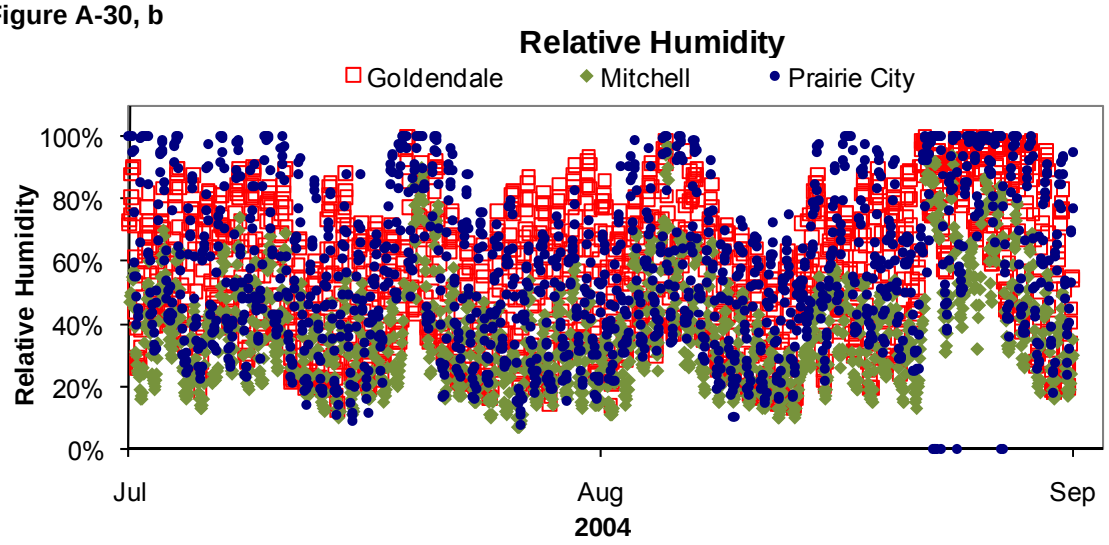

Figure A-30, c

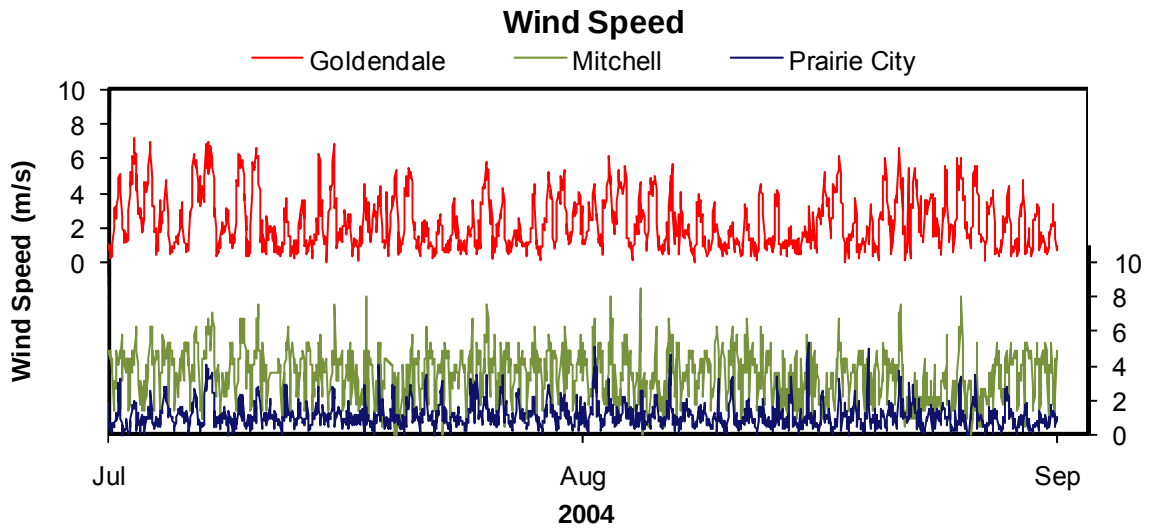

Figure A-30, d

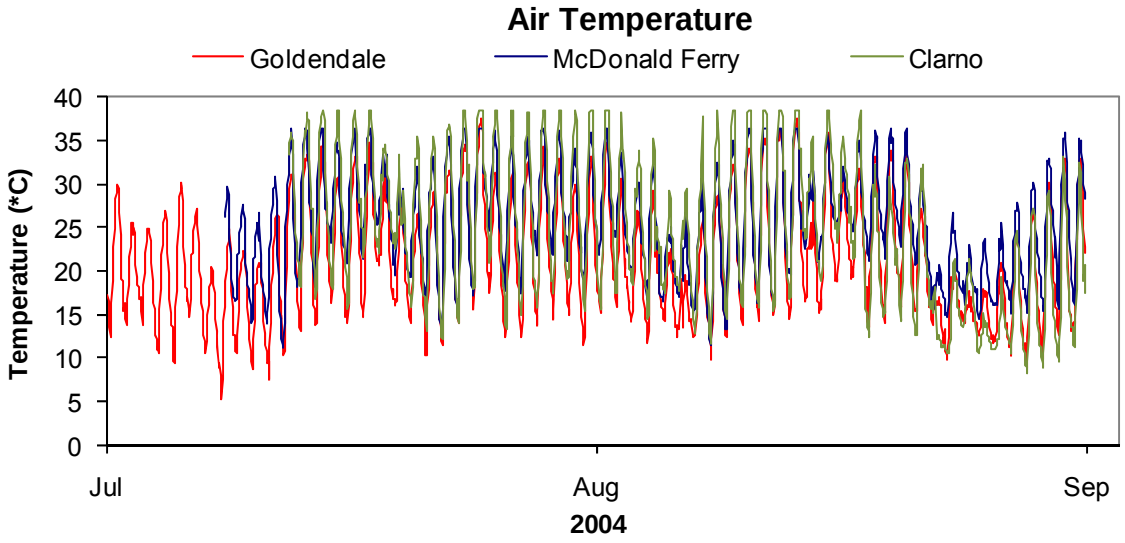

Figure A-30, e

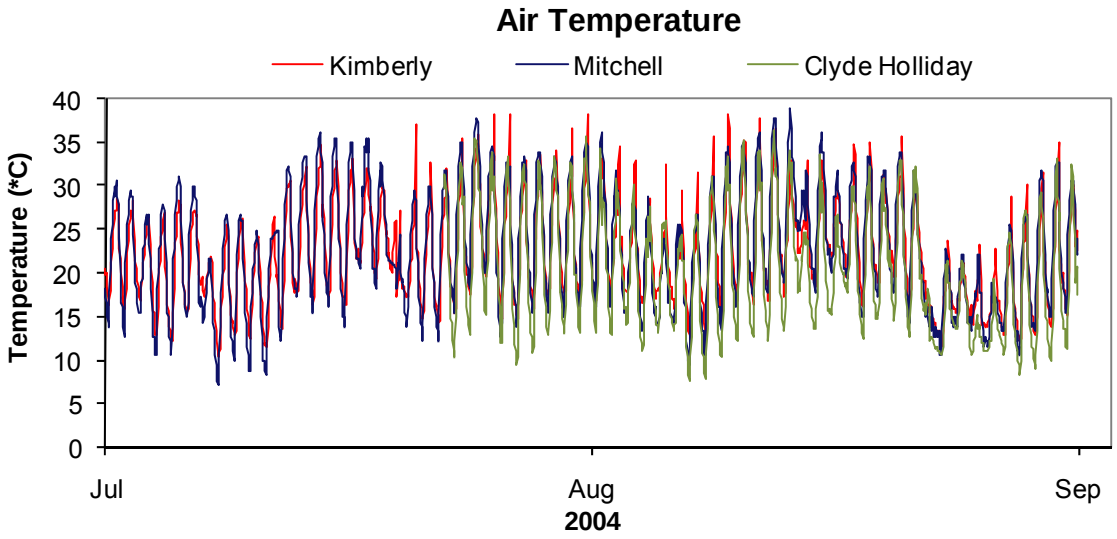

Figure A-30, f

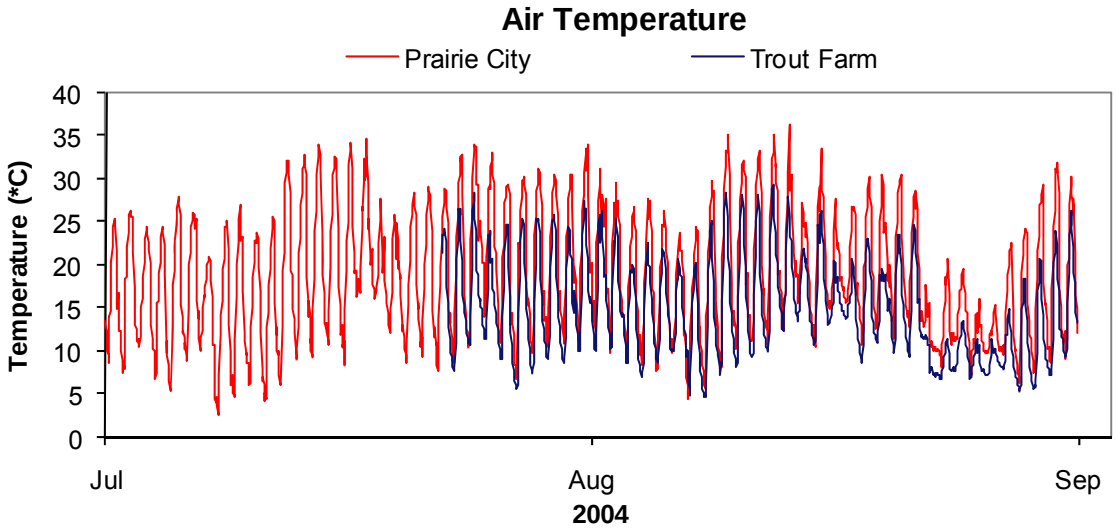

Flow and Temperature of Boundary Condition

The most upstream point of the John Day River model was at the Trout Farm Campground at river km 437.0. The volumetric flow at that point was calculated based on the continuous flow gage on the river near Blue Mountain Hot Springs. One flow sample was collected at Trout Farm on 8/19/04. This flow measurement was proportioned to the flow measured at Blue Mountain Hot Springs and that proportion used to calculate flows for the entire model period (**Figure A-31**). The relative flows at the boundary condition and in the upper tributaries were adjusted during model calibration. This is described further under the "Flow Inputs" section below.

The temperature inputs at the model boundary were measured by a continuous monitoring logger from 7/14/04 18:00 through the end of the model period (**Figure A-32**). For the period prior to July 14, boundary condition temperatures were calculated by proportioning temperatures to a continuous

monitoring logger at the mouth of nearby Deardorff Creek. Data was available at both sites for the period July 15-18. The ratio of temperatures at Trout Farm to temperatures on Deardorff Creek was determined for each hour during these four days. An average ratio was determined for each hour of the day and applied to the period July 1- 0:00 – June 14 17:00 when measured data were not available at Trout Farm.

Figure A-31. Volumetric flow of the boundary condition of the John Day River model

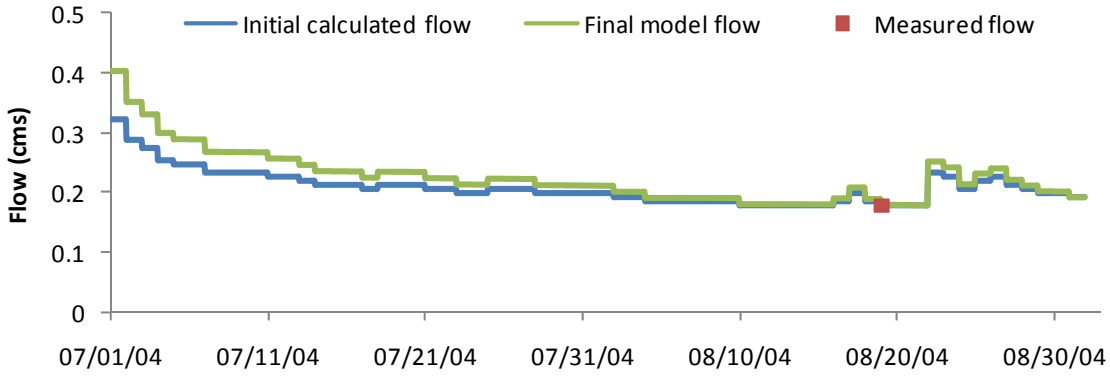

Figure A-32. Temperature of headwaters boundary condition of the John Day River model

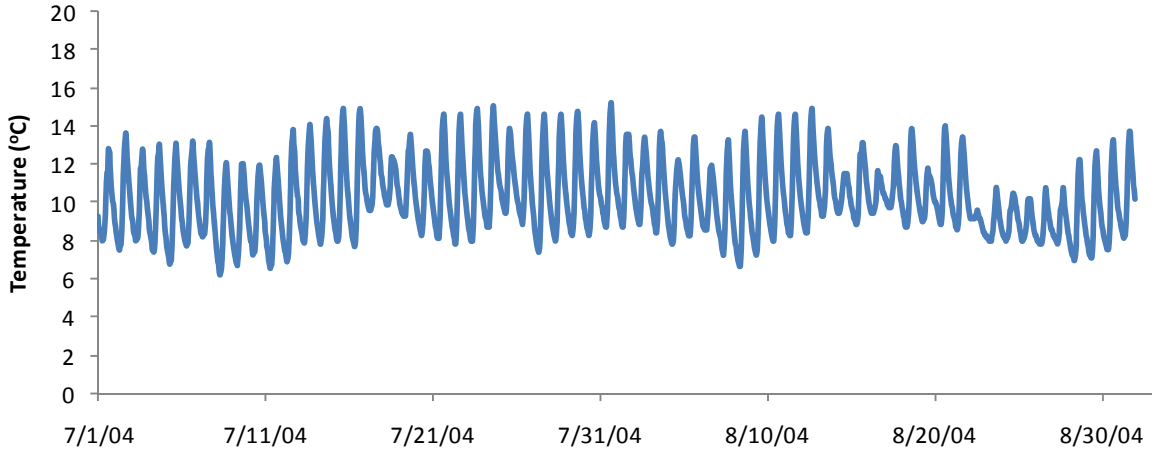

Flow Inputs

A total of forty-three tributaries, springs, return flows and diversions were represented as water inputs/outputs to the John Day River model (**Table A-12**). This is quite a simplification of the actual inputs and outputs to the system, as there are hundreds of inflows and diversions, hardly any of which have measured data. There were only three continuous flow data sets available for tributaries to the John Day River during the model period: South Fork John Day River, North Fork John Day River, and lower Pine Creek. There were no flow or diversion data available for any of the other tributaries, return flows, springs or diversions.

Calculation of Tributary inflows. Measured data from the South Fork John Day River, Pine Creek and the John Day River at Blue Mt. Hot Springs were used to proportion flow data for the rest of the tributary inflows. **Figure A-33, a-c** shows measured flows of these sites along with the North Fork John Day River. Most tributaries had monthly estimates of stream flow from the OWRD Water Availability Basins (WABs). These monthly estimates represent average (50% exceedance interval) conditions. Monthly flow estimates were calculated from measured daily data for the gaged sites in 2004. The monthly WAB data

and gaged data were proportioned by month, with one value per month. Applying this value to the first of each month, the proportions were linearly interpolated between these dates so that a separate proportion value was determined for each day. These daily proportions were then used to calculate a flow for each day at the un-gaged site.

Flows in several of the upper river tributaries were modified during calibration. Modifications were made in order to: (1) better match modeled temperatures to measured temperatures; (2) better match modeled flows to measured flows or to flows estimated by the Water Master; or (3) to provide better hydraulic stability in the model. The two springs located in the upper 10 kilometers of the river were added for the same reasons. During calibration, the following tributary flows were decreased: Call Creek, Roberts Creek, Rail Creek, Deardorff Creek, and Reynolds Creek. Tributary inflows were increased in Strawberry Creek and Slyfe Creek. As needed, flows were either added to or subtracted from a nearby calibration node (see below) to ensure the hydraulics remained calibrated.

Calculation of spring and accretion inflows. There were numerous springs/seeps with a distinguishable temperature signal detected during the TIR flight (Watershed Sciences, 2004). While the majority of these did not appear to impact John Day River temperatures (and most were only 1-2^{o}C cooler than the river), a subset of the coldest springs (six) were added as inflows to the model, in part to help represent return flows to the river. Flow was based on mass balance calculations using TIR data inputs and instream flows. The flow from most of the springs was not enough to cause a detectable change in the mainstem river temperature. In this case, the spring flow rates were estimated as half the amount that would cause a detectable change in river temperature. For one of the springs, flows were increased during calibration in order to better match model temperatures to measured temperatures.

People familiar with the upper John Day River also suspect the presence of springs in the headwater area of the river and between the South Fork John Day River and Picture Gorge (D. Butcher, 2009, pers. comm.). These groundwater inputs are likely diffuse enough that they did not register in the TIR. Adding additional groundwater inputs in these two reaches also helped with model calibration. Groundwater was added in two ways: (1) two additional springs were added to upper 10 km of the river and represented as mass transfer nodes in the model; and (2) accretion flows were added to the model in both the upper river and in the area between South Fork John Day River and Picture Gorge (**Figure A-34**). A small volume of the accretion flows in the upper 10 km were attributed to the seepage of warm water in the vicinity of Blue Mt. Hot Springs. To maintain calibration of the model hydrology and because there were no diversions located in this upper reach of the river, continuous withdrawals were also added to this reach (**Figure A-35**).

Calculation of return flows. Given the large amount of irrigation in the upper river (above Picture Gorge), it is expected that there are probably significant return flow contributions. There are no measured data for these return flows, however. The OWRD Water Master indicated the location of several of the larger return flows and one was added to the model at km 375.9 to represent the Enterprise drain return flow. The Water Master estimated the flows from this return to be 1.5-3.0 CFS and an average value was used in the model (E. Julsrud, 2009, pers. comm.). The model also tried to capture return flows through the inclusion of “springs” and “calibration” flows.

Calculation of diversion/calibration flows. There are hundreds of diversions on the John Day River. In an effort to capture the impact of diversions, 17 diversions points were identified in the model to represent the geographic distribution of diversion points from the OWRD point of diversion database. Hourly flows were assigned to each of these points (**Figure A-36, a-c)** based on the flows necessary to balance the river hydrology between gaged locations on the river. These flows were both negative and positive, so positive “calibration” flows are another way that return flows are represented in the model.

Table A-12. Flow inputs and rates for the John Day River model

Stream km	Location name	Reference used for calculations
436.00	Upper springs	Added during calibration: variable based on hydrologic calibrations
434.85	Call Creek	Gage: JDR @ Blue Mt. Hot Springs
430.85	Roberts Creek	Gage: JDR @ Blue Mt. Hot Springs
430.70	Rail Creek	Gage: JDR @ Blue Mt. Hot Springs
429.85	Blue Mt. Hot Springs	TIR temperature balance: 0.00089 cms
429.75	Upper springs	Added during calibration: 0.11000
427.75	Graham Creek	Gage: JDR @ Blue Mt. Hot Springs
424.75	Deardorff Creek	Gage: JDR @ Blue Mt. Hot Springs
423.55	*Diversion/calibration flow*	Hydrology calibration
421.70	Reynolds Creek	Gage: JDR @ Blue Mt. Hot Springs
417.80	Return of side channel (Isham Creek?)	Gage: JDR @ Blue Mt. Hot Springs
413.80	*Diversion/calibration flow*	Hydrology calibration
412.15	Strawberry Creek	Gage: JDR @ Blue Mt. Hot Springs
408.95	Slyfe/Strawberry Creek	Gage: JDR @ Blue Mt. Hot Springs
408.40	Dixie Creek	Gage: JDR @ Blue Mt. Hot Springs
403.85	*Diversion/calibration flow*	Hydrology calibration
400.05	Indian Creek	Gage: JDR @ Blue Mt. Hot Springs
397.65	Pine Creek (upper)	Gage: JDR @ Blue Mt. Hot Springs
392.70	Seep (near Dean & Dissel Creeks)	TIR temperature balance: 0.00001 cms
392.15	*Diversion/calibration flow*	Hydrology calibration
384.70	Canyon Creek	Gage: JDR @ Blue Mt. Hot Springs
379.60	*Diversion/calibration flow*	Hydrology calibration
376.35	Laycock Creek	Gage: JDR @ Blue Mt. Hot Springs
376.10	*Diversion/calibration flow*	Set to zero during hydrology calibration
375.90	Enterprise drain return flow	OWRD Water Master: 0.05663 cms
370.55	Beech Creek	Gage: South Fork John Day River
369.45	*Diversion/calibration flow*	Hydrology calibration
360.50	Spring (near Birch Ck)	TIR temperature balance: 0.00708 cms
357.15	Spring	TIR temperature balance: 0.00198 cms originally, changed to 0.10198 during calibration
352.15	Belshaw Creek & Fields Creek	Gage: South Fork John Day River
346.35	*Diversion/calibration flow*	Hydrology calibration
330.40	*Diversion/calibration flow*	Set to zero during hydrology calibration
329.00	Spring	TIR temperature balance: 0.00085 cms
328.30	Dayville WWTP	Measured (no diversion during model period)
326.00	S. Fork John Day River	Measured
324.10	*Diversion/calibration flow*	Hydrology calibration
318.95	Cottonwood Creek	Gage: South Fork John Day River
314.25	Rock Creek (upper)	Gage: South Fork John Day River
306.25	Squaw Ck.	Gage: South Fork John Day River
295.15	*Diversion/calibration flow*	Hydrology calibration
294.50	Seep (RB) (near Branson Creek)	TIR temperature balance: 0.00001 cms
283.50	Johnson Creek	Gage: South Fork John Day River
282.20	N. Fork John Day River	Measured

278.15	Bologna Canyon	Gage: South Fork John Day River
275.10	*Diversion/calibration flow*	Set to zero during hydrology calibration
260.55	*Diversion/calibration flow*	Hydrology calibration
256.95	Parrish Creek & Kahler Creek	Gage: South Fork John Day River
241.85	Alder Creek	Gage: South Fork John Day River
226.70	Shoofly Creek	Gage: South Fork John Day River
217.60	Spring/seep (near Girds Creek)	TIR temperature balance: 0.00001 cms
215.65	*Diversion/calibration flow*	Hydrology calibration
202.25	Bridge Creek	Gage: South Fork John Day River
173.35	*Diversion/calibration flow*	Hydrology calibration
164.50	Pine Creek (lower)	Measured
146.55	*Diversion/calibration flow*	Hydrology calibration
139.65	Butte Creek	Gage: Pine Creek
118.15	Thirtymile Creek	Gage: Pine Creek
30.10	Hay Creek	Gage: Pine Creek
22.85	*Diversion/calibration flow*	Hydrology calibration
17.25	Rock Creek (lower)	Gage: Pine Creek

Figure A-33, a-c. Measured flow records used as basis for derived tributary flows

Figure A-33, a

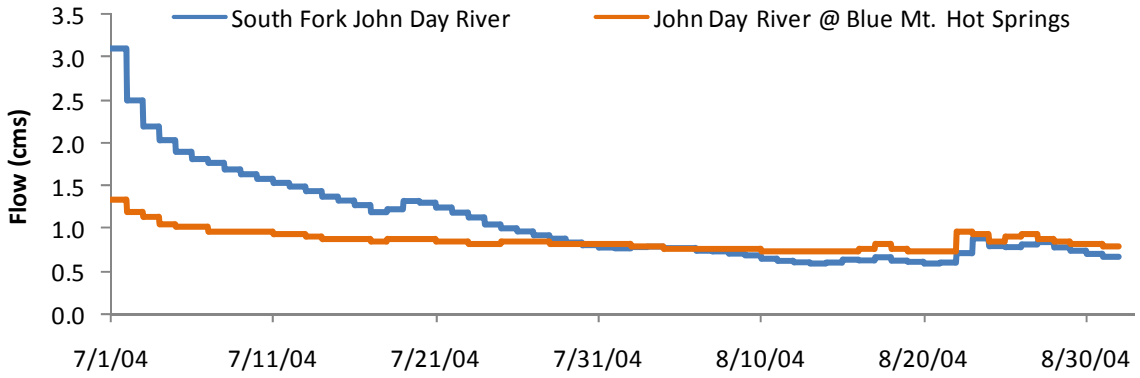

Figure A-33, b

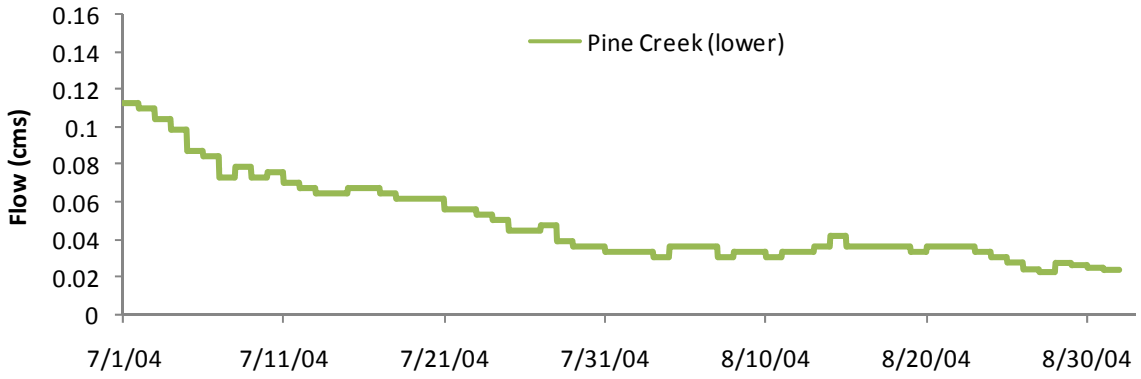

Figure A-33, c

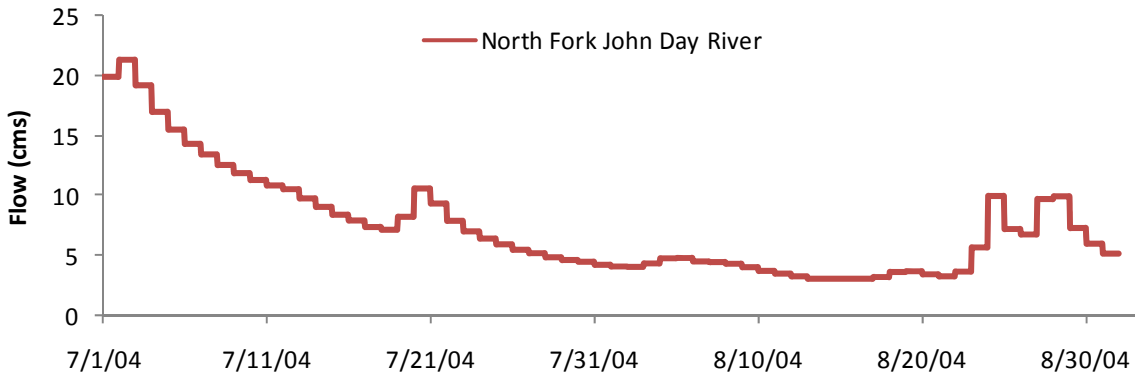

Figure A-34. Constant accretion flows into the John Day River model

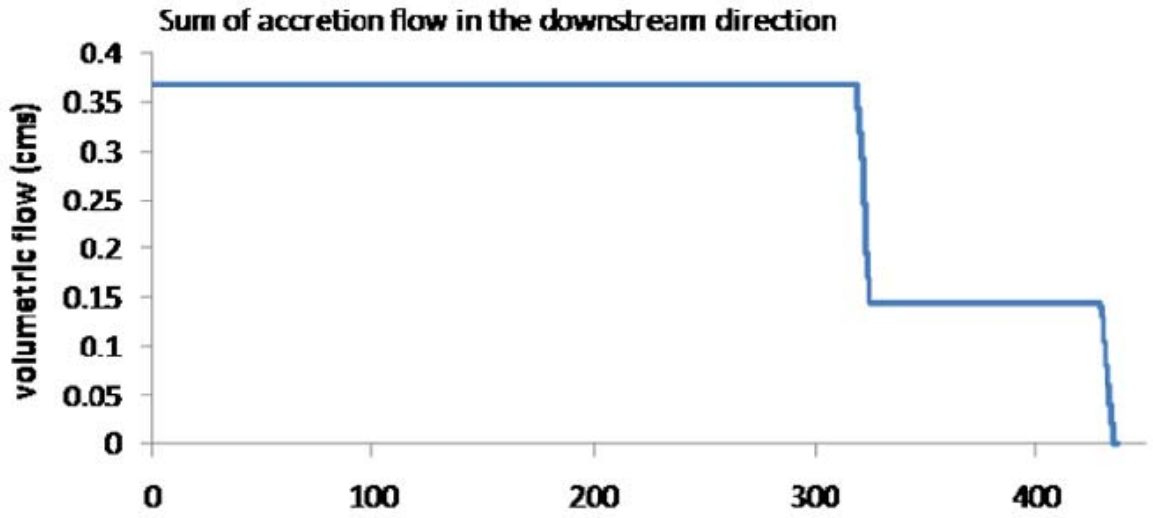

Figure A-35. Constant water withdrawals from the John Day River model

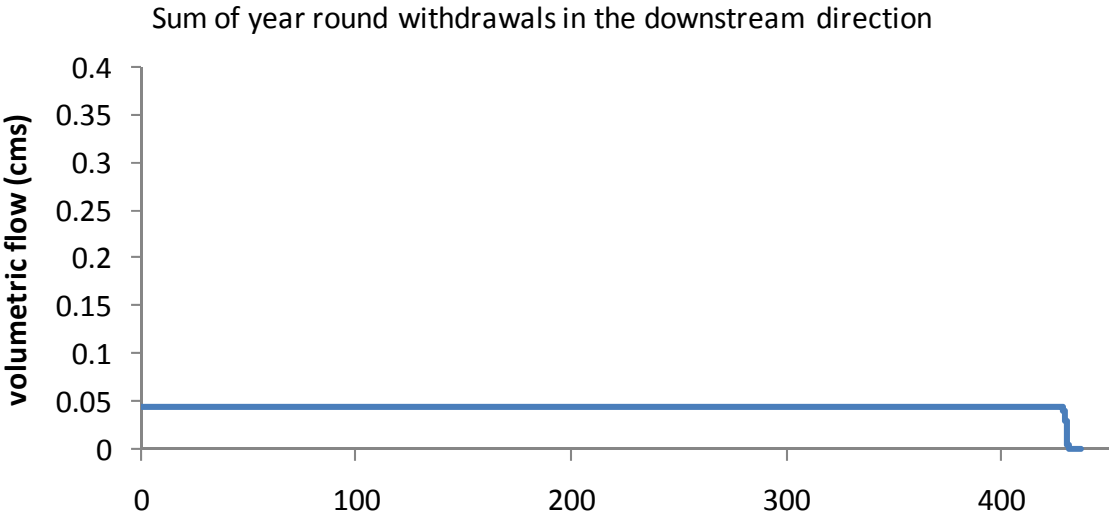

Figure A-36, a-c. Calculated calibration flows to/from the John Day River

Figure A-36, a

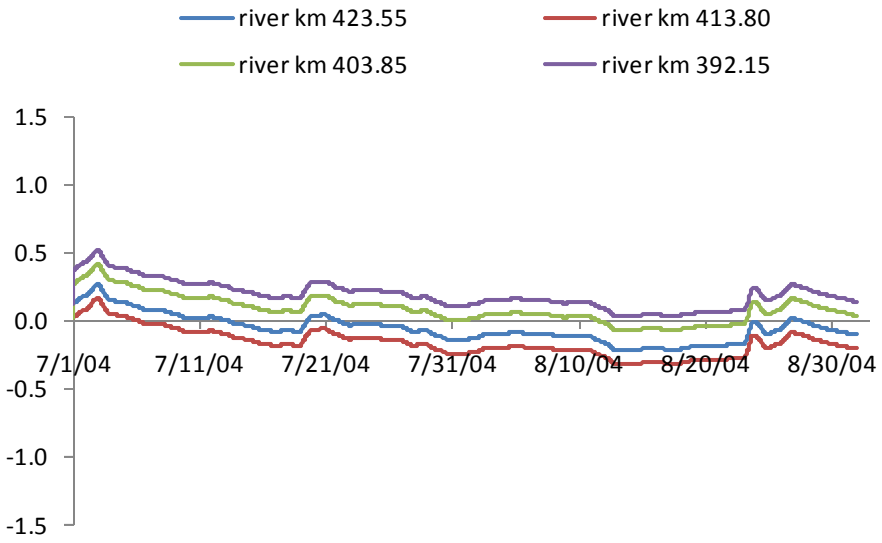

Figure A-36, b

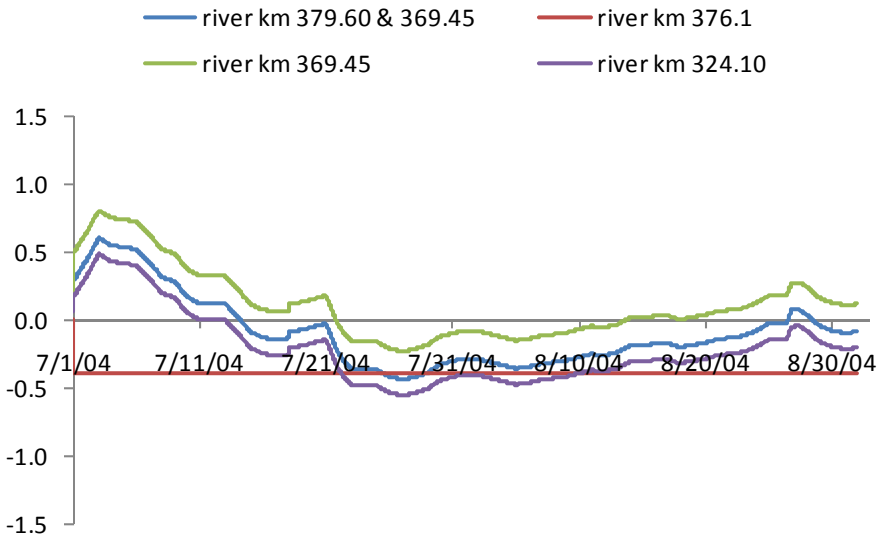

Figure A-36, c

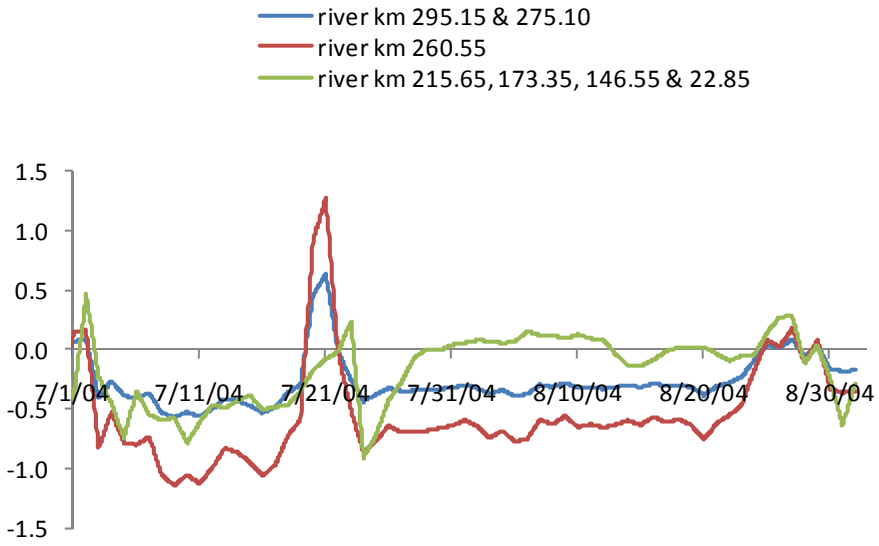

Flow Calibration

The modeled flows resulting from the above input data were compared with measured flow records for the John Day River at five gage locations over the period of the model: Blue Mt. Hot Springs, John Day, Picture Gorge, Service Creek and McDonald Ferry (**Figure A-37, a-e**). In addition, the longitudinal performance of the John Day River model was evaluated on August 17-19, 2004 by comparing measured field data with model results (**Figure A-38, Figure A-39, Figure A-40,** and **Figure A-41**).

Figure A-37, a-e. Temporal flow profiles at gage stations on the John Day River

Figure A-37, a

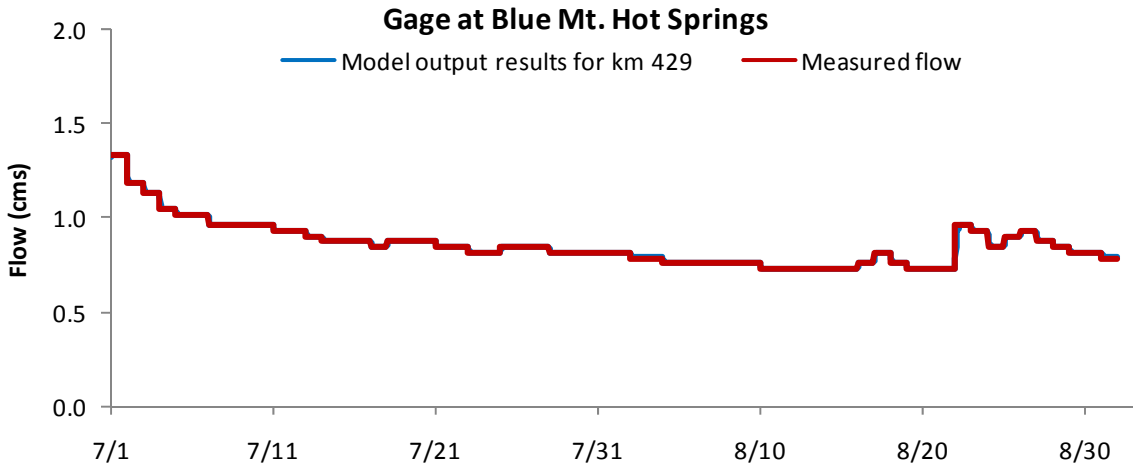

Figure A-37, b

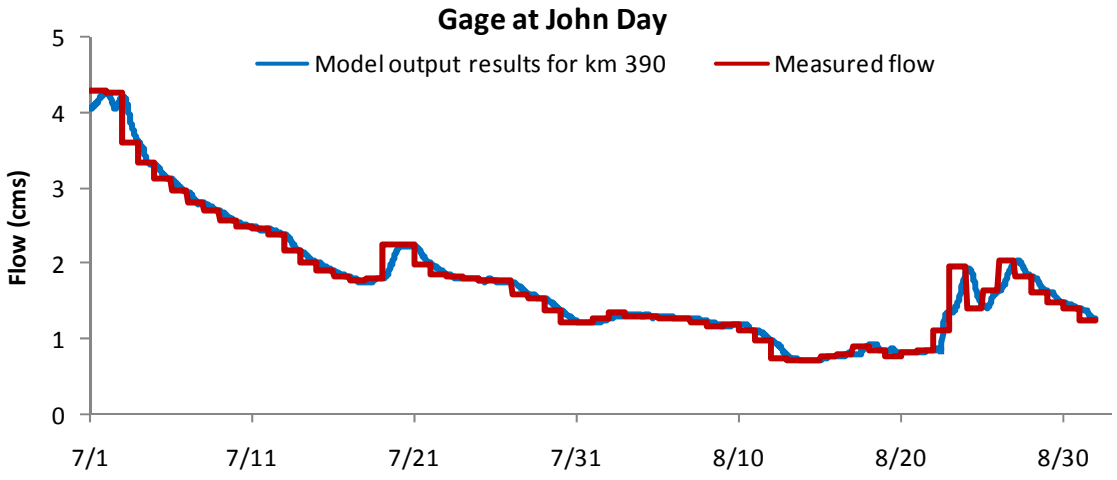

Figure A-37, c

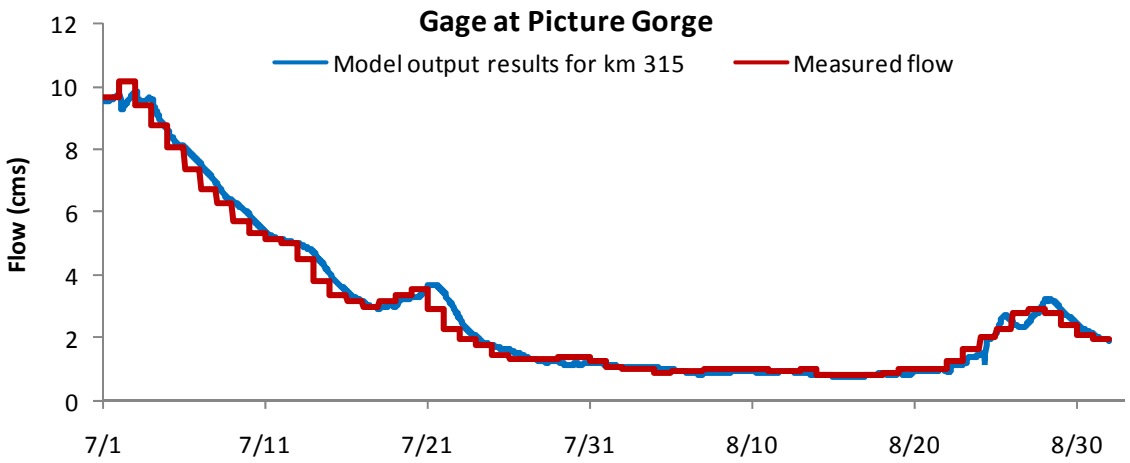

Figure A-37, d

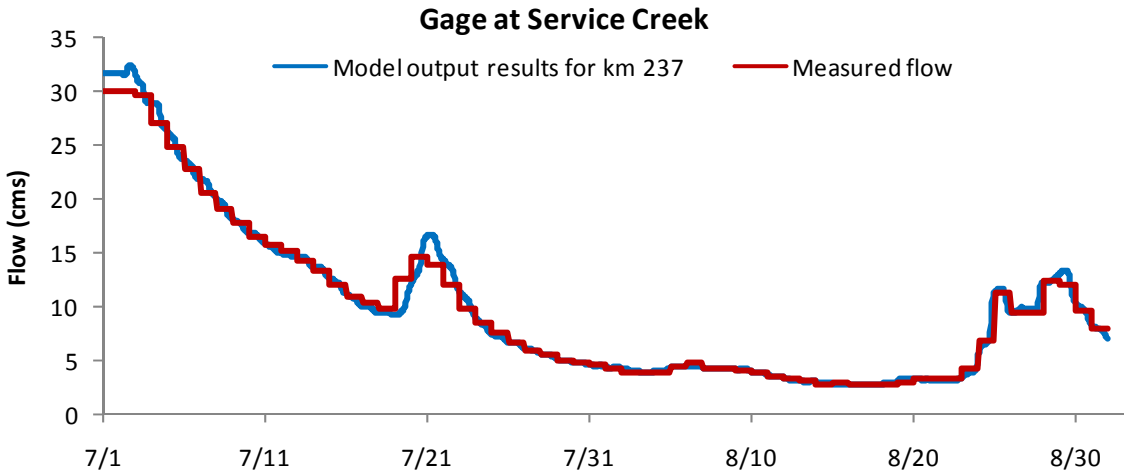

Figure A-37, e

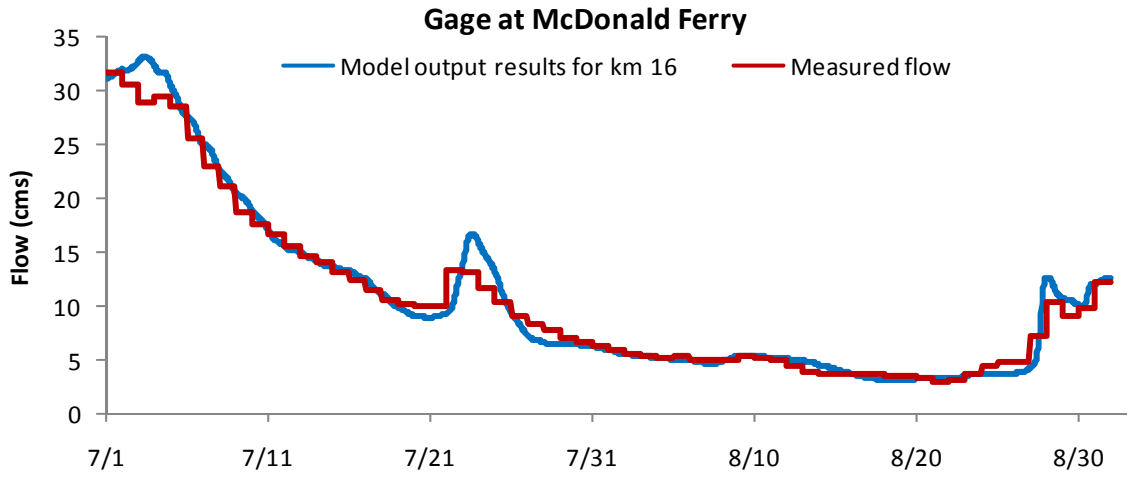

Figure A-38. Longitudinal profile of model results with measured flow

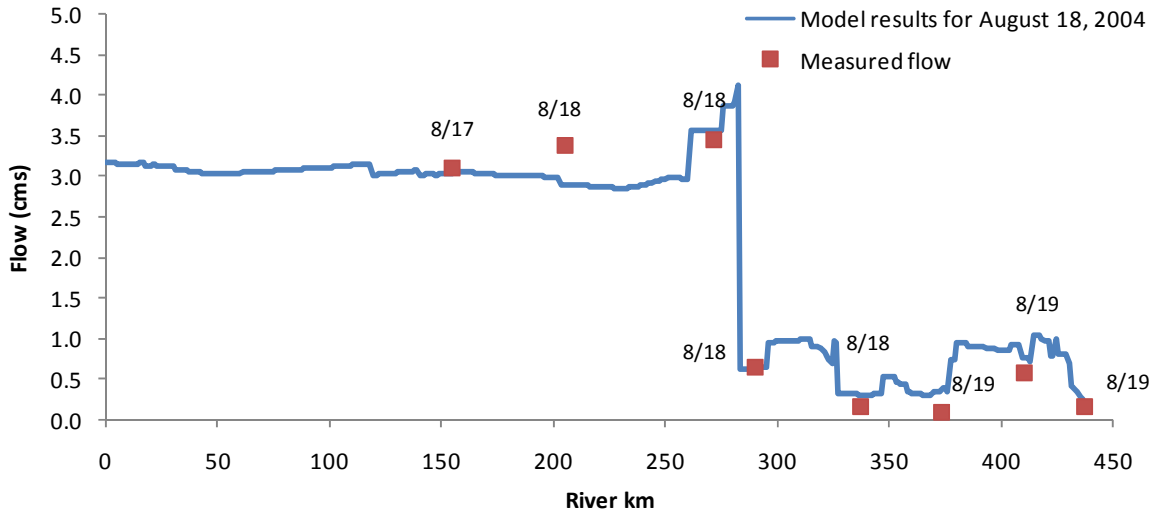

Figure A-39. Longitudinal profile of model results with measured velocity

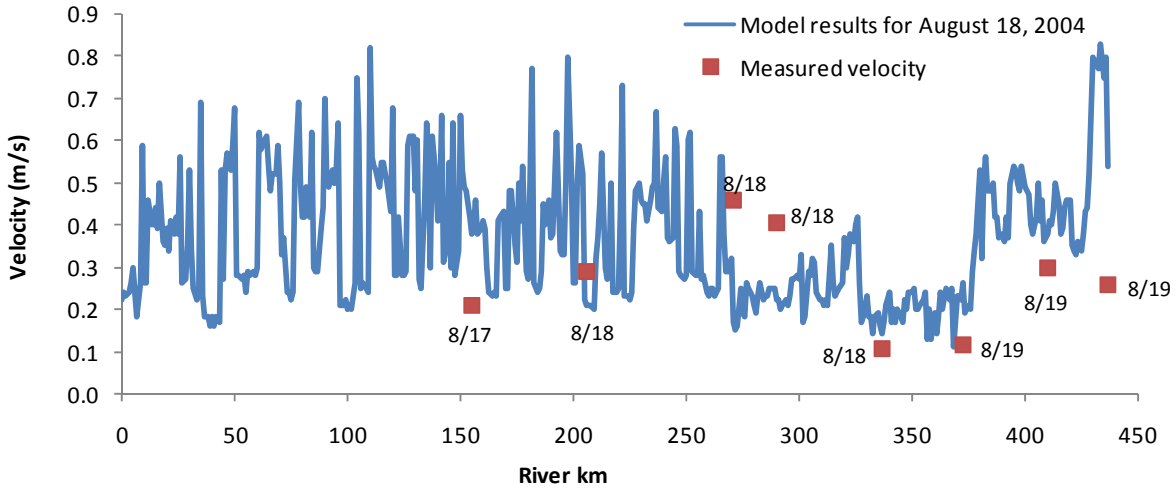

Figure A-40. Longitudinal profile of model results with measured top widths

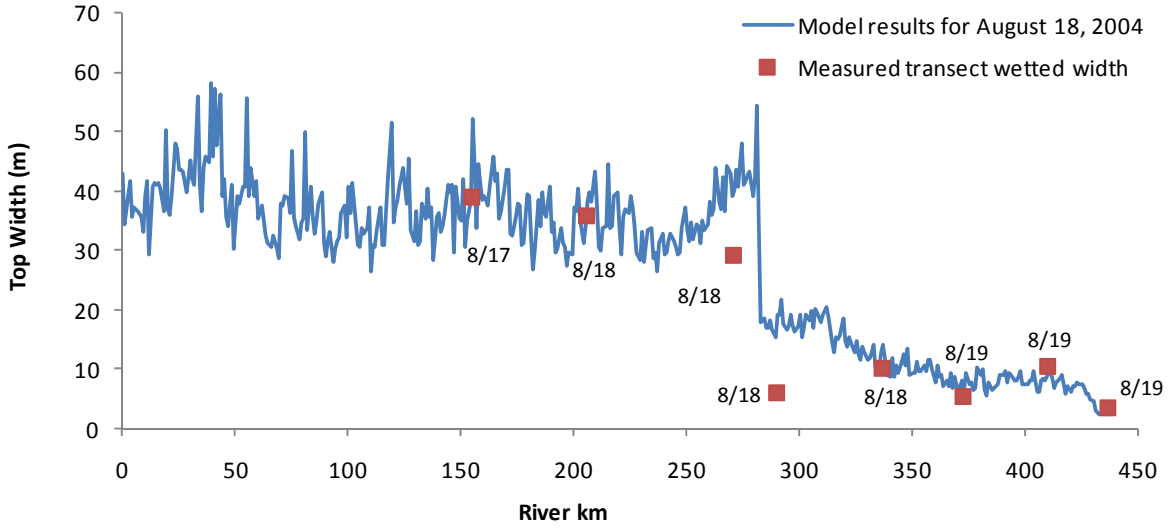

Figure A-41. Longitudinal profile of model results with measured hydraulic depths

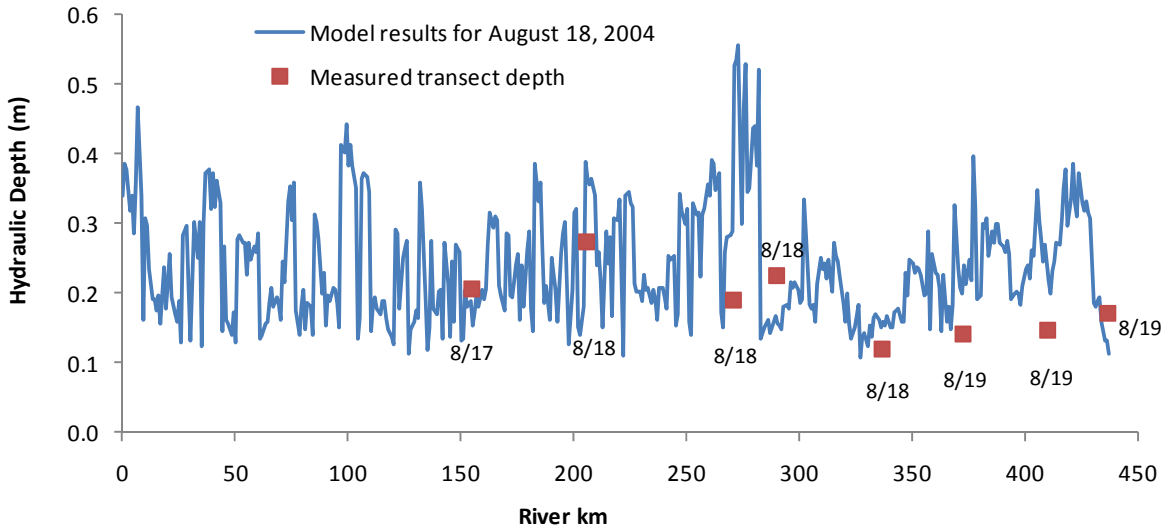

Temperature Input

There were nine tributaries with continuous temperature data for at least some portion of the model period (**Figure A-42, Figure A-43,** and **Figure A-44**). Five of these tributaries had data for the entire model period of July 1-August 31, 2004, while four had data for a portion of the model period. Many of the tributaries and/or springs had an instantaneous TIR temperature measurement for one point in time on either 8/29/04 or 8/30/04. Temperature data were entirely unavailable for many of tributary inflows.

To fill in data gaps where there were no measured data, the temperature was calculated for each inflow (**Table A-13**) using one of several different methods:

(1) For sites where only a portion of the model period was measured, temperature data for the missing time period was calculated by comparing that site with data from another tributary. In most cases, data was compared for the first two days with overlapping data. An average ratio of temperatures between the two sites was determined for this 48 hour period and then applied to the period of missing data. In several instances where this average ratio method did not yield good results, hourly data were compared over a three-day over-lapping period. An average ratio was determined for each hour of the day (rather than an average over the entire period) and then applied to the time period with missing data.

(2) For tributaries with an instantaneous TIR temperature measurement (but no hourly measurements), the input temperature was calculated using a ratio of the TIR temperature of the target creek and a nearby creek, with associated hourly data

(3) For tributaries without either hourly or TIR measurements, the input temperature was developed by using either TIR or hourly data from a nearby stream or spring/seep. This method was used for the diversion/calibration flows, since in some instances, the mass transfers acted as inflows.

(4) Data arrays for springs/seeps were developed either by (a) using a ratio to a nearby tributary based on TIR measurements; or (b) assigning a constant value to the spring/seep for the entire model period during determined through calibration.

(5) Accretion flows added directly to the model were assigned estimated groundwater or hot springs temperatures (**Figure A-45**). Temperatures were estimated based on best professional judgment.

Figure A-42. Tributary continuous measured temperature profile

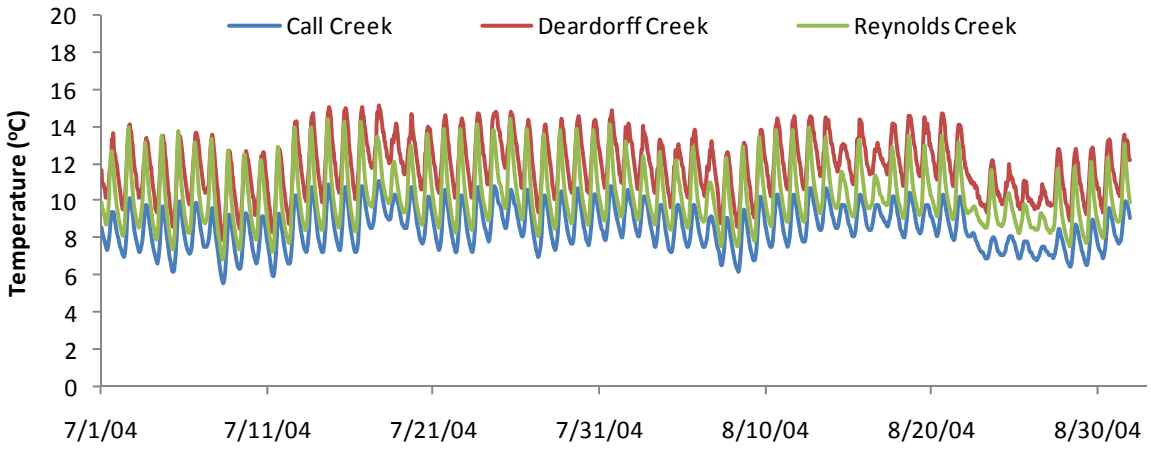

Figure A-43. Tributary continuous measured temperature profile

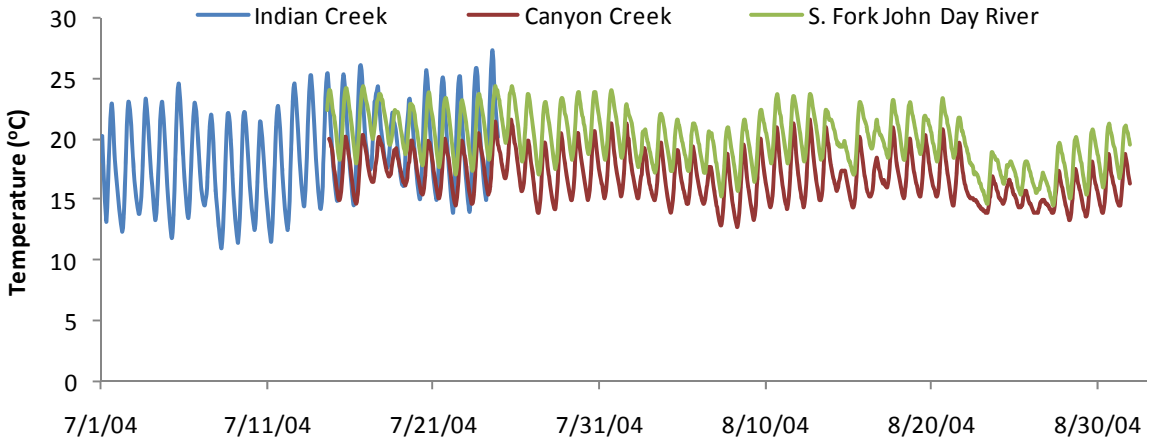

Figure A-44. Tributary continuous measured temperature profile

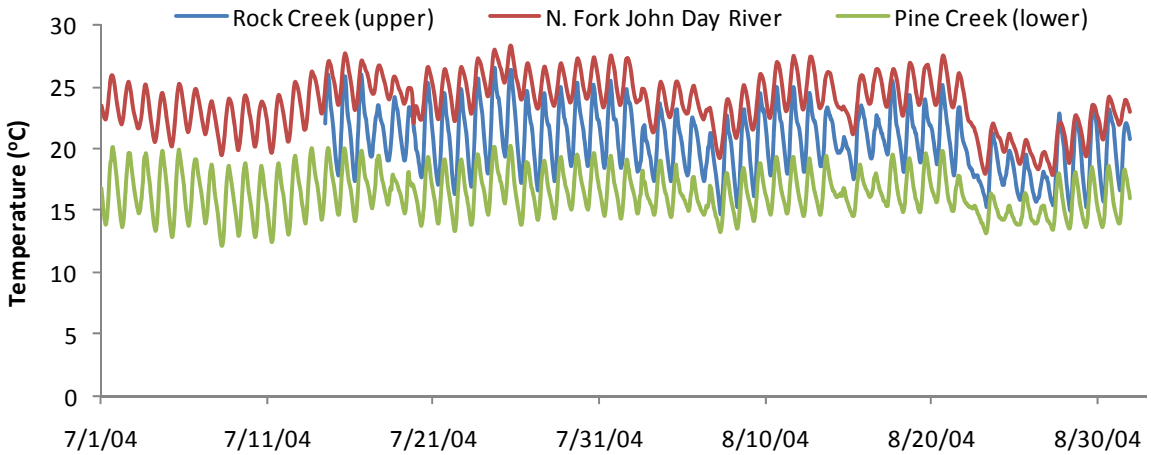

Table A-13. Temperature inputs and rates for the John Day River model

Stream km	Location name	Based on	Creek used for comparison	Ratio
436.00	Upper springs	Estimated groundwater temperature (11.5°C), (best professional judgment)		
434.85	Call Creek	Measured data		
430.85	Roberts Creek	No TIR data, used Call Creek data	Call Creek	1.00
430.70	Rail Creek	TIR data	Call Creek	1.00
429.85	Blue Mt. Hot Springs	Estimated temperature from DOGAMI (58°C) (DOGAMI website).		
429.75	Upper springs	Estimated groundwater temperature (11°C) , (best professional judgment)		
427.75	Graham Creek	TIR data	Deardorff Creek	1.05
424.75	Deardorff Creek	Measured		
423.55	*Diversion/calibration flow*	Deardorff Creek data	Deardorff Creek	1.00
421.70	Reynolds Creek	Measured		
417.80	Return of side channel (Isham Creek?)	TIR data from nearby unnamed tributary (km 411.1)	Canyon Creek	1.07
413.80	*Diversion/calibration flow*	TIR data from nearby unnamed tributary (km 411.1)	Canyon Creek	1.07
412.15	Strawberry Creek	TIR data from nearby unnamed tributary (km 411.1)	Canyon Creek	1.07
408.95	Slyfe/Strawberry Creek	TIR data from nearby unnamed tributary (km 411.1)	Canyon Creek	1.07
408.40	Dixie Creek	TIR data from Shaw Gulch (km 404.9)	Canyon Creek	0.95
403.85	*Diversion/calibration flow*	TIR data from Shaw Gulch (km 404.9)	Canyon Creek	0.95
400.05	Indian Creek	Measured through 7/24; hourly ratio after that	Canyon Creek	Varied by hour, 0.95-1.35
397.65	Pine Creek (upper)	TIR data from Fish Creek (km 398.65)	Canyon Creek	1.13
392.70	Seep (near Dean & Dissel Creeks)	TIR data	Canyon Creek	1.14
392.15	*Diversion/calibration flow*	Canyon Creek data	Canyon Creek	0.90
384.70	Canyon Creek	Measured after 7/14; average 48 hour ratio before that	Pine Creek (lower)	1.02
379.60	*Diversion/calibration flow*	Canyon Creek data	Canyon Creek	1.00
376.35	Laycock Creek	TIR data	Canyon Creek	1.16
376.10	*Diversion/calibration flow*	Not applicable - no inflow		
375.90	Enterprise drain return flow	Canyon Creek data	Canyon Creek	0.90
370.55	Beech Creek	TIR data	Canyon Creek	1.23
369.45	*Diversion/calibration flow*	Beech Creek data	Beech Creek	1.00
360.50	Spring (near Birch Ck)	TIR data	Canyon Creek	1.10
357.15	Spring	TIR data, assumed constant TIR temperature (16.9°C)		
352.15	Belshaw Creek & Fields Creek	TIR data from spring (km 360.5)	Canyon Creek	1.10
346.35	*Diversion/calibration flow*	TIR data from Cummings Creek (km 346.65)	Canyon Creek	1.22
330.40	*Diversion/calibration flow*	Not applicable - no inflow		
329.00	Spring	TIR data	Canyon Creek	1.26
328.30	Dayville WWTP	Measured (no discharge during model period)		

Stream km	Location name	Based on	Creek used for comparison	Ratio
326.00	S. Fork John Day River	Measured after 7/14; average 48 hour ratio before that	Pine Creek (lower)	1.25
324.10	*Diversion/calibration flow*	TIR data from Rattlesnake Creek (km 316.5)	Pine Creek (lower)	1.24
318.95	Cottonwood Creek	TIR data from Rattlesnake Creek (km 316.5)	Pine Creek (lower)	1.24
314.25	Rock Creek (upper)	Measured after 7/14; average 48 hour ratio before that	Pine Creek (lower)	1.26
306.25	Squaw Ck.	TIR data from Rattlesnake Creek (km 316.5) & Rock Creek (averaged)	Pine Creek (lower)	1.25
295.15	*Diversion/calibration flow*	Rock Creek data	Rock Creek (upper)	1.00
294.50	Seep (RB) (near Branson Creek)	TIR data	Pine Creek (lower)	1.21
283.50	Johnson Creek	TIR data from Rattlesnake Creek (km 316.5) & Rock Creek (averaged)	Pine Creek (lower)	1.25
282.20	N. Fork John Day River	Measured		
278.15	Bologna Canyon	TIR data	Pine Creek (lower)	1.18
275.10	*Diversion/calibration flow*	Not applicable - no inflow		
260.55	*Diversion/calibration flow*	Johnson Creek data	Johnson Creek	1.00
256.95	Parrish Creek & Kahler Creek	TIR data from Kahler Creek	Pine Creek (lower)	1.50
241.85	Alder Creek	TIR data	Pine Creek (lower)	1.49
226.70	Shoofly Creek	TIR data from Alder Creek & Bridge Creek (averaged)	Pine Creek (lower)	1.45
217.60	Spring/seep (near Girds Creek)	TIR data	Pine Creek (lower)	1.18
215.65	*Diversion/calibration flow*	Bridge Creek data	Bridge Creek	1.00
202.25	Bridge Creek	TIR data	Pine Creek (lower)	1.41
173.35	*Diversion/calibration flow*	Pine Creek data	Pine Creek (lower)	1.00
164.50	Pine Creek (lower)	Measured		
146.55	*Diversion/calibration flow*	Butte Creek data	Butte Creek	1.00
139.65	Butte Creek	TIR data from Muddy Creek (km 172.05) & Thirtymile Creek (averaged)	Pine Creek (lower)	1.305
118.15	Thirtymile Creek	TIR data	Pine Creek (lower)	1.34
30.10	Hay Creek	TIR data	Pine Creek (lower)	1.32
22.85	*Diversion/calibration flow*	Rock Creek data	Rock Creek (lower)	1.00
17.25	Rock Creek (lower)	TIR data	Pine Creek (lower)	1.27

Figure A-45. Temperature of constant accretion flows in John Day River model

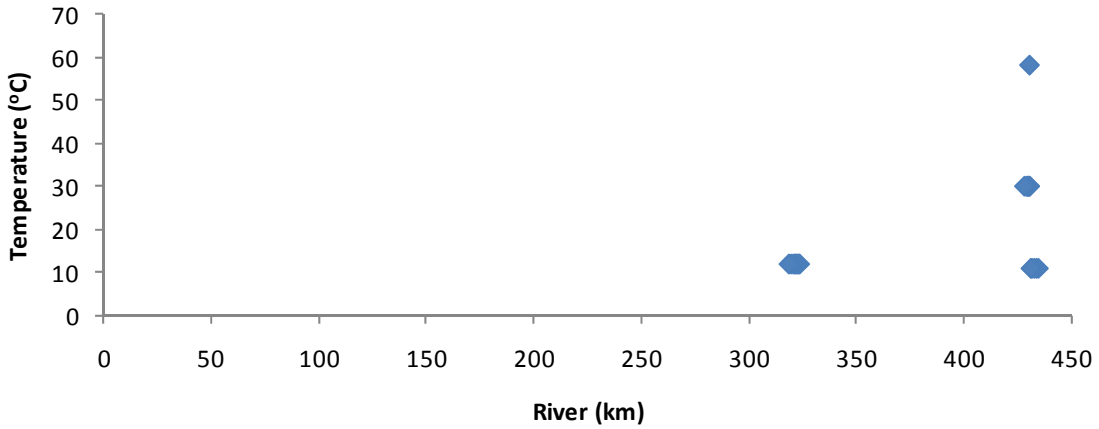

Temperature Calibration

DEQ, BLM, and Confederated Tribes of the Warm Springs Reservation provided continuous temperature data for calibration in the John Day River at 21 locations. Two locations were not used because the temperature data was not within the modeled time period. The model generally reproduces spatially and temporal varying temperature measurements (**Table A-14**, **Figure A-46**, **Table A-15, Figure A-47**). Two of the BLM sites (Picture Gorge and Service Creek) were originally going to be discarded because the measured data did not match the seasonal patterns of other sites and did not match the TIR data. On a closer evaluation of the data, it was determined that the data was correct, but was shifted approximately 9 days. The same shift was true for the North Fork John Day site (described above in the temperature input data). For the Picture Gorge site, the shift appeared to be 9 days and 4 hours; for the Service Creek and North Fork John Day sites the shift appeared to be 9 days and 1 hour. These shifts were made in the data and used in the model. Though, there were no QAQC provided, data went through a external QC screening for anomalous diel that could indicate air exposure, and the daily fluctuation is consistent for upstream and downstream QA records. TIR data was collected on the mainstem over the course of two days – 8/29/04 and 8/30/04, following a seasonally unusual storm in the 2nd week of August (Watershed Sciences, 2004).

The largest challenge in calibrating the model was attempting to reproduce the diel swing in temperature throughout the model period. The data show a smaller diel swing toward the beginning and end of the model period while the middle period has a larger diel swing (see for example **Figure A-47**, sites 12 and 16). Despite varying channel bottom widths, Manning's n, hyporheic flow and meteorological parameters during the calibration process, the model was not able to reproduce this pattern. The simplifying assumptions of a trapezoidal channel, hyporheic flow rate based on a constant percent of the stream flow and meteorology derivation could have led to the model's inability to reproduce this pattern. DEQ chose to try to reproduce the daily maximum temperatures during the warmest period, rather than focus on reproducing the diel pattern in the less-critical time period. In context of the larger calibration effort and the good calibration statistics, this limitation of the model is minor and does not limit the application of the model to be used to help determine sources of pollution, calculate natural thermal potential or determine of allocations.

Table A-14. TIR error statistics

Error type	Value
Mean	-0.43
Absolute mean	0.63
Root mean square	0.82
Nash-Sutcliffe	0.94

Figure A-46. Longitudinal profile of measured temperatures using Thermal Infrared Radiometry and model results. The instream temperature measurements are from the same hour as the TIR collection time, at that location.

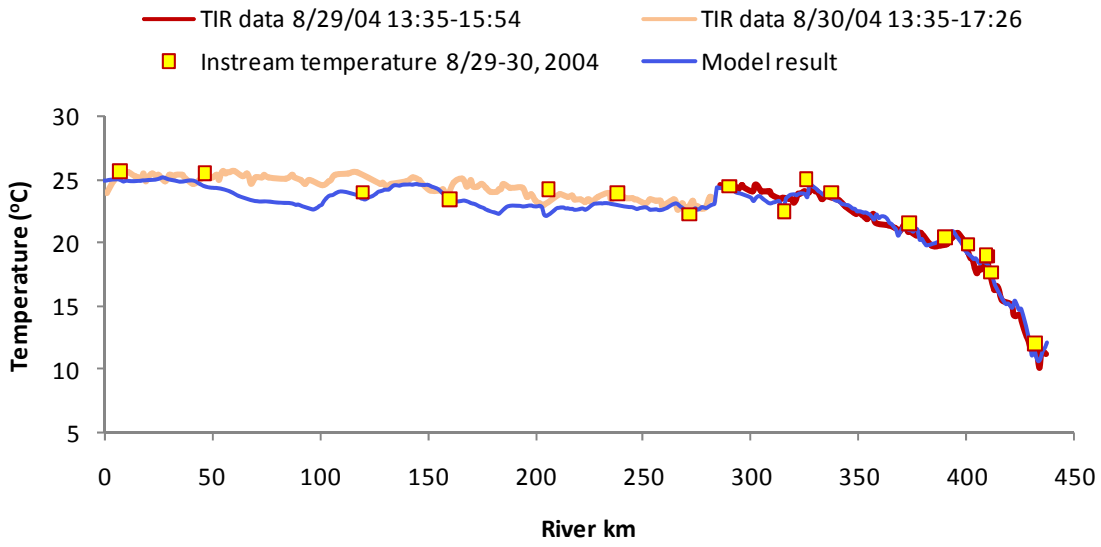

Table A-15. Continuous monitoring error statistics

Site Name	Source of temperature data	Ref	rKM	All data				
				n	Mean Error	Abs Mean Error	RMSE	Nash-Sutcliffe
John Day River u/s Blue Mt. Hot Springs	CTWSR	1	431.55	1053	0.07	0.60	0.85	0.77
John Day River at USFS Boundary above Prairie City	BLM	2	431.20	No measured data during model period				
John Day River 2 km u/s Prairie City	CTWSR	3	411.05	1488	-0.60	0.96	1.18	0.81
John Day River 0.9 km u/s Prairie City	CTWSR	4	409.75	1488	-0.58	0.91	1.14	0.85
John Day River at Prairie City	CTWSR	5	408.85	1488	-0.56	0.91	1.14	0.85
John Day River 7.5 km d/s Prairie City	CTWSR	6	400.35	1487	0.03	0.65	0.85	0.91
John Day River 17 km d/s Prairie City	CTWSR	7	389.50	1488	0.17	0.78	1.11	0.86
John Day River at John Day WWTP	DEQ	8	384.15	858	0.30	0.66	0.91	0.85
John Day River at Clyde-Holliday State Park	DEQ	9	372.95	969	0.74	1.08	1.32	0.80
John Day River at ODFW Bridge above Dayville	DEQ	10	336.75	1161	0.54	1.24	1.57	0.75
John Day River d/s Dayville	CTWSR	11	325.25	1488	0.96	1.22	1.42	0.75
John Day River at Picture Gorge	BLM	12	315.30	1488	0.06	1.51	1.84	0.51
John Day River u/s Bone Creek	DEQ	13	289.95	1164	0.17	1.21	1.57	0.73
John Day River u/s Kimberly	BLM	14	283.95	No measured data during model period				
John Day River at Shady Grove Wayside	DEQ	15	271.40	1165	-0.32	0.77	0.98	0.79
John Day River near Service Creek	BLM	16	237.70	1488	-0.69	1.23	1.60	0.33
John Day River at Priest Hole BLM Boat Ramp	DEQ	17	205.80	1209	-0.34	1.07	1.39	0.63
John Day River at Hwy218 Clarno	DEQ	18	160.05	1211	0.16	1.50	1.86	0.21
John Day River u/s Pine Hollow	BLM	19	119.95	1199	0.29	1.12	1.47	0.58
John Day River at Hwy 206	DEQ	20	46.80	612	0.37	1.48	1.87	0.51
John Day River at River Mile 15	BLM	21	7.15	1488	0.06	1.43	1.86	0.49
				Average	0.04	1.07	1.36	0.68

Figure A-47. Measured steam temperature (thinner, blue line) versus model results (thicker, orange line)

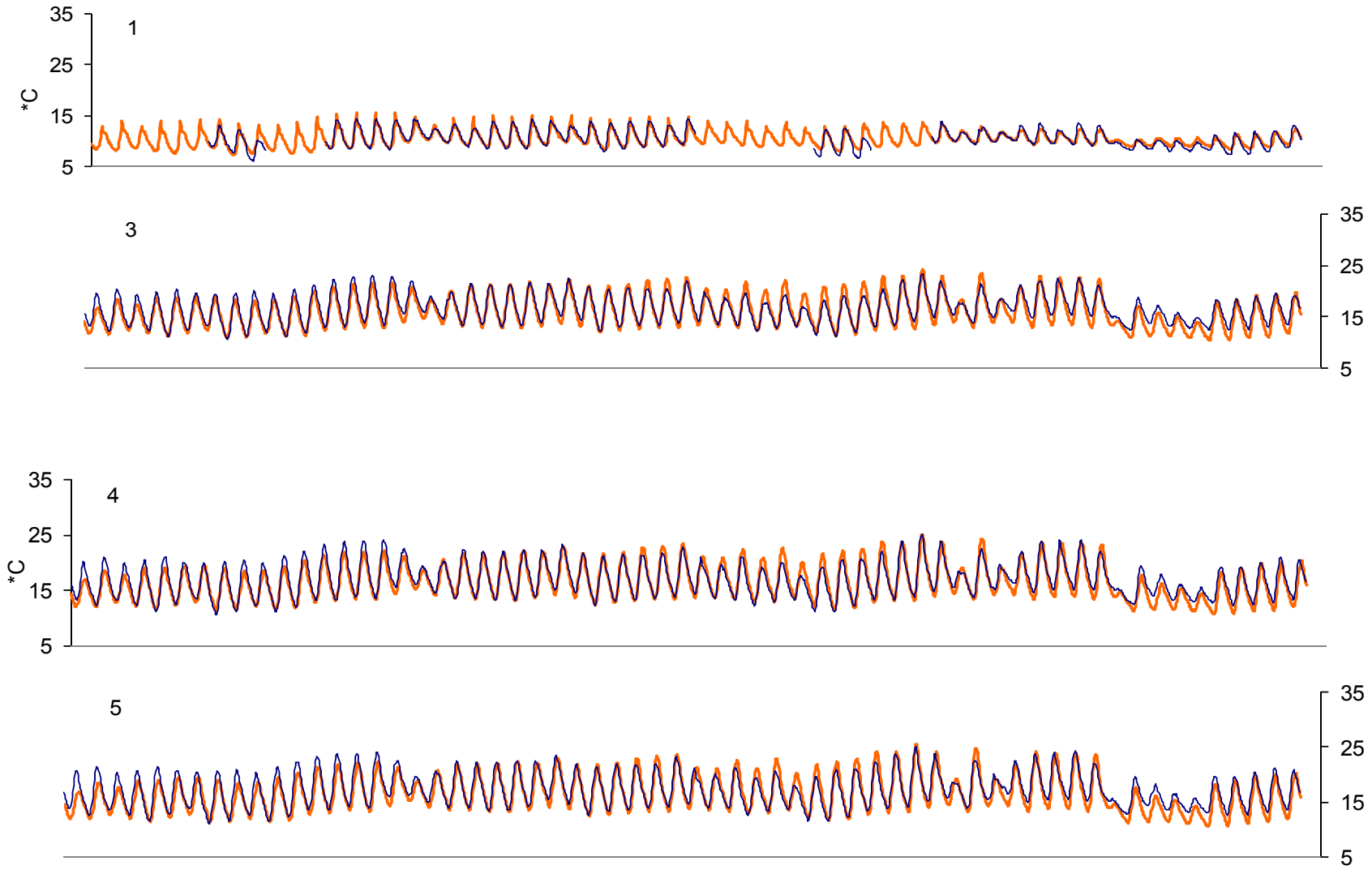

Figure A-47 (Continued). Measured steam temperature (thinner, blue line) versus model results (thicker, orange line)

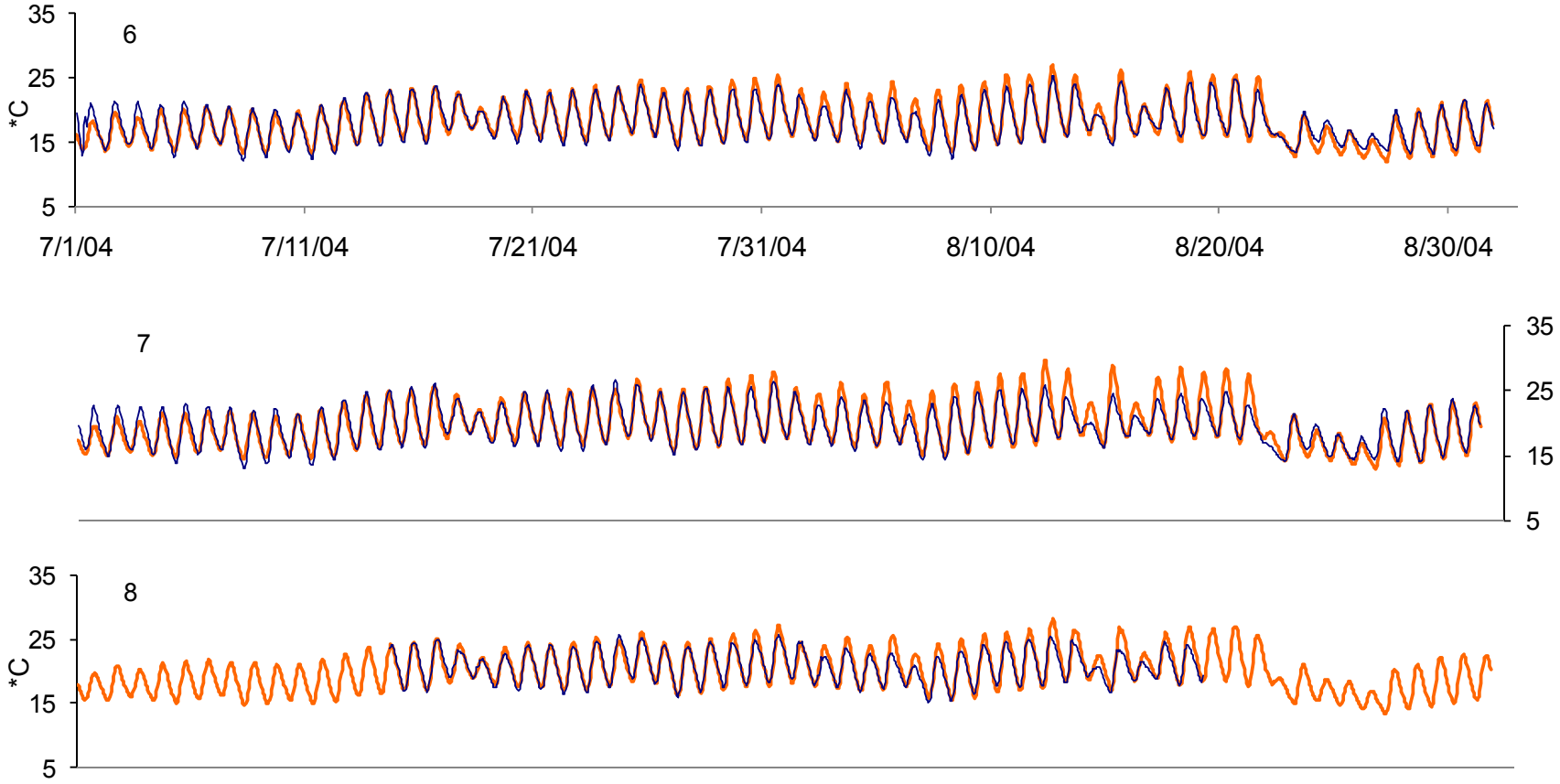

Figure A-47 (Continued). Measured steam temperature (thinner, blue line) versus model results (thicker, orange line)

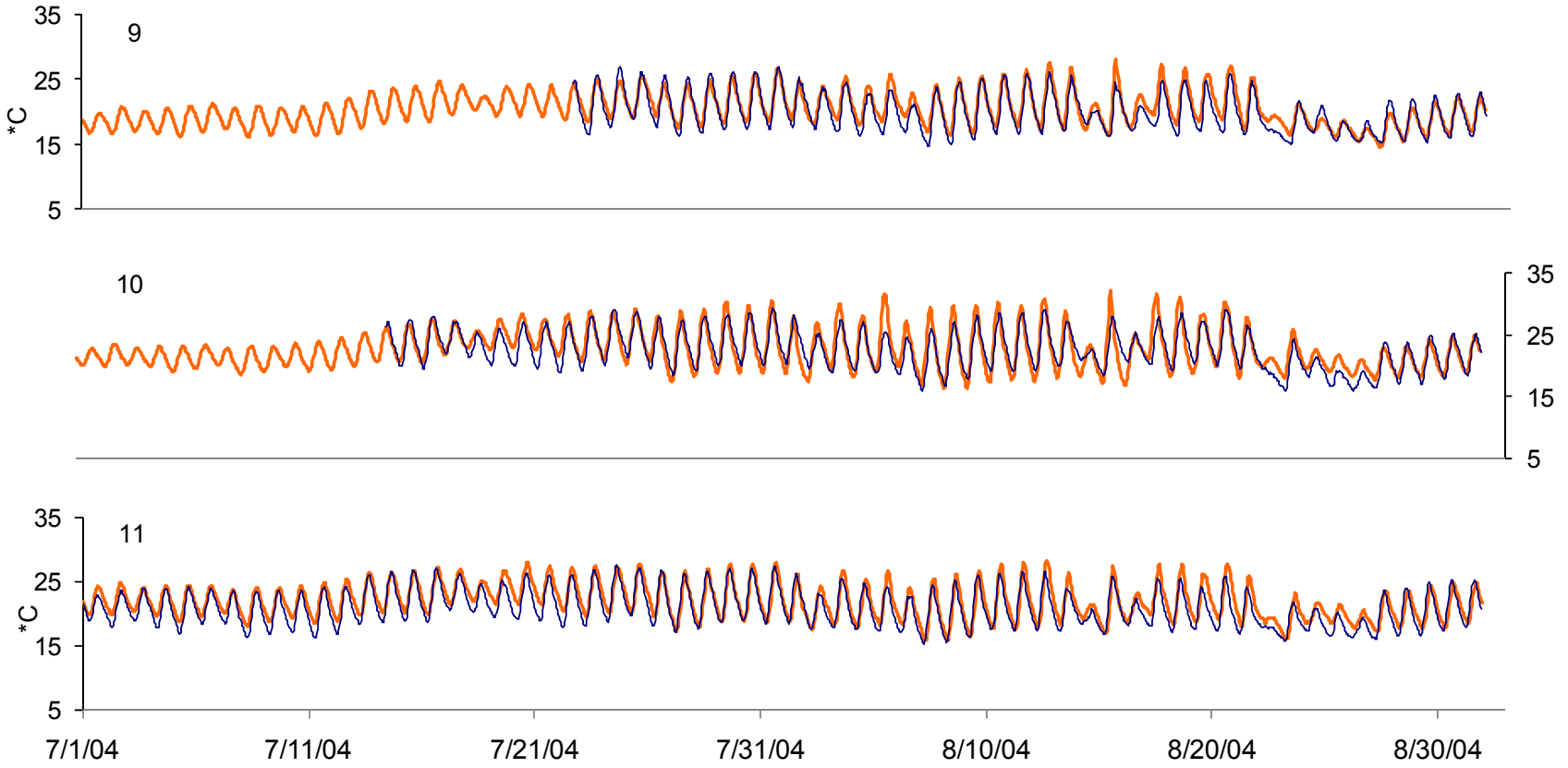

Figure A-47 (Continued). Measured steam temperature (thinner, blue line) versus model results (thicker, orange line)

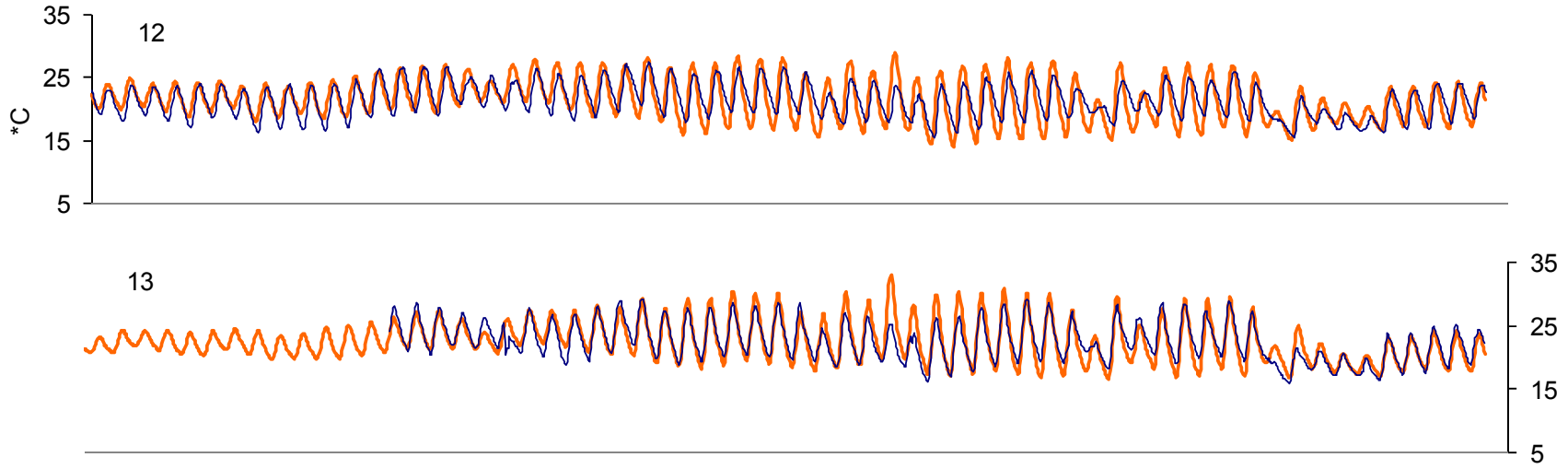

Figure A-47 (Continued). Measured steam temperature (thinner, blue line) versus model results (thicker, orange line)

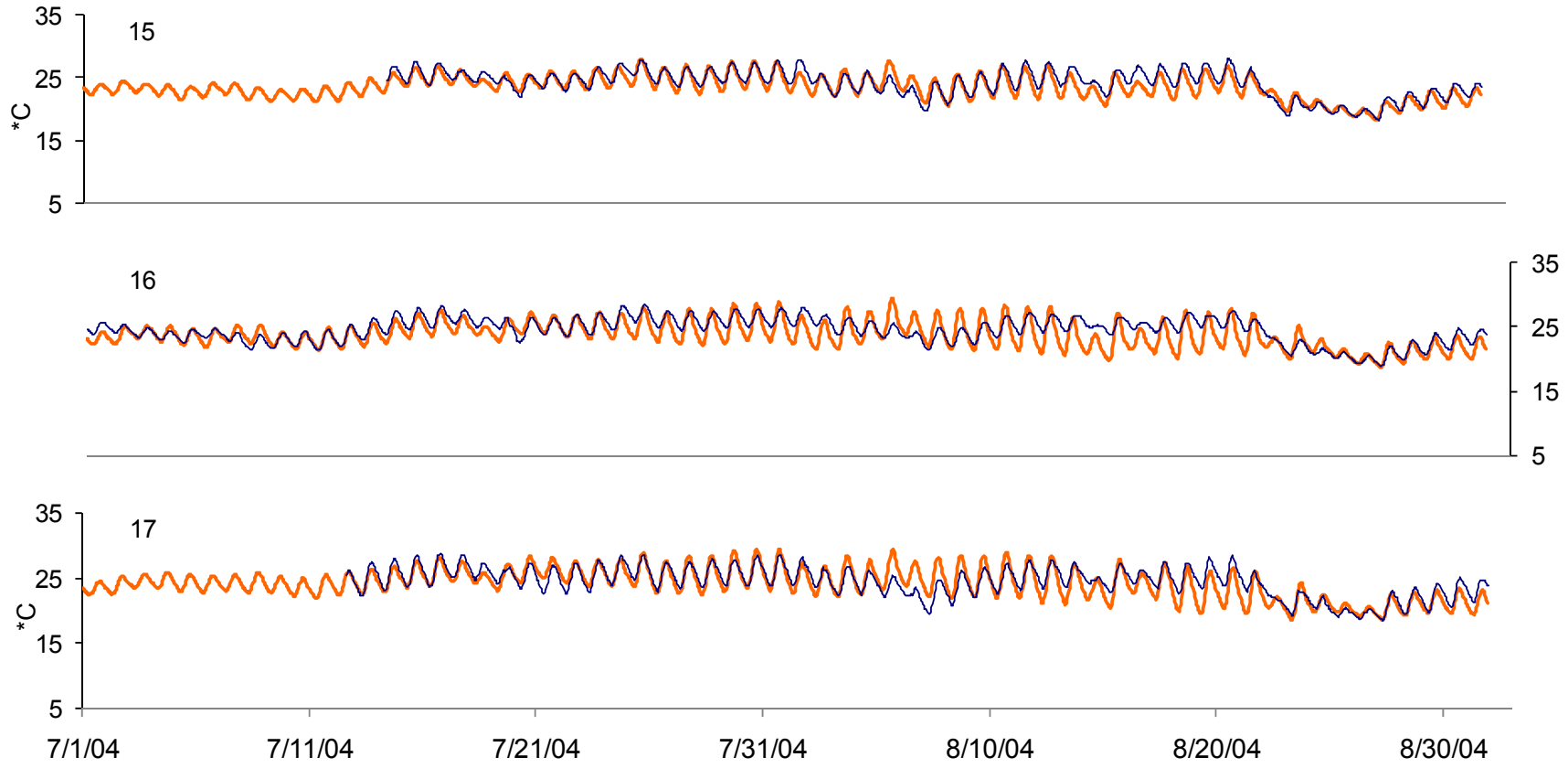

Figure A-47 (Continued). Measured steam temperature (thinner, blue line) versus model results (thicker, orange line)

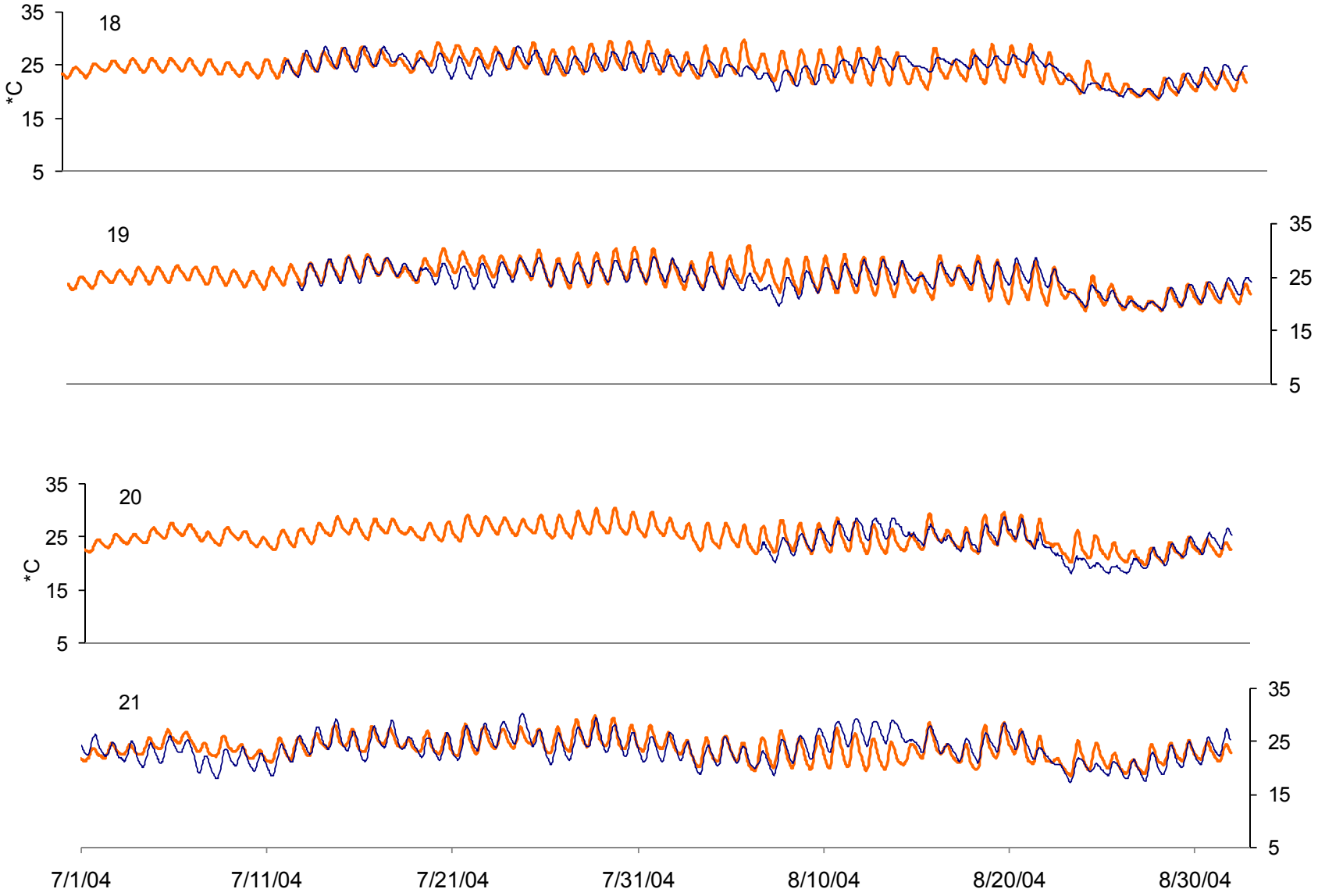

3.3 North Fork John Day River

The North Fork John Day River is a tributary to the John Day River. The North Fork John Day River Subbasin comprises an area of 1,182,711 acres and is referenced by the 4th field Hydrologic Unit Code (HUC) 17070202. Instream temperature was simulated for 172.9 km of the North Fork John Day River from the mouth to the confluence with Baldy Creek. The following documents the calibration methods and decisions and ultimately describes the model used in the North Fork John Day River TMDL.

Overview

Stream Name: North Fork John Day River
Model: Heat Source version 8.0.4
Beginning date: 6/15/2002
Ending date: 9/1/2002
Time step: 0.5 minute
Distance step: 100 m
Transverse sample rate: 20m
"Deep alluvium" option on at 12°C
Initial flush condition: 10 days
Extent: mouth to confluence with Baldy Creek (172.9 km) (**Figure A-48**).

Figure A-48. Extent of the North Fork John Day River temperature model

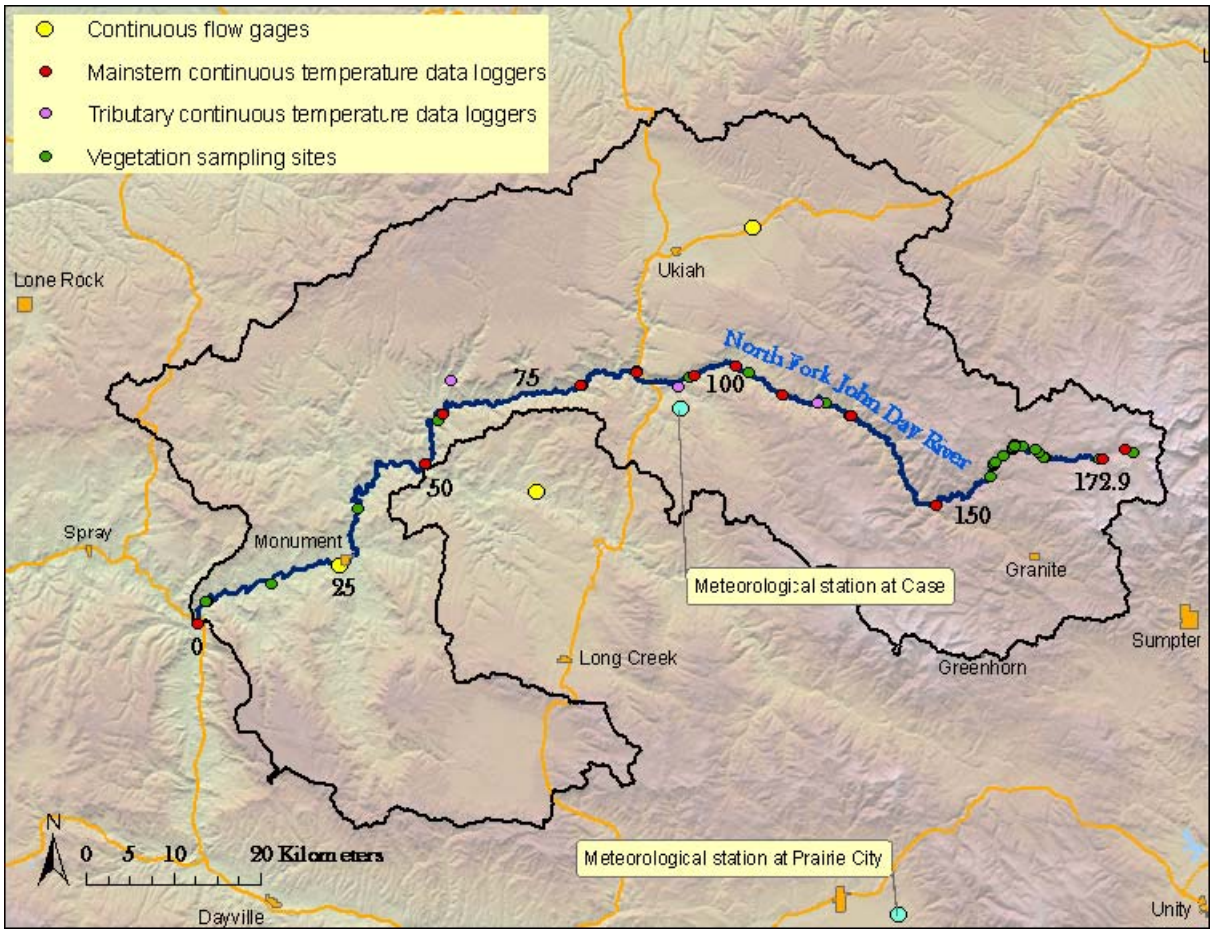

Reach Properties

Table A-16 identifies the sources of spatial GIS data used in the model. See **Section 2.3** for methodology. The elevation profile and reach gradient were determined using DEM files, and then each reach gradient was averaged over the neighboring seven reaches before input to the model (**Figure A-49**). The bankfull channel widths were measured from DOQ images and verified by field measurements (**Figure A-50**). Additional aerial images were used as supplemental sources of information for both channel morphology and riparian vegetation mapping. The channel depths were estimated to be between 0.25m and 0.8m and were varied longitudinally (**Figure A-51**). Bottom widths were initially estimated to be 10% less than bankfull width (not shown). Using these estimates, **Equation A-2** and assuming a trapezoidal channel as depicted in **Figure A-52**, channel angle z values were estimated. To calibrate the model, the bottom widths and channel angle z values were altered to better reflect observed temperature responses to morphological variability. During calibration, the bottom widths were quartered, and the channel angle z values were doubled (**Figure A-53** and **Figure A-54**). Manning's n and percent hyporheic exchange values were iteratively altered during calibration so that the model temperatures approximately reproduced measured temperatures (**Figure A-55**). Topographic shade angles used in the model are presented in **Figure A-56**. The average of the vegetation heights and densities sampled at each node is presented in **Figure A-57** and **Figure A-58**. Using these channel morphology and shade inputs, the North Fork John Day River model's ability to simulate shade is shown in **Figure A-59**.

Table A-16. Spatial Data and Application

Spatial Data	Data Source	Application
10-Meter Digital Elevation Models (DEM)	10-m DEM files provided by OGDC	Measure Stream Elevation and Gradient Measure Topographic Shade Angles
Aerial Imagery – Digital Orthophoto Quads	0.5-m uncompressed National Agriculture Imagery Program (NAIP) lowermost 2.4km used 1-m compressed color NAIP	Map Vegetation Map Channel Morphology Measure Active Channel Widths Map Roads, Development, Structures
Thermal Infrared Radiometry (TIR) Stream Temperature Data	Upper watershed 1998 Lower watershed 2002 Watershed Sciences, LLC	Measure Surface Temperatures Develop Longitudinal Temperature Profiles Identify Subsurface Hydrology, Groundwater Inflow, Springs

Figure A-49. Model setup channel elevation and gradient

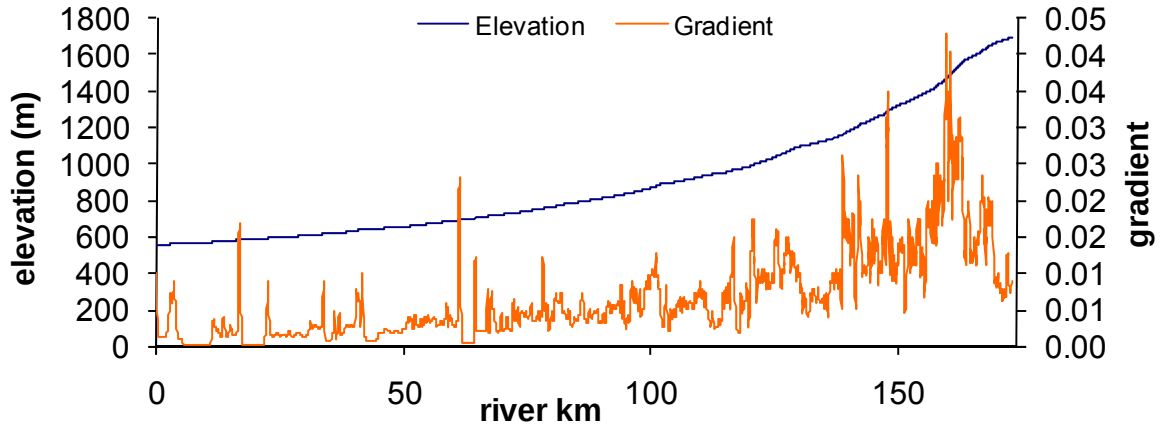

Figure A-50. Model setup for bankfull width

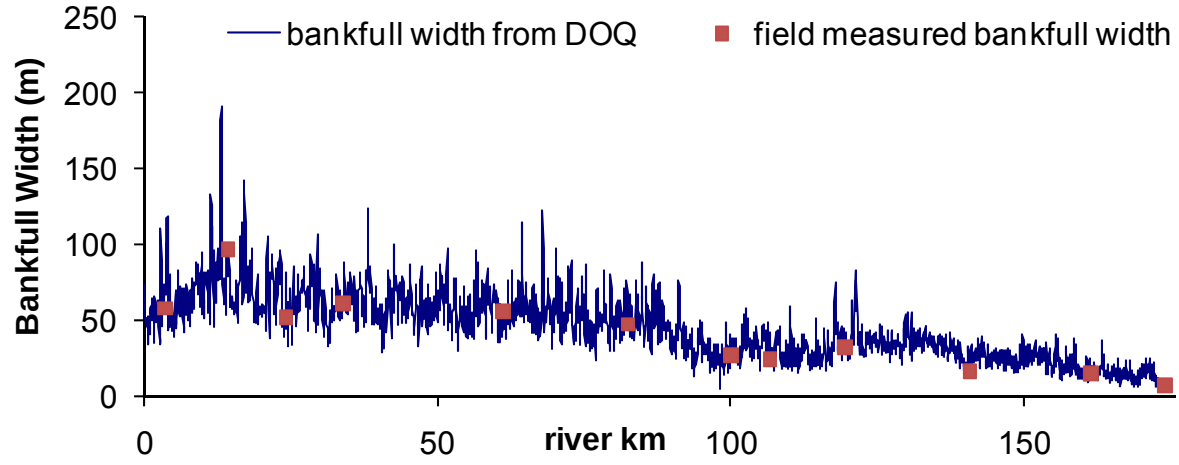

Figure A-51. Depth values used for model

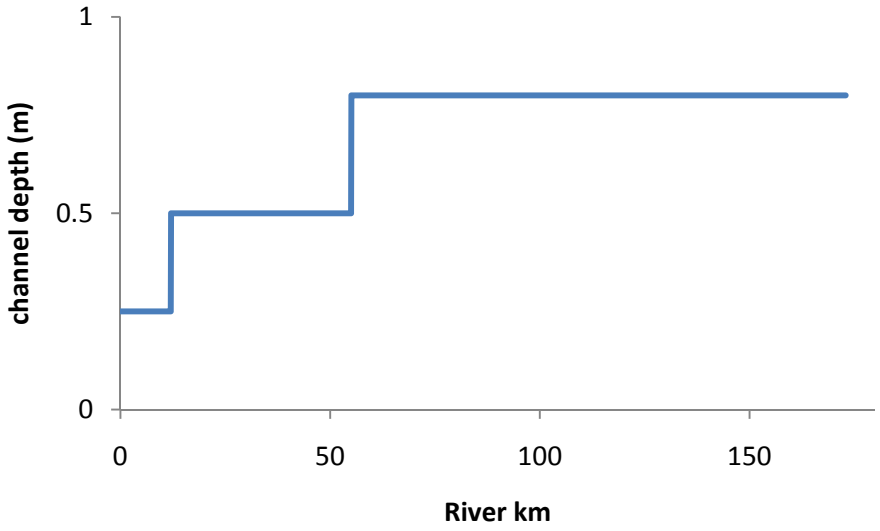

Equation A-2. $z = \frac{b_1 - b_2}{2D}$

Figure A-52. Calculation of channel angle z for model setup

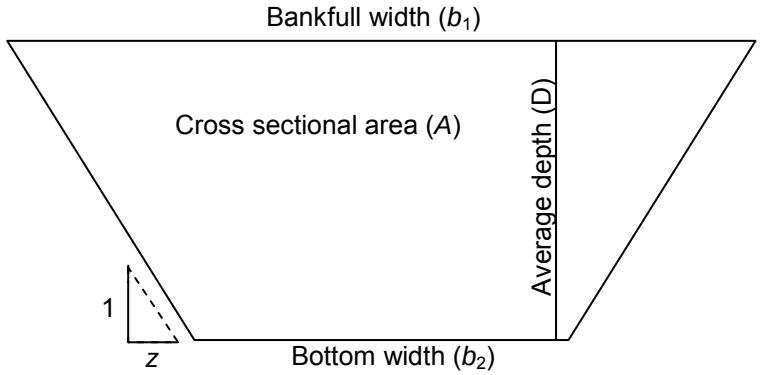

Figure A-53. Model setup for bottom width determined from sampled bankfull width, cross sectional area, and average depth values used in models

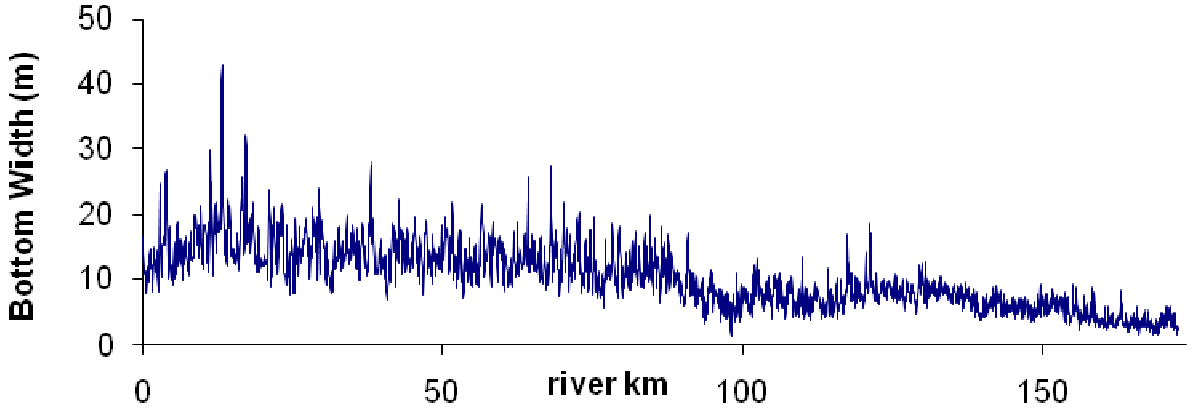

Figure A-54. Model setup for channel angle z determined from sampled bankfull width, cross sectional area, and average depth values used in models

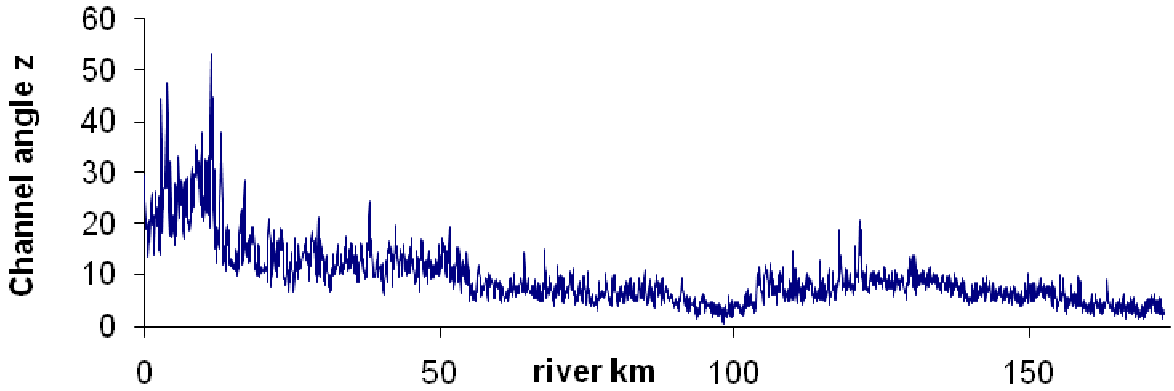

Figure A-55. Model setup for Manning's n and percent hyporheic exchange

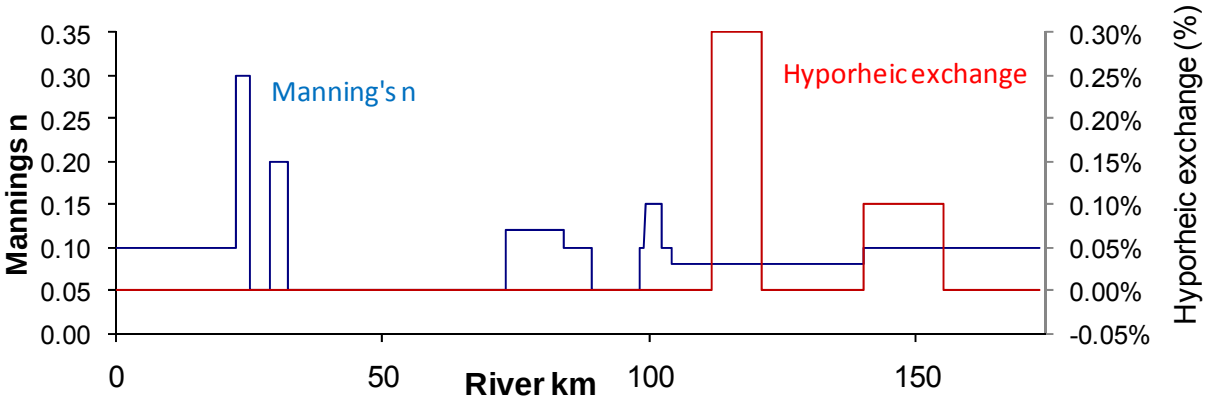

Figure A-56. Model setup for topographic shade angle

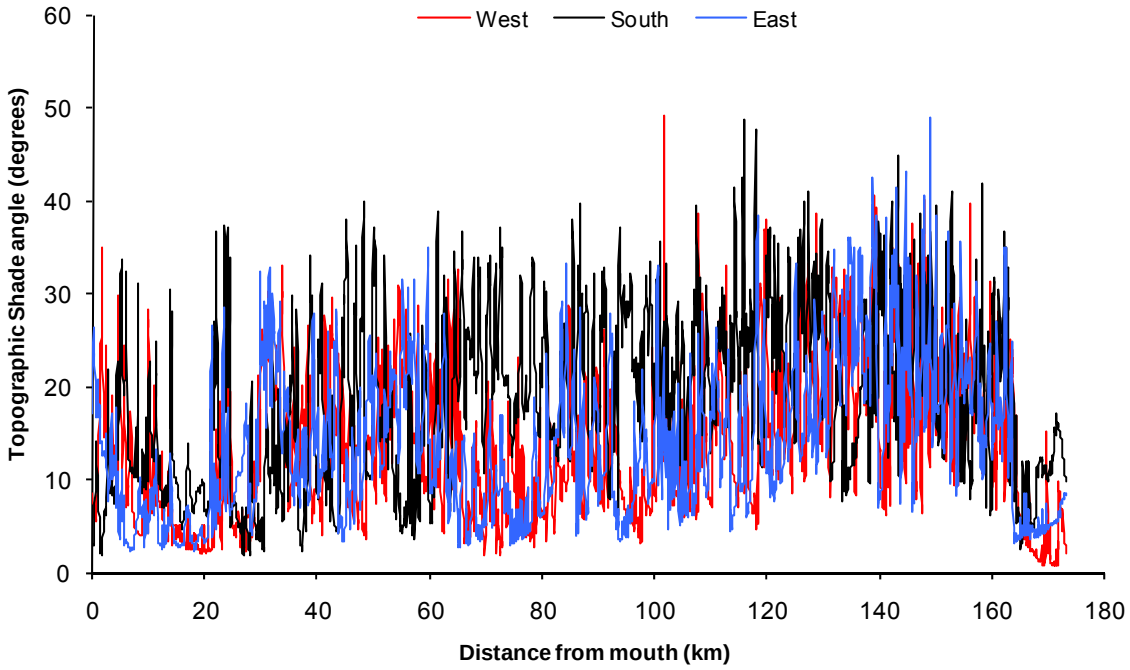

Figure A-57. Model setup for average height of streamside vegetation

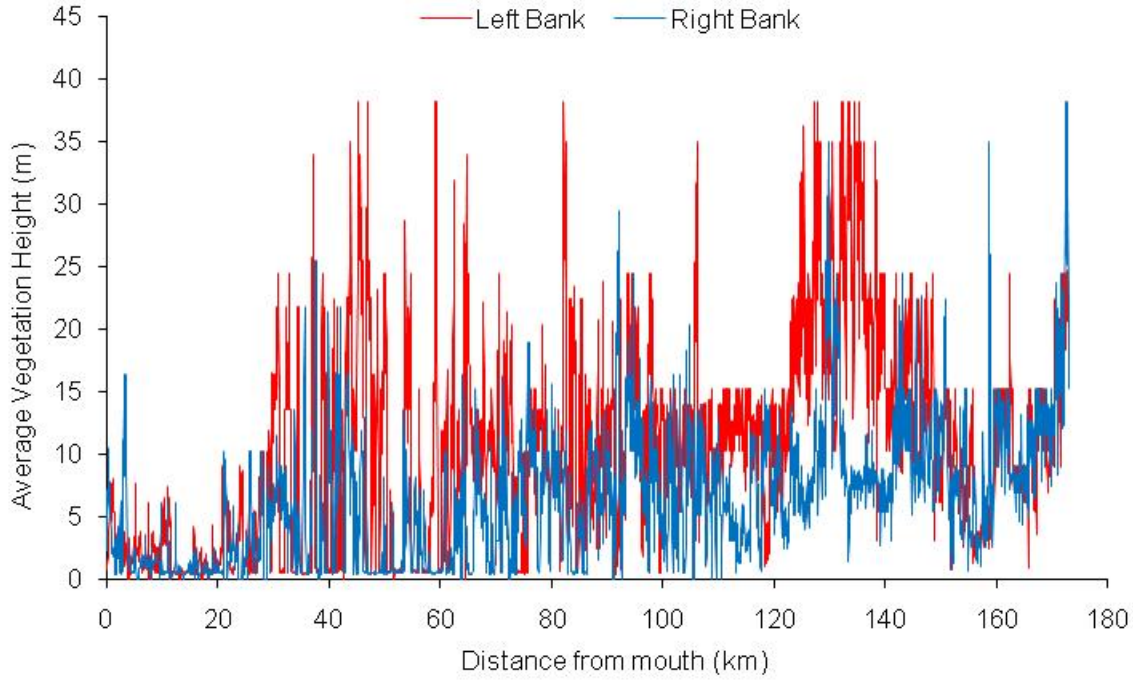

Figure A-58. Model setup for average density of streamside vegetation

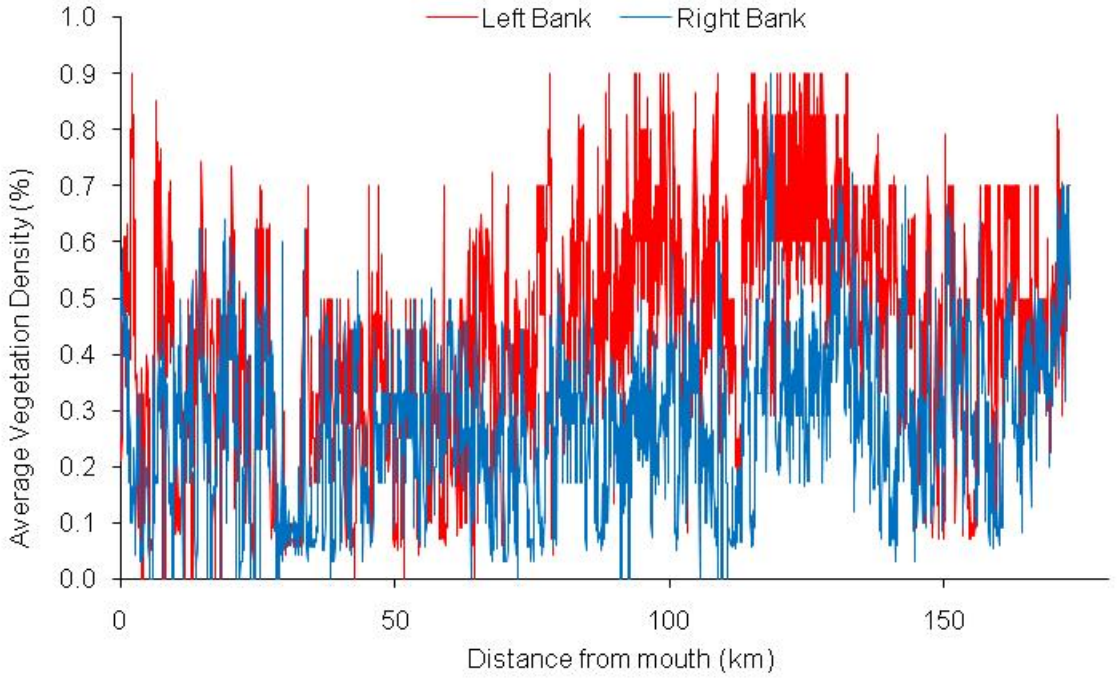

Figure A-59. Predicted shade on North Fork John Day River

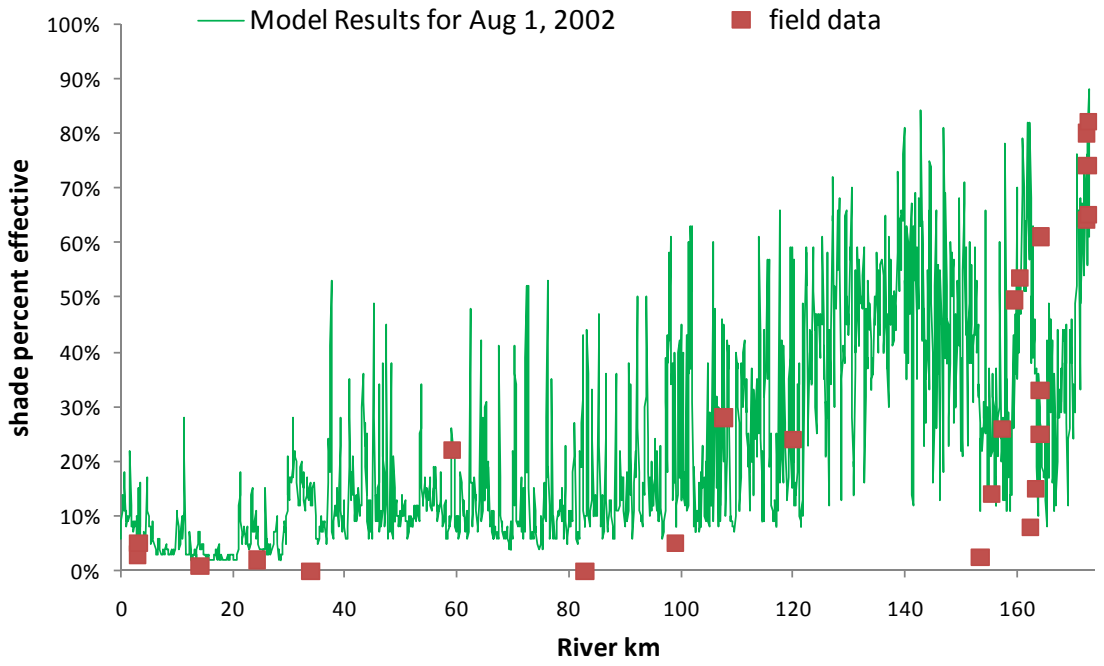

Meteorology

Meteorological data were collected at the Case and Prairie City stations in the basin (**Table A-17**). The meteorological inputs varied by stream kilometer based on proximity to the weather station and are presented in **Table A-18**. The air temperature data were adjusted from the Case station to the continuous data node based on elevation and the dry adiabatic lapse rate of 9.8ºC/km, according to the following equation: Adjustment for dry adiabatic lapse rate = 9.8*($Elev_{metstation}$ – $Elev_{contnode}$)/1000, where Elev is the elevation in meters. Relative humidity from the Case station was used without any modifications. Where used, wind speed data came from the Prairie City meteorological station. A multiplicative wind sheltering coefficient was applied to the wind speed for calibration. Cloudiness was determined by calculating the deviation of solar radiation measured at the Prairie City station from the theoretical maximum solar radiation on a rolling 24 hour average. The meteorological observations are presented in **Figure A-60, a-d**.

Table A-17. Data inputs for North Fork John Day River model

Site	Source	Elevation (m)	Meteorological Parameters
Prairie City	USBR	1144	Cloudiness, wind speed
Case	DRI-RAWS	1159	Relative humidity, air temperature

Table A-18. Data inputs by river km

Range (river km)	Adiabatic Adjustment (additive, °C)	Wind sheltering Coefficient (multiplicative)
172.9 - 132.7	-0.4	0.0
132.7 - 118.3	1.3	0.0
118.3 - 109.2	2.1	0.0
109.2 - 102.7	2.5	0.0
102.7 - 95.6	2.9	0.0
95.6 - 87.1	3.3	0.0
87.1 - 69.3	5.1	0.3
69.3 - 50.2	4.8	1.0
50.18 - 26.4	5.1	1.0
26.4 - 0.0	5.7	1.0

Figure A-60, a-d. Meteorology inputs for model setup

Figure A-60, a

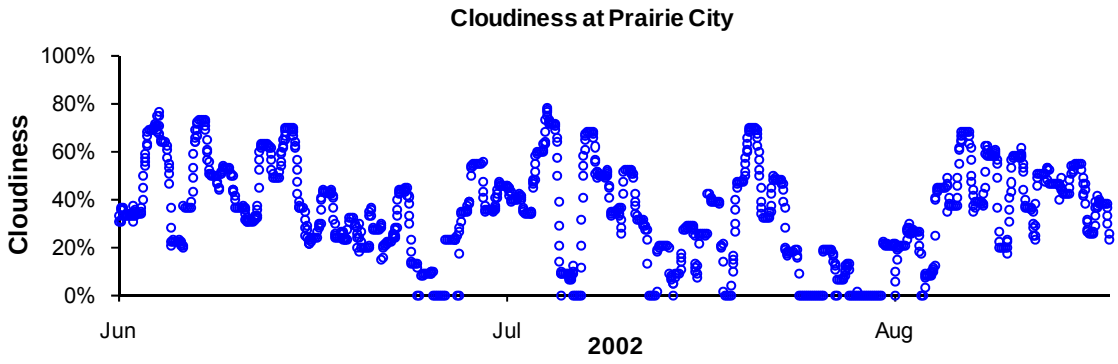

Figure A-60, b

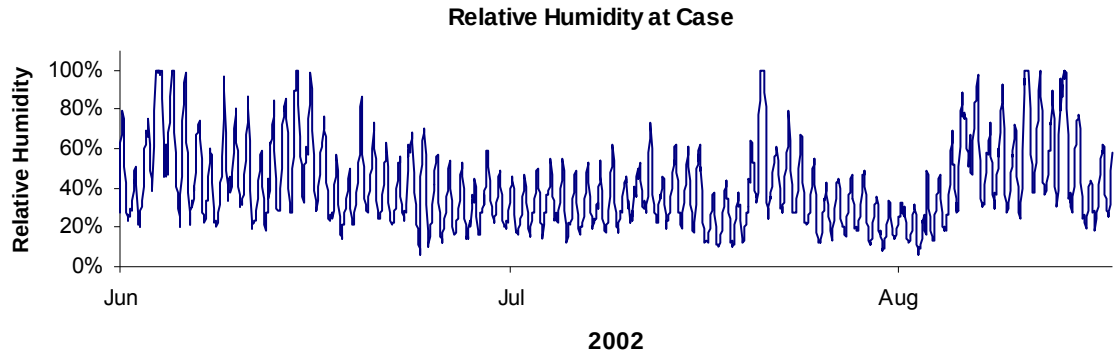

Figure A-60, c

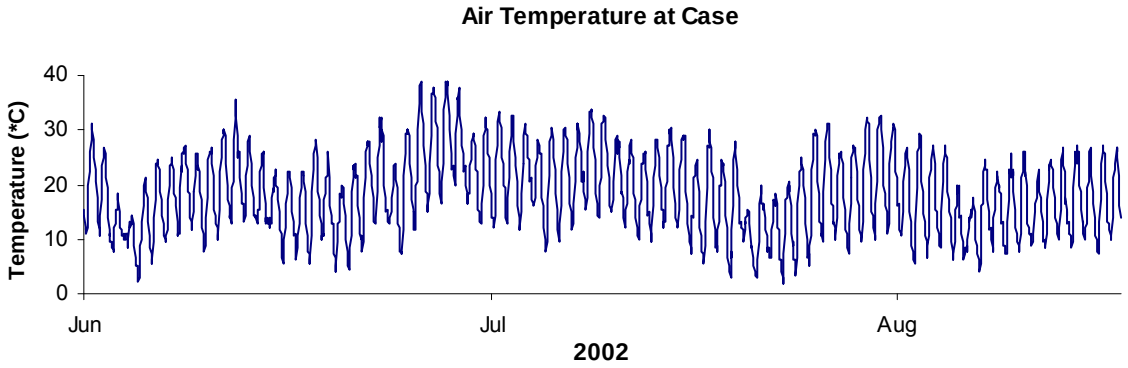

Figure A-60, d

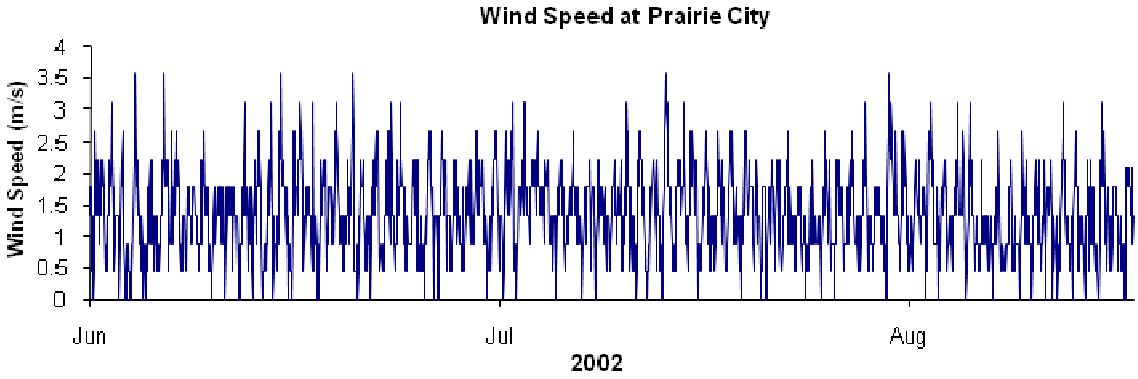

Flow and Temperature of Boundary Condition

The most upstream point of the North Fork John Day River model was downstream of Baldy Creek at river km 172.9. North Fork flow was measured at thirteen sites along the model corridor in early August near or on the day of the 2002 TIR flight. This included a 9/8/2002 measurement at the model upper boundary. In order to estimate the boundary flow on other days the Monument flow gage was utilized. North Fork boundary flows were estimated as daily averages reported for the Monument gage multiplied by 0.0674, which is the 9/8/2002 measured flow at the boundary divided by that at the gage. A temporal flow profile is shown in **Figure A-61**. The temperature inputs at that point were measured by a continuous monitoring logger (**Figure A-62**, DEQ monitoring, LASAR).

Figure A-61. Volumetric flow of the boundary condition of the North Fork John Day River model

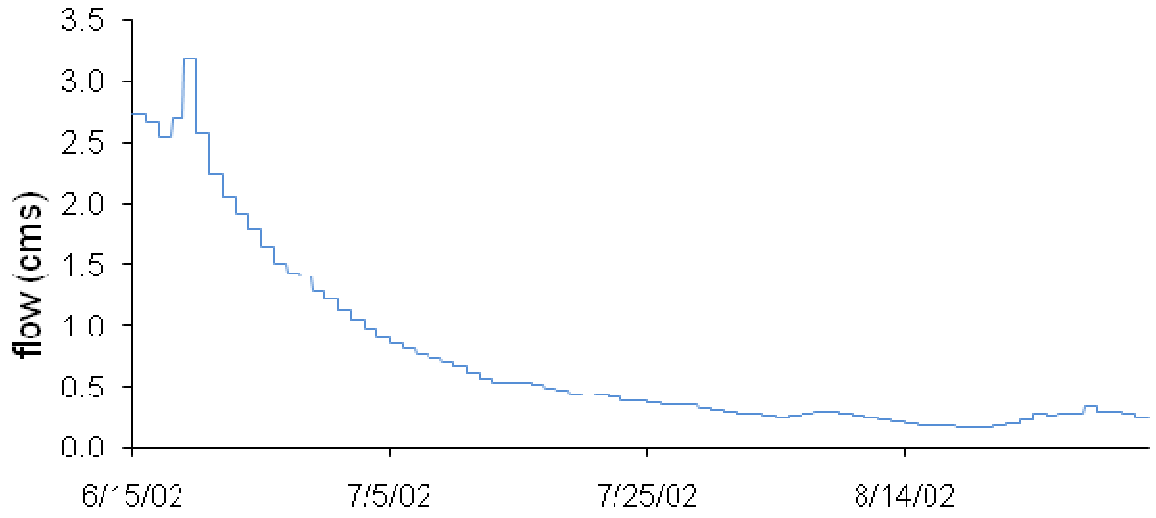

Figure A-62. Temperature of boundary condition of the North Fork John Day River model

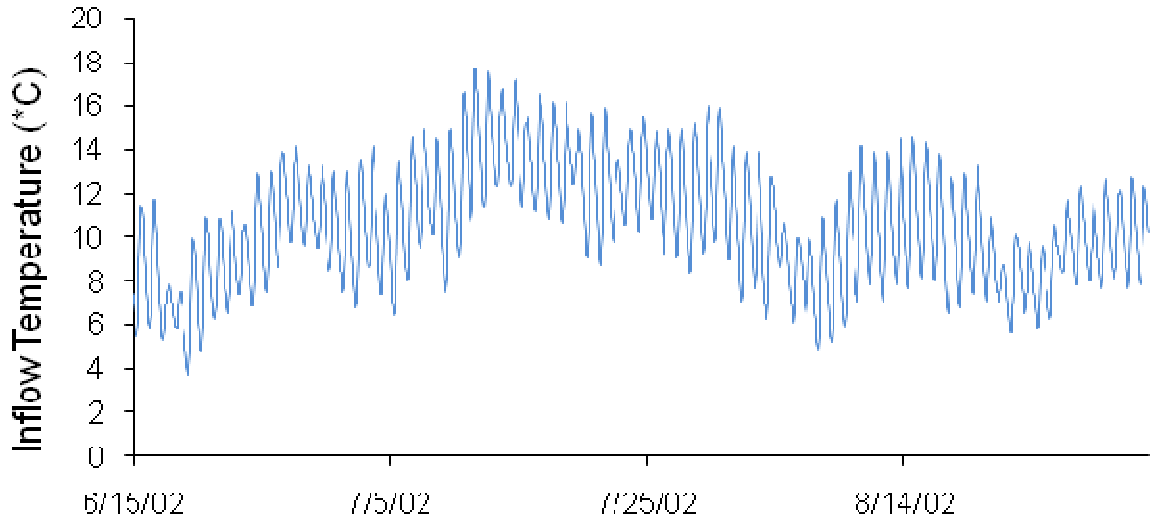

Flow Inputs

Thirty tributaries were represented as water inputs to the North Fork John Day River model (**Table A-19**). Input flows were derived using several methods. There were only two continuous flow data sets collected on the tributaries, Middle Fork John Day River at Ritter and Camas Creek, during the model period (**Figure A-63** and **Figure A-64**). Instantaneous flow measurements were collected by DEQ on some tributaries in August 2002. For these tributaries, the daily record was estimated by applying the Ritter/synoptic flow ratio, on the day of the synoptic measurement, to the Ritter daily record for the model period. Flow data was entirely unavailable for many other tributaries. For these, the model period record of the Ritter gage was proportioned to the un-measured tributary, based on the drainage area ratio by approximating the area 1:100,000 stream layer. For two tributaries, flow was based on temperature balance calculations derived from TIR data and the Camas Creek records. Where appropriate, these values were then varied during model calibration to match instream measurements (termed 'calibration factor' in **Table A-19**). Finally, the continuous flow records on the North Fork John Day River at

Monument were compared to the model prediction at the same point (river km 24.25). The difference in the flow was added into the model as represented by a "calibration flow" tributary near the Middle Fork John Day River (**Figure A-65**). Water diversions and withdrawals were spatially based on OWRD's water rights data and represented in the model by many constant gradual water withdrawals as well as one larger out-flowing tributary at a concentrated area of withdrawals. The amount of water withdrawal increased during the later part of the model season, probably correlated with increased irrigation (**Figure A-66** and **Figure A-67**).

Table A-19. Flow inputs and rates for the North Fork John Day River model

Stream km	Location name	Based on	Flow factor	Calibration factor
164.40	Onion Ck	Watershed area	0.009	--
163.80	Trail Ck	Instantaneous flow measurement	0.094	--
159.70	Trout Ck	Watershed area	0.023	--
153.85	Crane Ck	Watershed area	0.016	--
146.30	Bear Gulch on left	Watershed area	0.006	--
141.40	Granite Ck	Instantaneous flow measurement	0.268	1.5
139.40	Backout Ck	Watershed area	0.014	2.0
134.85	Glade Ck	Watershed area	0.006	2.0
129.50	Basin Ck	Watershed area	0.013	4.0
123.60	Big Ck	Watershed area	0.142	3.2
118.20	Oriental Ck	Instantaneous flow measurement	0.020	4.0
115.05	Otter Ck	Watershed area	0.005	4.0
105.50	Texas Bar Ck	Instantaneous flow measurement	0.018	--
97.20	Desolation Ck	TIR temperature balance	1.062	1.5
96.45	Meadowbrook Ck	Watershed area	0.152	2.0
91.45	Camas Ck	Recorded measurements	--	--
75.50	Spring (LB)	Watershed area	0.001	--
72.10	Stony	Watershed area	0.037	--
61.95	Potamus	Watershed area	0.097	--
60.40	Mallory	Watershed area	0.038	--
56.60	Ditch	Watershed area	0.023	--
51.65	Middle Fork	Recorded measurements	--	--
44.80	Cabin	Watershed area	0.013	0.8 (after 8/1)
35.95	Wall	Watershed area	0.380	0.8 (after 8/1)
27.85	Deer	Watershed area	0.084	--
25.35	Cottonwood	TIR temperature balance	0.500	--
8.30	Rudio	Instantaneous flow measurement	0.016	--
51.00	Calibration flow	calibration	--	--

Figure A-63. Measured flow record used as basis for watershed area and instantaneous flow measurement methods

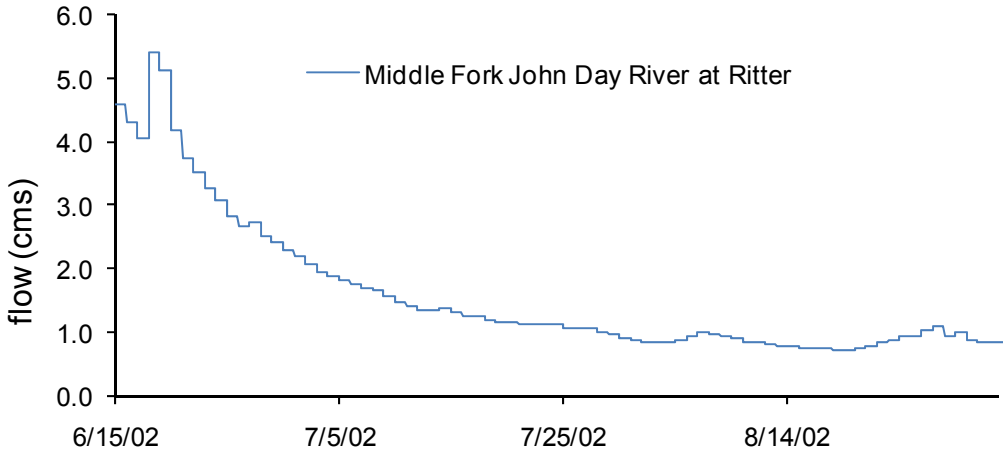

Figure A-64. Measured flow record used as basis for TIR temperature balance method

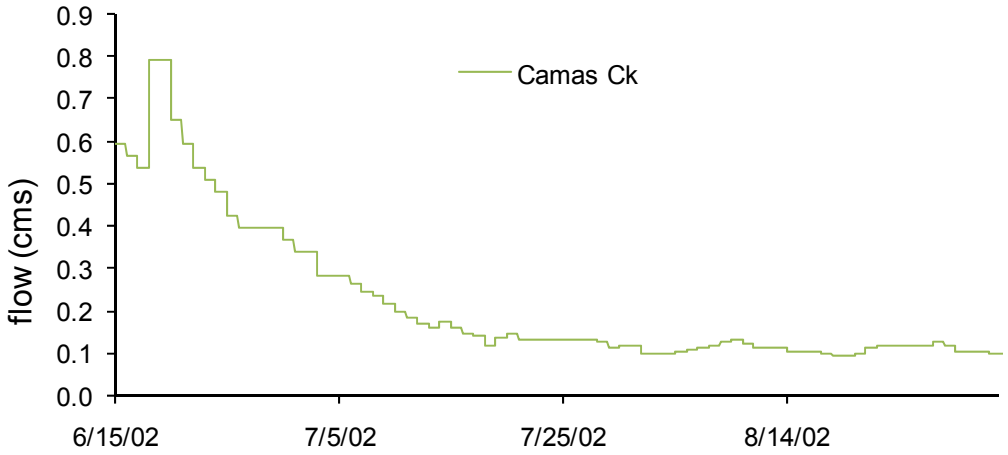

Figure A-65. Calibration inflow to the North Fork John Day River model at river km 51.00

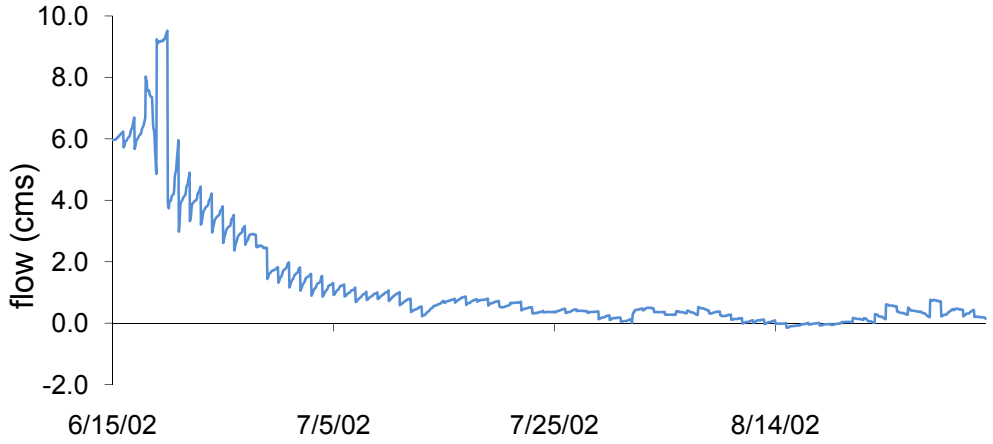

Figure A-66. Withdrawals from the North Fork John Day River model (June 15 – July 31, 2002)

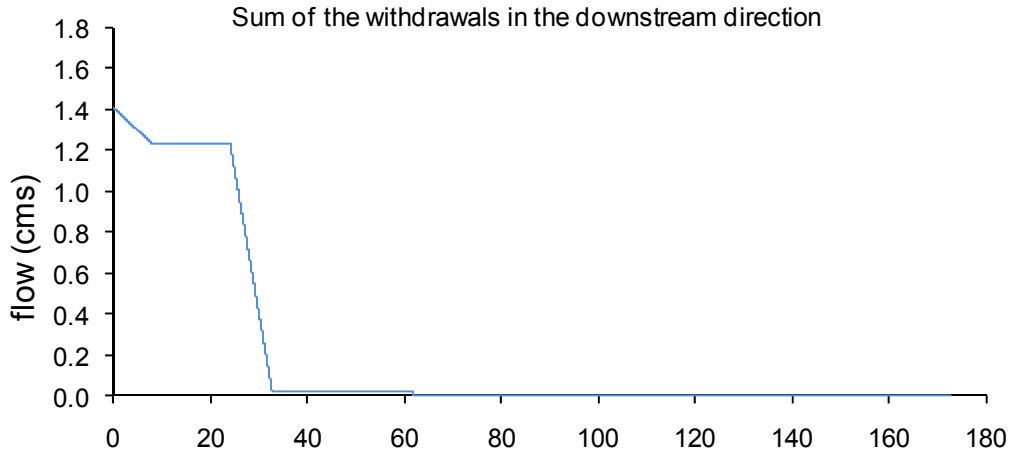

Figure A-67. Withdrawals from the North Fork John Day River model (August 1 – September 1, 2002)

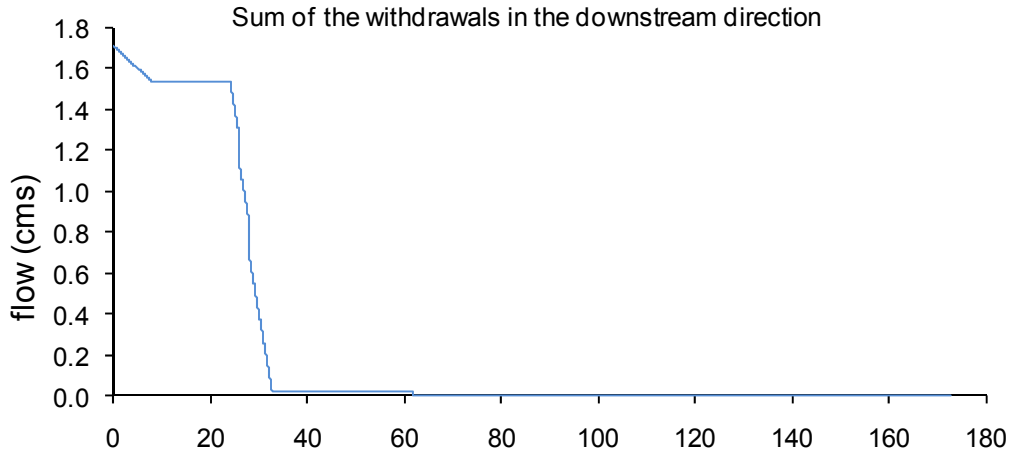

Flow Calibration

The modeled flows resulting from the above inputs were compared with flow measured at North Fork John Day River at Monument (**Figure A-68**). In addition, the longitudinal performance of the North Fork John Day River model was compared to field measurements collected on Aug 8 and 9, 2002 (**Figure A-69, Figure A-70, Figure A-71,** and **Figure A-72**).

Figure A-68. Temporal flow profile at river km 24.25 after calibration

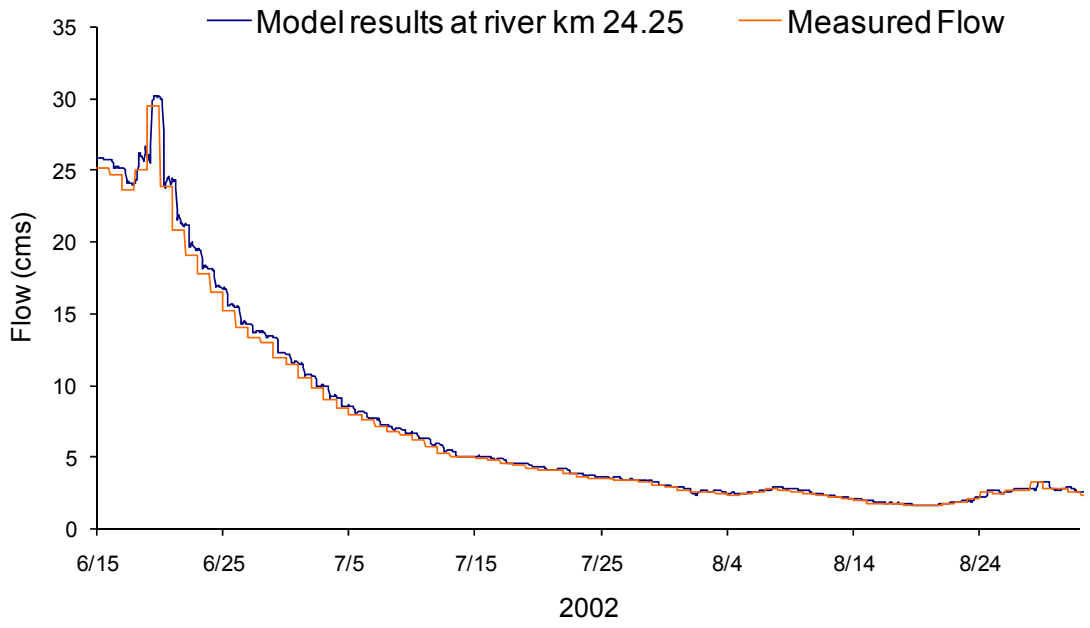

Figure A-69. Longitudinal profile of model results with measured flow. Model results are represented by lines and measurements by points

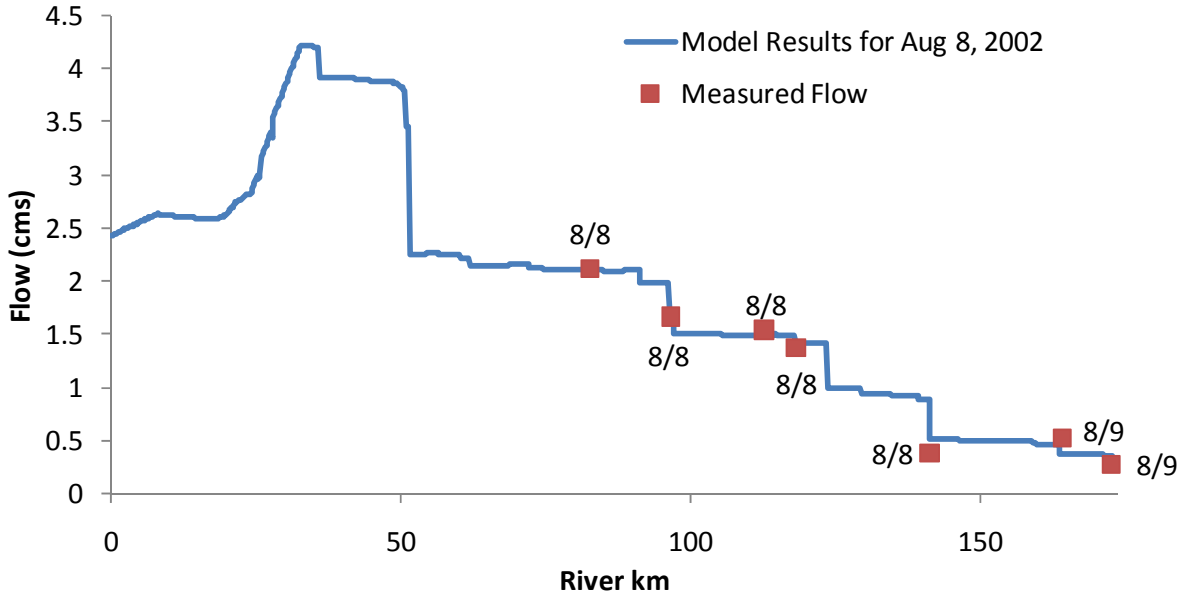

Figure A-70. Longitudinal profile of model results on Aug 8, 2002 with measured velocity. Model results are represented by lines and measurements by points

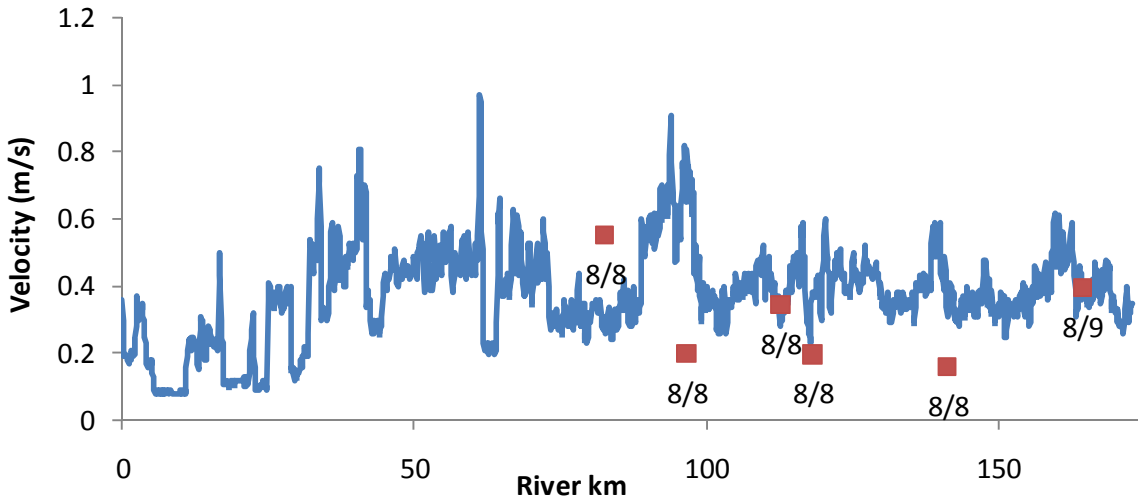

Figure A-71. Longitudinal profile of model results on Aug 8, 2002 with measured hydraulic widths. Model results are represented by lines and measurements by points

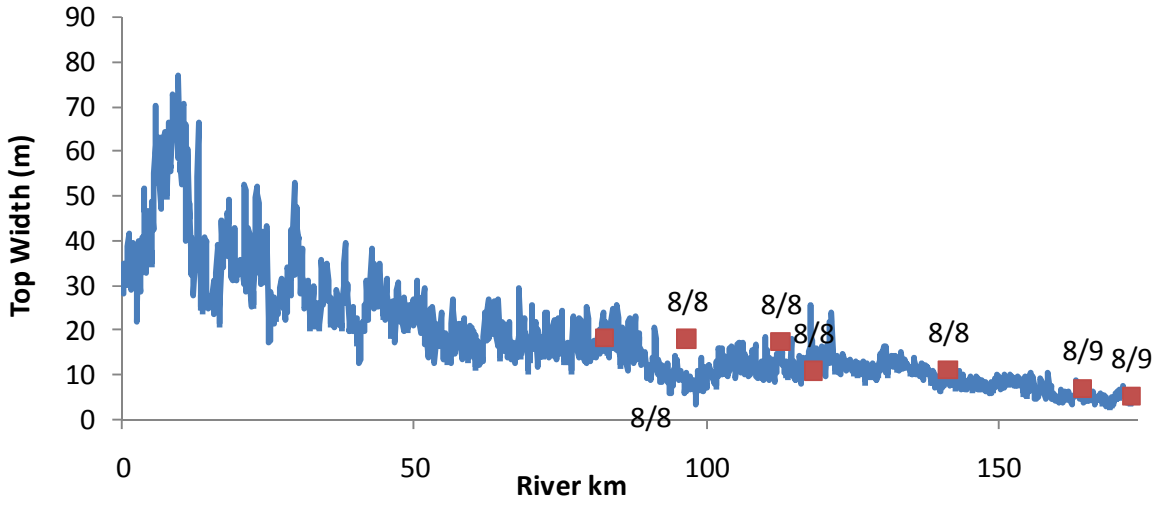

Figure A-72. Longitudinal profile of model results on Aug 8, 2002 with measured hydraulic depths. Model results are represented by lines and measurements by points

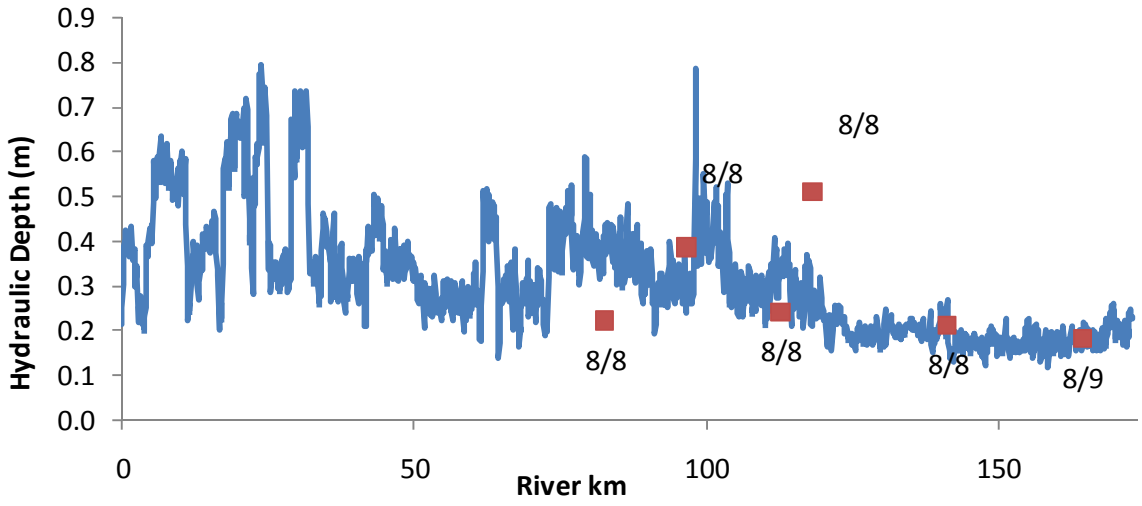

Temperature Input

There were six complete continuous temperature data sets collected on tributaries during the model period (**Figure A-73, Figure A-74,** and **Figure A-75**). Eight tributary temperature data sets were discontinuous during some part of the model period (**Figure A-76, Figure A-77, Figure A-78,** and **Figure A-79**). In order to estimate temperatures for data gaps, a generic data set was prepared for the model year, by compositing measured data from different sites. Compositing served because no single site was represented with year round data. A generic array provides a template that reflects the temporal pattern for the period and can be adjusted in magnitude to "fit' with other data. *Though year round modeling was not employed due to other data and model capability limitations, the generic record was prepared for the full year encompassing the model period as a starting point (see inset below).* The generic data set (**Figure A-80**) is based on streams from across the North Fork drainage area, as shown in the following inset, which includes the Middle Fork drainage. Accordingly, it serves to address both subbasins.

This workbook produces a single full year water temperature dataset synthesized from 4 other incomplete records with the objective of generating a typical diel and daily fluctuation for Middle Fork and North Fork tributaries, that can be proportioned to other records to fill in data gaps.

For the modeled rivers, no single QA data record addresses the entire model year
In order to represent a full year, records are combined from different sites

Galena	Mid Fk	1/1-3/14
abv Desolation	North Fk	1/1-10/27
Lower North Fork trib	Rudio Ck	1/2-5/30
Sunshine RS	Mid Fk	6/4 - 11/14

Records overlap, so the selection within the overlap was based on this hierarchy, from with first preference from top to bottom:

- ► Mid Fk at Sunshine RS
- ► Mid Fk at Galena
- ► Rudio Creek (North Fork trib
- ► N fk abv Desolation

Other Notes

►The data were screened to replace all negative numbers with zeroes.
►1.0 degrees Celsius was subtracted from Rudio, for fit
►The North Fork was given least preference, because though it covered a gap otherwise unaddressed, its diel is low when compared to typical mid fk tributaries

To complete the discontinuous data sets, the generic data array was adjusted to overlap the measured data. For the streams having measured continuous temperature data, but not for the full simulation period, the gaps were filled with the generic data set and these cells multiplied uniformly by a single adjustment factor of actual/generic at the point where the data sets joined. In some instances gaps in the array occurred for times before and after the measured array, and a different adjustment factor would be used for each, as needed to 'edge-match' the data. If a gap occurred within a measured array, it would be filled with generic data, in this case adjusted to split the difference between any beginning and ending mismatch.

Temperature data were unavailable for many tributaries and springs. For these, the generic temperature record developed for this basin was proportioned to the un-measured tributary, based on the instantaneous TIR temperature measurement collected in August 1998 or 2002. For tributaries with no measured continuous, discontinuous, or TIR data, a factor of 0.850 was applied to the generic data (**Table A-20)** as an adjustment that placed its temporal profile in the mid-range of North and Middle Fork tributary measured arrays. Additional flow that was added as a tributary for calibration was assigned a temperature profile from the Middle Fork John Day River (**Figure A-81**).

Figure A-73. Tributary continuous temperature profile

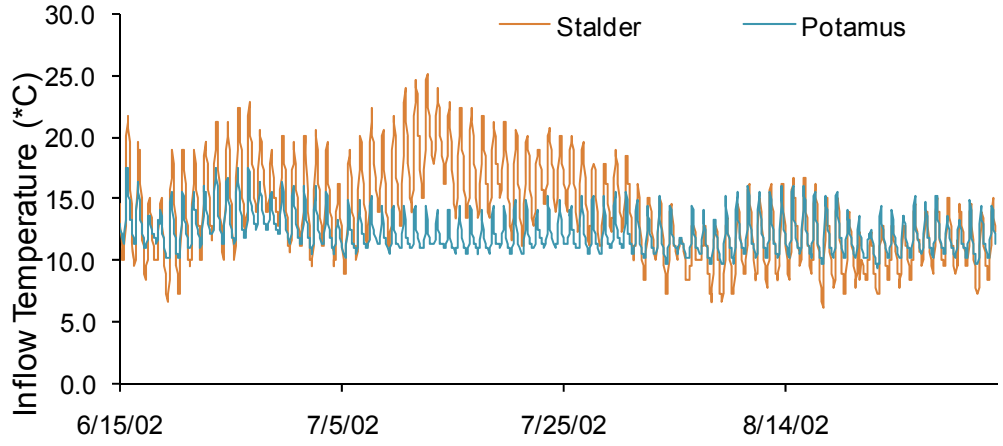

Figure A-74. Tributary continuous temperature profile

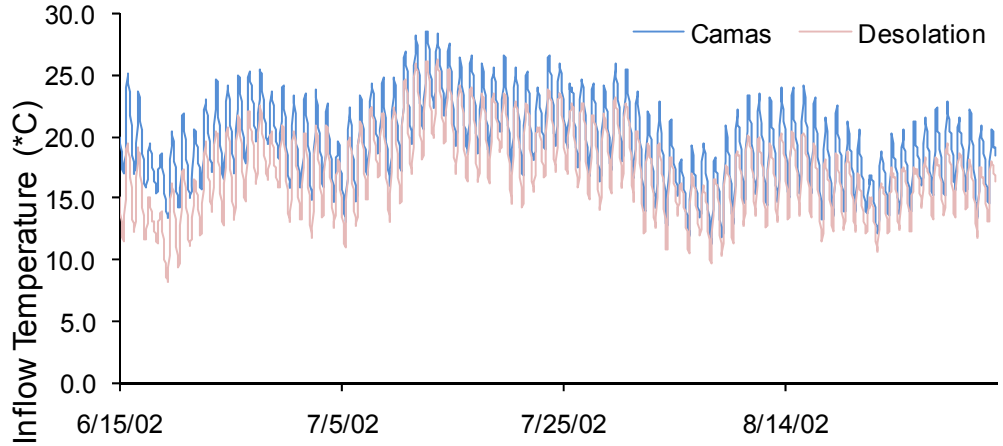

Figure A-75. Tributary continuous temperature profile

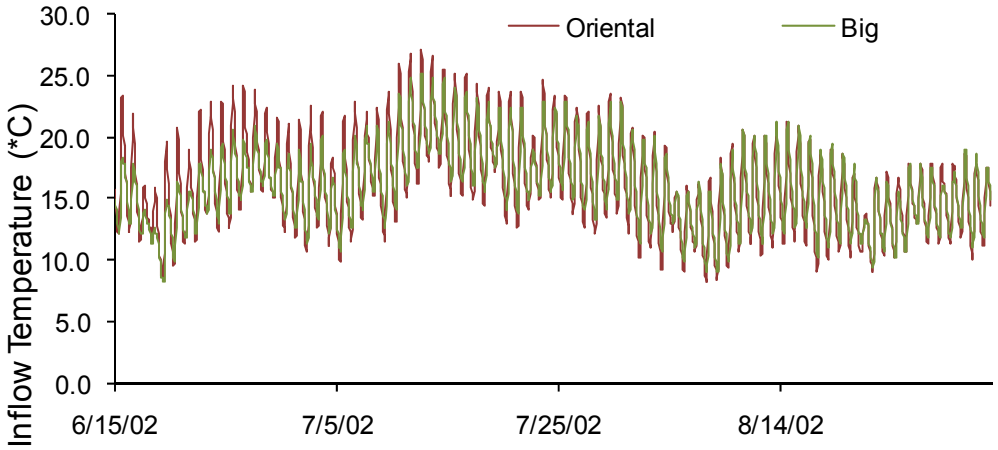

Figure A-76. Discontinuous inflow temperature data sets

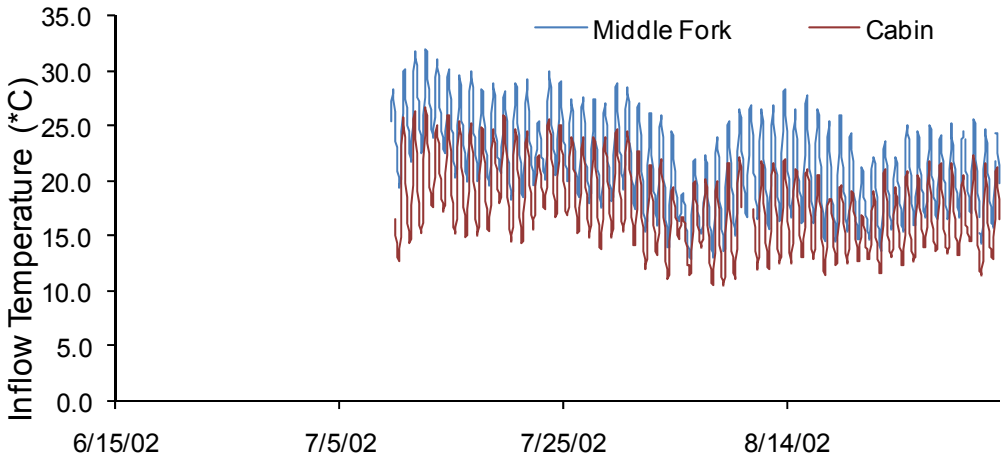

Figure A-77. Discontinuous inflow temperature data sets

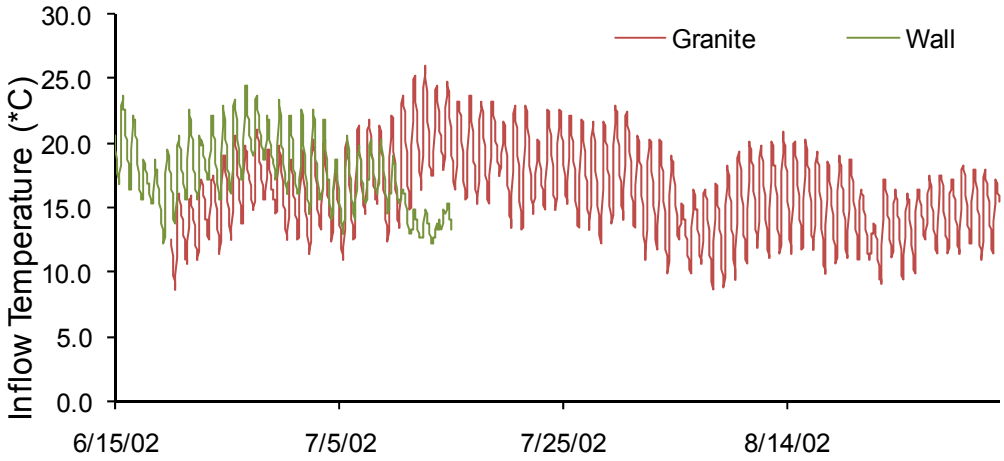

Figure A-78. Discontinuous inflow temperature data sets

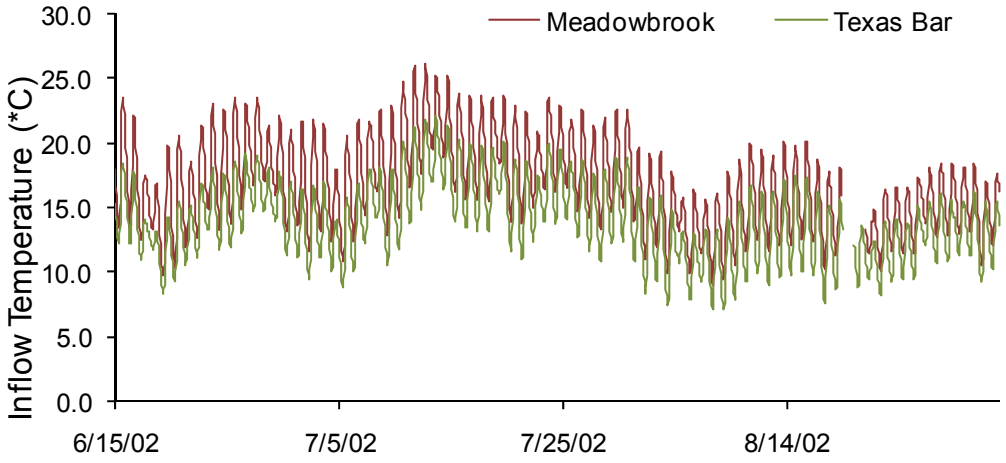

Figure A-79. Discontinuous inflow temperature data sets

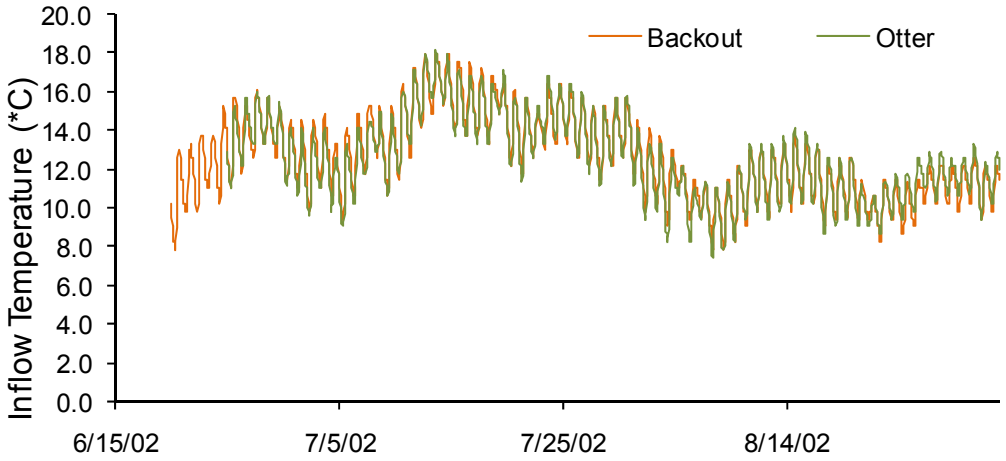

Figure A-80. Generic temperature set

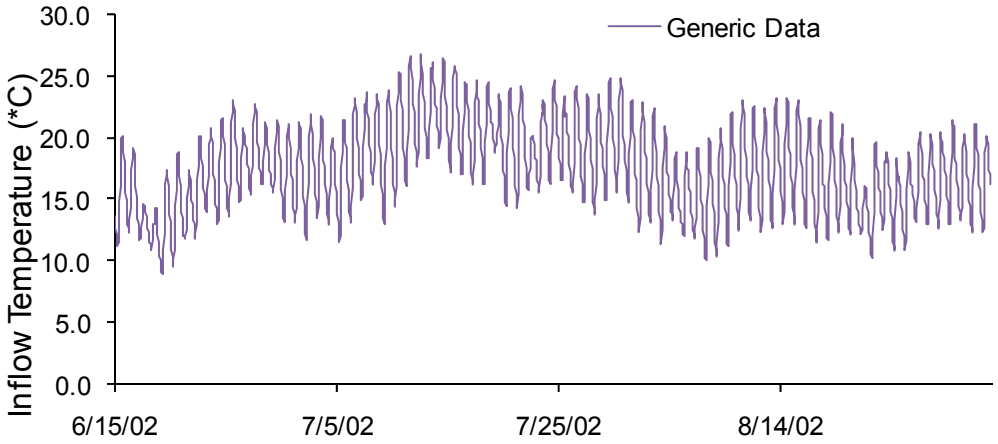

Table A-20. Temperature inputs and rates for the North Fork John Day River model

Stream km	Location name	Based on	Temperature factor
164.40	Onion Ck	TIR 1998	0.765
163.80	Trail Ck	TIR 1998	1.075
159.70	Trout Ck	TIR 1998	1.027
153.85	Crane Ck	TIR 1998	0.923
146.30	Bear Gulch on left	TIR 1998	0.880
141.40	Granite Ck	Discontinuous data set	1.012
139.40	Backout Ck	Discontinuous data set	0.823
134.85	Glade Ck	TIR 1998	1.063
129.50	Basin Ck	TIR 2002	0.743
123.60	Big Ck	Continuous data set	--
118.20	Oriental Ck	Continuous data set	--
115.05	Otter Ck	Discontinuous data set	0.779
105.50	Texas Bar Ck	Discontinuous data set	0.799
97.20	Desolation Ck	Continuous data set	--
96.45	Meadowbrook Ck	Discontinuous data set	0.940
91.45	Camas Ck	Continuous data set	--
75.50	Spring (LB)	TIR 2002	0.992
72.10	Stony Ck	Generic	0.850
61.95	Potamus Ck	Continuous data set	--
60.40	Mallory Ck	Continuous data set	--
56.60	Ditch Ck	Generic	0.850
51.65	Middle Fork John Day	Discontinuous data set	1.109
44.80	Cabin Ck	Discontinuous data set	0.859
35.95	Wall Ck	Discontinuous data set	0.646 +4
27.85	Deer Ck	Generic	0.850
25.35	Cottonwood Ck	Generic	0.850
8.30	Rudio Ck	Generic	0.850
51.00	Calibration flow	Middle Fork	--

Figure A-81. Temperature of calibration inflow to the North Fork John Day River model (cont.)

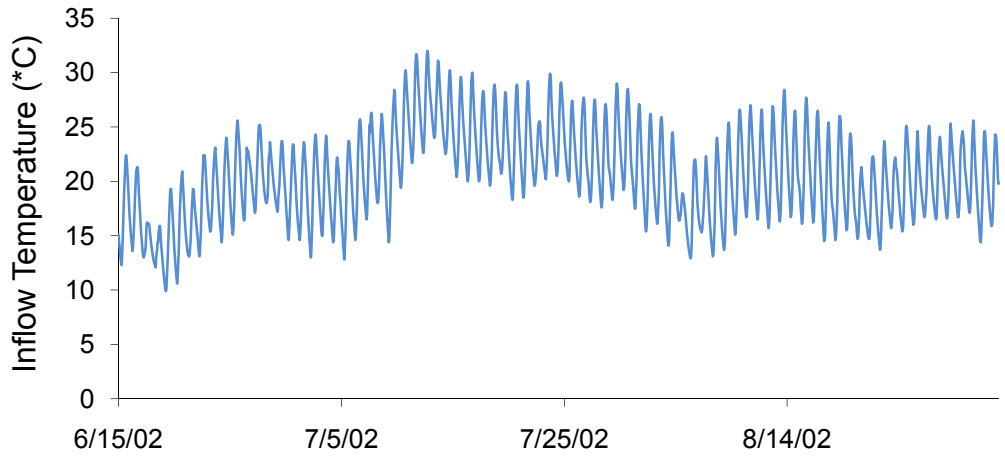

Temperature Calibration

DEQ, Umatilla National Forest, and BLM provided continuous temperature data for calibration in the North Fork John Day River at 10 instream locations. The model generally reproduces spatially and temporal varying temperature measurements (**Table A-21, Figure A-82, Table A-22,** and **Figure A-83**). The most downstream continuous data logger (reference point J) was audited twice, at the beginning and end of its deployment. Between the audit dates, the logger recorded daily maximum temperatures at 10am. Compared with the data from the same point in 2004, the temperature profile appears shifted by 7 hours, possibly explaining the poor error statistics at that point. The longitudinal profile generally matches the TIR data collected on 8/11/2002, except the uppermost and lowermost 20 km. TIR data were collected in two separate years, but overlapped spatially by 45.2 km. The non-overlapping TIR data collected in 1998, upstream of river km 141.90, were adjusted by subtracting the typical difference within the zone of overlap, 3.5°C, from each median value to approximate 2002 temperatures. The upper river rapid increase in the 1998 adjusted temperatures was captured by the model. The modeled results in the most downstream 20 km did not match the TIR profile. The model results are warmer than the observations. Adjusting the parameters Manning's n, channel morphology and percent hyporheic exchange did not create a closer visual match. See previous statistics discussion at the beginning of **Section 3.1** for definitions. Given the limited TIR data collection, the model was deliberately calibrated to decrease the error associated with the instream continuous temperature loggers (see following section) rather than calibrating to the TIR.

Table A-21. TIR error statistics

Error type	Value
Mean	-0.44
Absolute mean	1.37
Root mean square	1.79
Nash-Sutcliffe	0.74

Figure A-82. Longitudinal profile of measured temperatures using Thermal Infrared Radiometry and model results

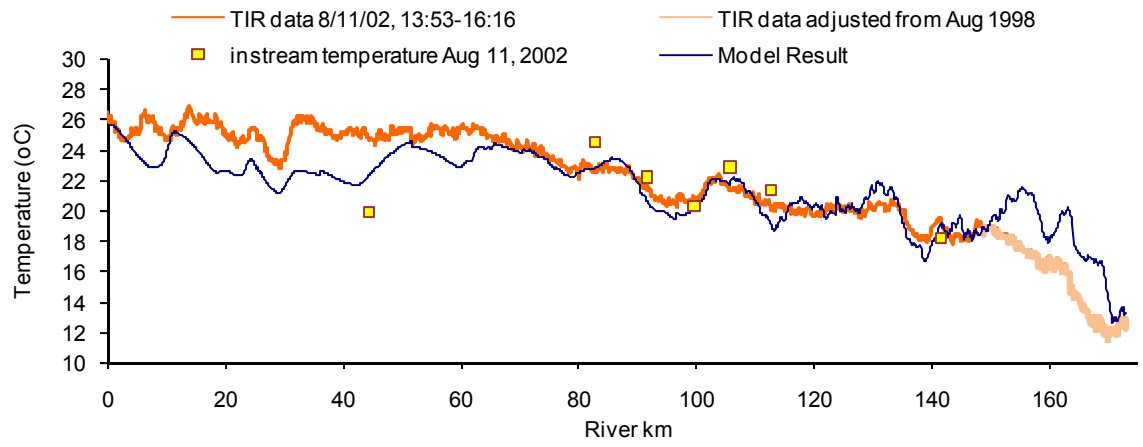

Table A-22. Continuous monitoring error statistics

Site Name	Source of temperature data	Ref	rKM	All data				
				n	Mean Error	Abs Mean Error	RMSE	Nash-Sutcliffe
North Fork John Day River above Granite Ck	ODEQ	A	141.50	575	0.84	1.07	1.31	0.77
North Fork John Day River above Big Ck	UNF	B	123.80	1345	-0.56	0.85	1.07	0.92
North Fork John Day River above Camp Creek	UNF	C	112.70	1390	-0.65	1.09	1.48	0.78
North Fork John Day River above Texas Bar Ck	ODEQ	D	105.70	1500	-0.64	1.54	2.08	0.62
North Fork John Day River above Desolation Ck	ODEQ	E	99.60	1848	0.23	0.77	0.98	0.92
North Fork John Day River above Camas Ck	UNF	F	91.55	1775	-0.10	0.74	0.94	0.92
North Fork John Day River below Sulphur Gulch	UNF	G	82.70	930	-0.24	1.49	1.83	0.64
Jd_070	BLM	H	55.95	300	2.97	3.44	3.92	-0.26
Jd_071	BLM	I	44.40	1293	3.00	3.03	3.37	0.12
North Fork John Day River above Rudio Creek	ODEQ	J	8.45	990	-1.61	2.17	2.88	-0.84
				Average	0.32	1.62	1.99	0.46

Figure A-83. Measured steam temperature versus model results

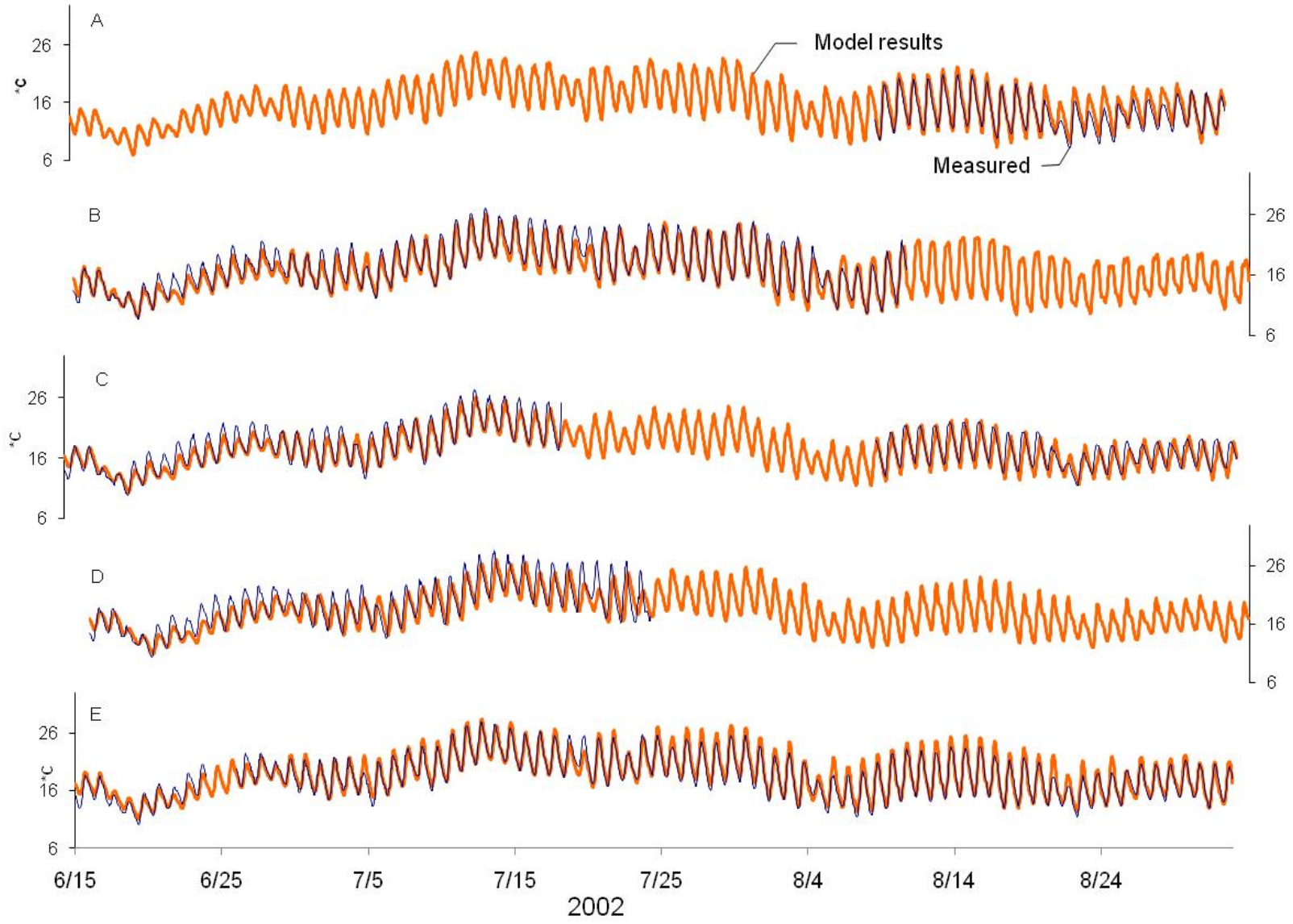

Figure A-83. Measured steam temperature versus model results (cont.)

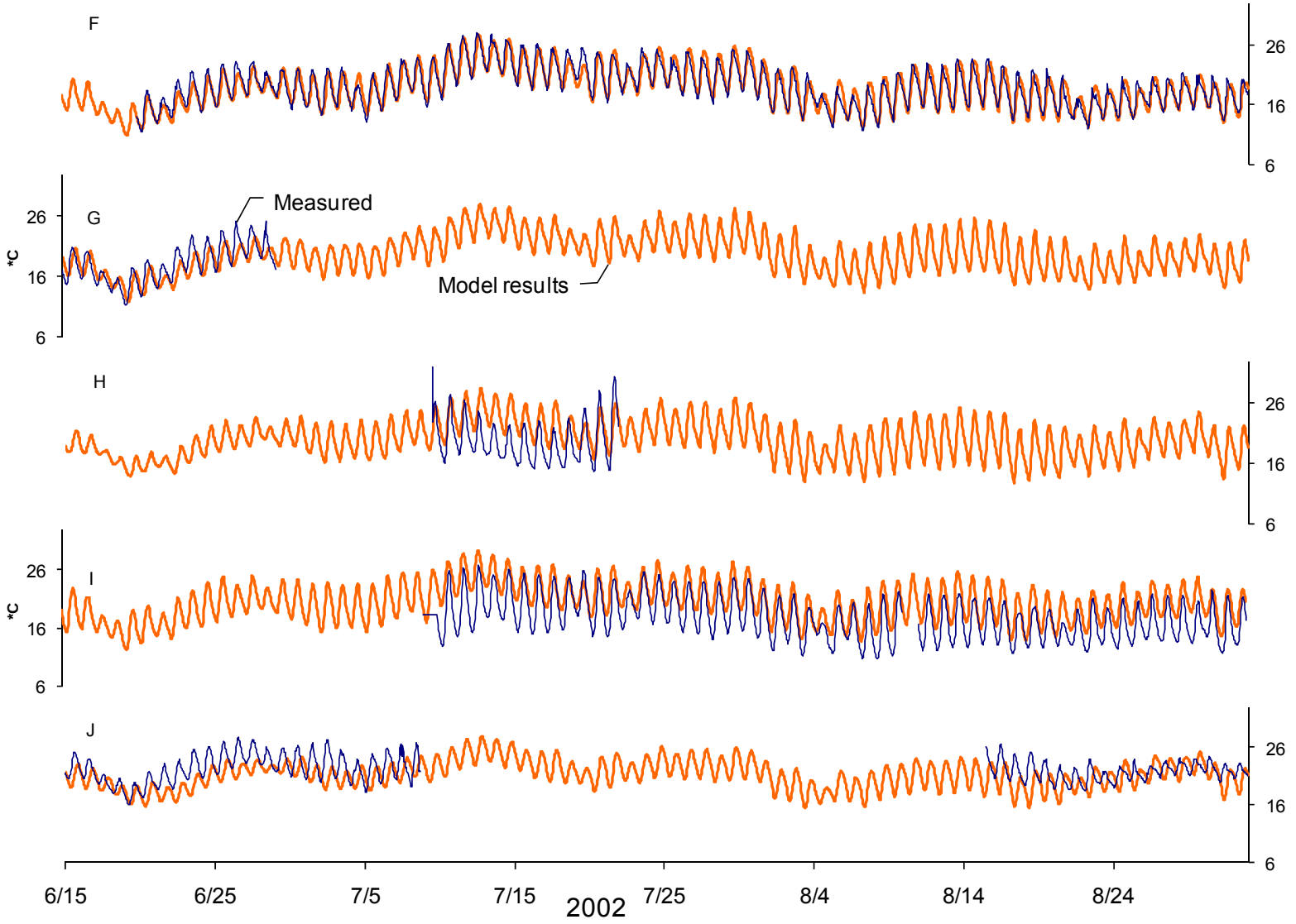

3.4 Middle Fork John Day River

The Middle Fork John Day River is a tributary to the John Day River. The Middle Fork John Day River subbasin comprises an area of 506,784 acres and is referenced by the 4th field Hydrologic Unit Code (HUC) 17070203. Instream temperature was simulated for 112.95 km of the Middle Fork John Day River from mouth to just downstream of confluence with Clear Creek. The following documents the calibration methods and decisions and ultimately describes the model used in the Middle Fork John Day River TMDL.

Overview

Stream Name: Middle Fork John Day River
Model: Heat Source version 8.0.4
Beginning date: 05/01/2002
Ending date: 10/31/2002
Time step: 0.5 minute
Distance step: 200 m
Transverse sample rate: 10m
"Deep alluvium" option on at 12°C
Initial flush condition: 5 days
Extent: mouth to just downstream of confluence with Clear Creek (112.95 km) (**Figure A-84**).

Figure A-84. Extent of the Middle Fork John Day River temperature model

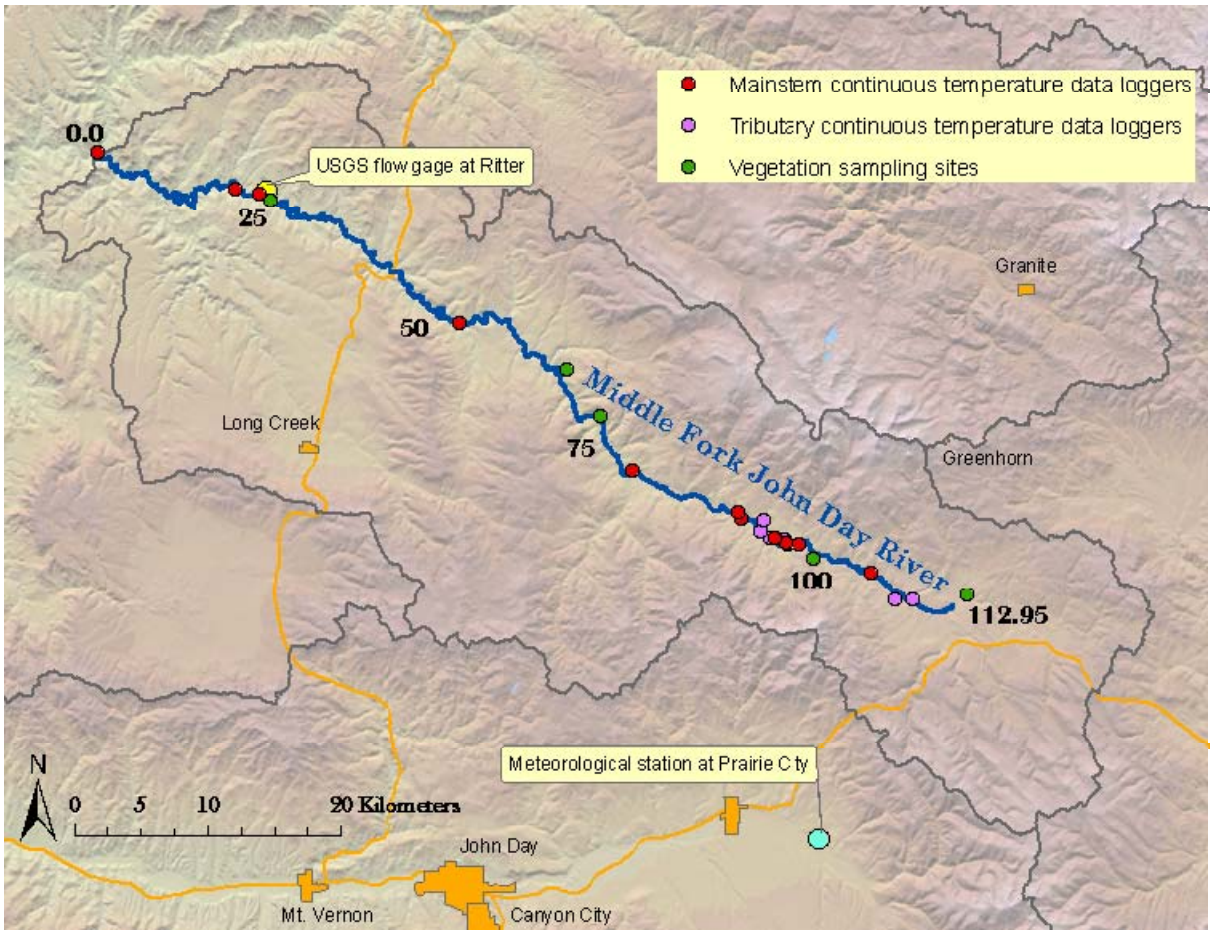

Reach Properties

Table A-23 identifies the sources of spatial GIS data used in the model. See **Section 2.3** for methodology. The reach gradient was determined using DEM files. The reach gradient was averaged over the neighboring seven reaches because overly steep gradients resulted from the coarse DEM scale, leading to numeric instability in the hydraulic routines of the model (**Figure A-85**). The bankfull channel widths were measured from DOQ images and verified by field measurements (**Figure A-86**). Additional aerial images were used as supplemental sources of information for both channel morphology and riparian vegetation mapping. The channel angle z values in the model were based on data collected by DEQ in 2002 and visually fitted trapezoids from surveyed transects (**Figure A-87**). A constant depth of 0.762 m was used, which was the average channel depth (m) from visually fitted trapezoids. Assuming a trapezoidal channel, bottom widths (**Figure A-88**) were estimated using calculated and measured values and **Equation A-3** and the relationship depicted in **Figure A-89** . The wetted widths resulting from the model were compared to the wetted widths calculated based on LiDAR data. In order for the model to simulate the observed wetted widths, the bottom widths were reduced by half. Where appropriate, especially from river km 104.3-112.95, these values were then further reduced during model calibration (reflected in **Figure A-88**). Manning's n and percent hyporheic exchange values were iteratively altered during calibration so that the model temperatures approximately reproduced measured temperatures (**Figure A-90**). No hyporheic exchange was necessary for calibration. Topographic shade angles used in the model are presented in **Figure A-91**. The average of the vegetation heights and densities sampled at each node is presented in **Figure A-92** and **Figure A-93**. Using these channel morphology and shade inputs, the Middle Fork John Day River model's ability to simulate shade is shown in **Figure A-94**.

Table A-23. Spatial Data and Application

Spatial Data	Data Source	Application
10-Meter Digital Elevation Models (DEM)	10-m DEM files provided by OGDC	Measure Stream Elevation and Gradient Measure Topographic Shade Angles
Aerial Imagery – Digital Orthophoto Quads	0.5-m uncompressed National Agriculture Imagery Program (NAIP)	Map Vegetation Map Channel Morphology Measure Active Channel Widths Map Roads, Development, Structures
Thermal Infrared Radiometry (TIR) Stream Temperature Data	Upper watershed 1998 Lower watershed 2002 Watershed Sciences, LLC	Measure Surface Temperatures Develop Longitudinal Temperature Profiles Identify Subsurface Hydrology, Groundwater Inflow, Springs
LiDAR vegetation data	LiDAR 2006 Watershed Sciences, LLC	Verify vegetation heights Measure wetted widths

Figure A-85. Model setup channel elevation and gradient

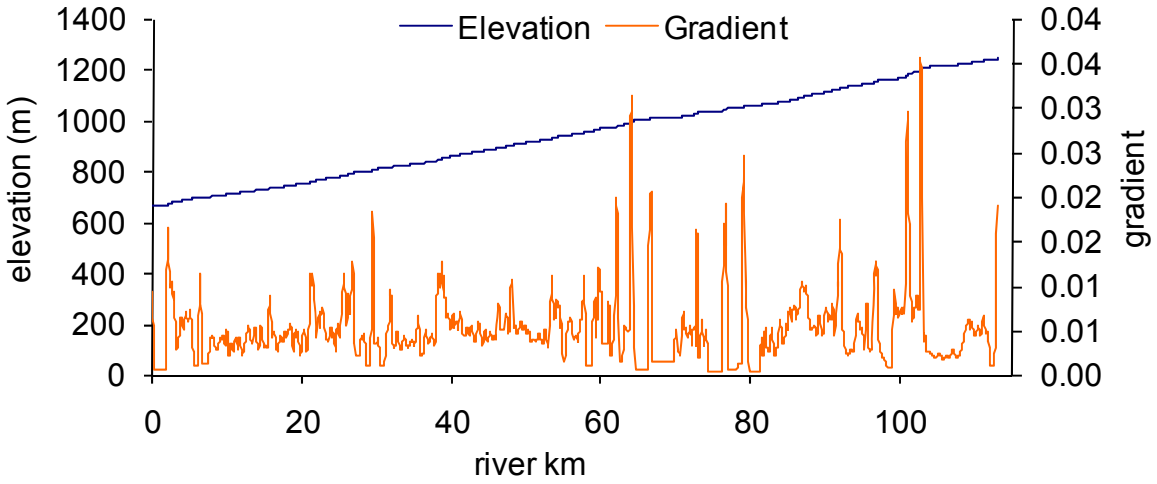

Figure A-86. TTools measurements for bankfull width used to calculate bottom width and channel angle z

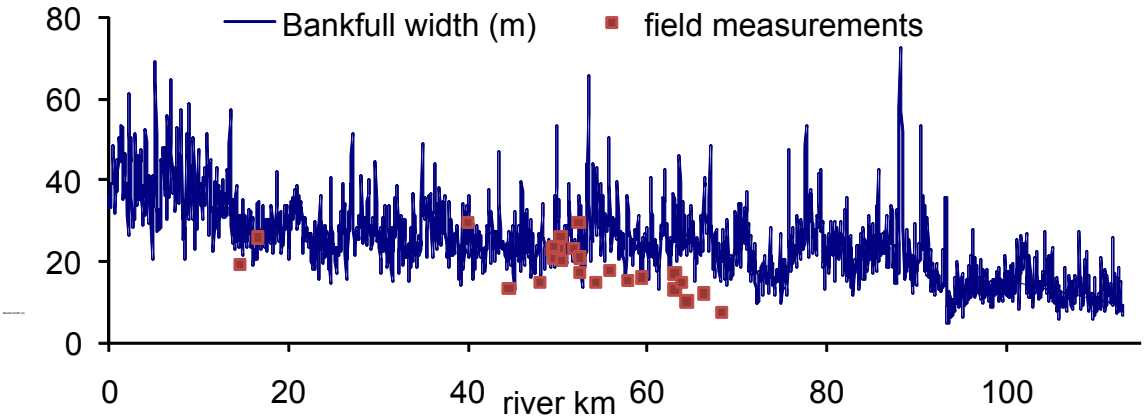

Figure A-87. Model setup for channel angle z determined from sampled bankfull width, cross sectional area, and average depth values used in models

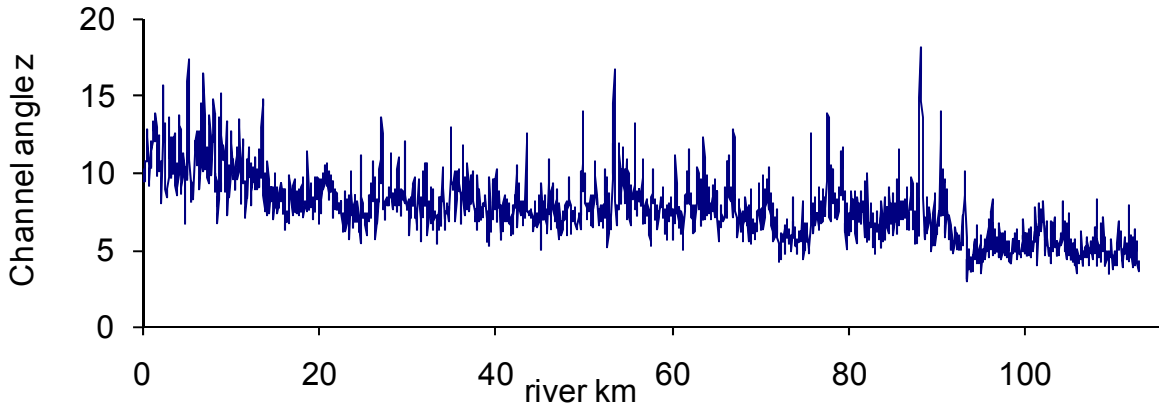

Figure A-88. Model setup for bottom width determined from sampled bankfull width, cross sectional area, and average depth values used in models

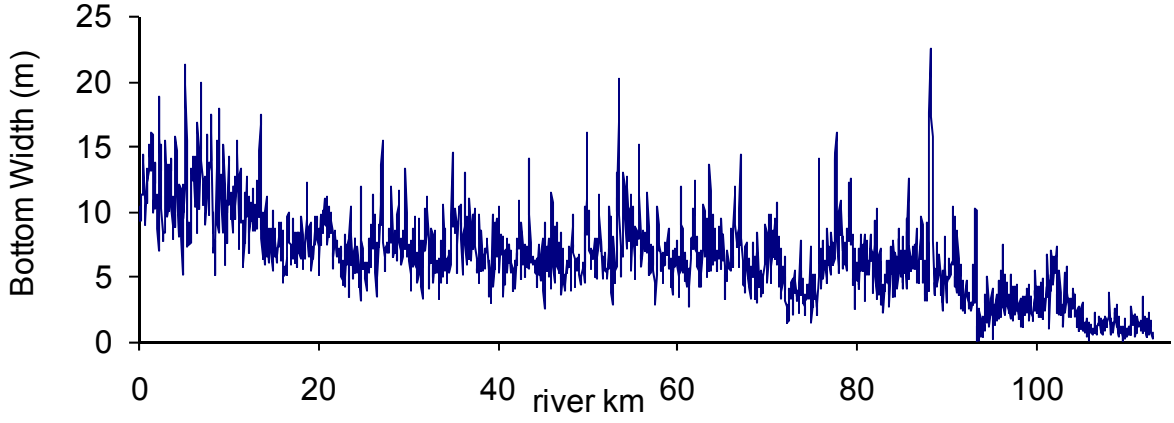

Equation A-3.

$$b_2 = b_1 - 2zD$$

Figure A-89. Calculation of channel angle z for model setup

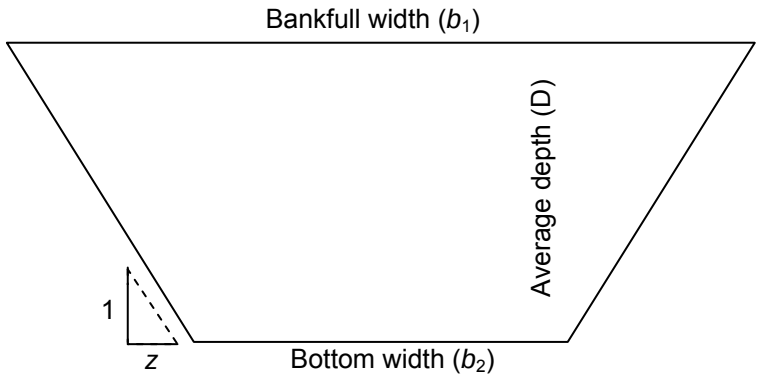

Figure A-90. Model setup for Manning's n and percent hyporheic exchange

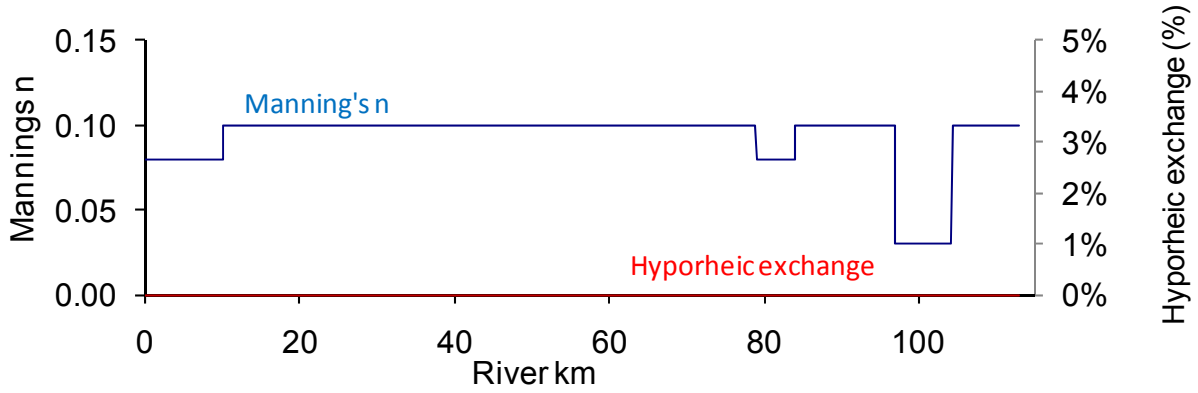

Figure A-91. Model setup for topographic shade angle

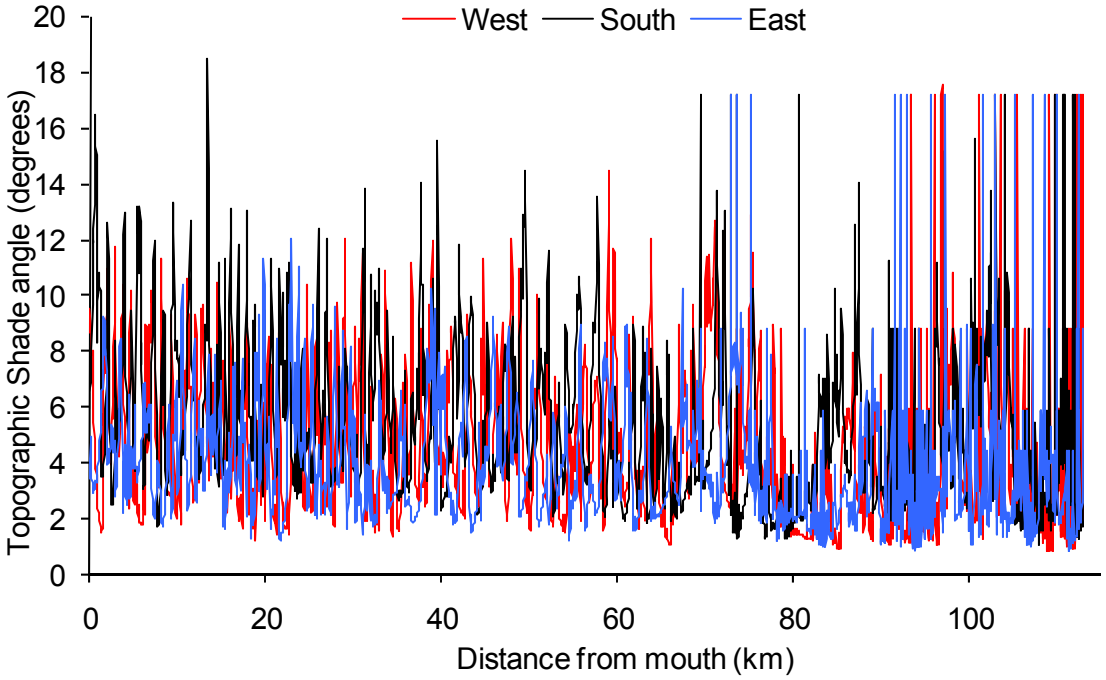

Figure A-92. Model setup for average height of streamside vegetation

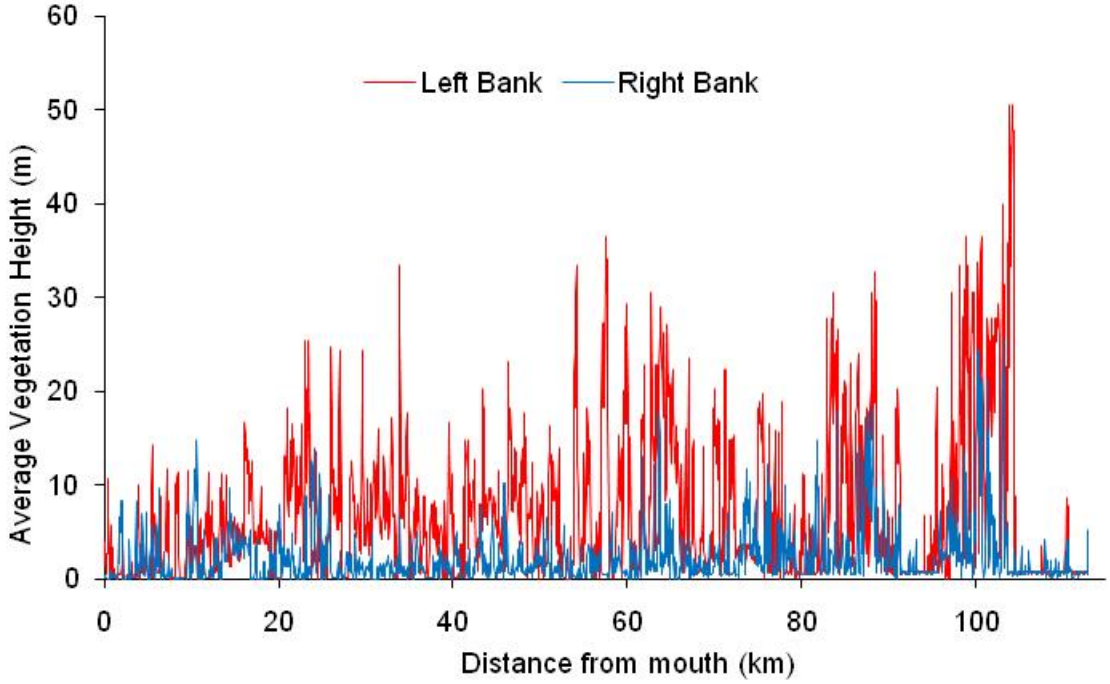

Figure A-93. Model setup for average density of streamside vegetation

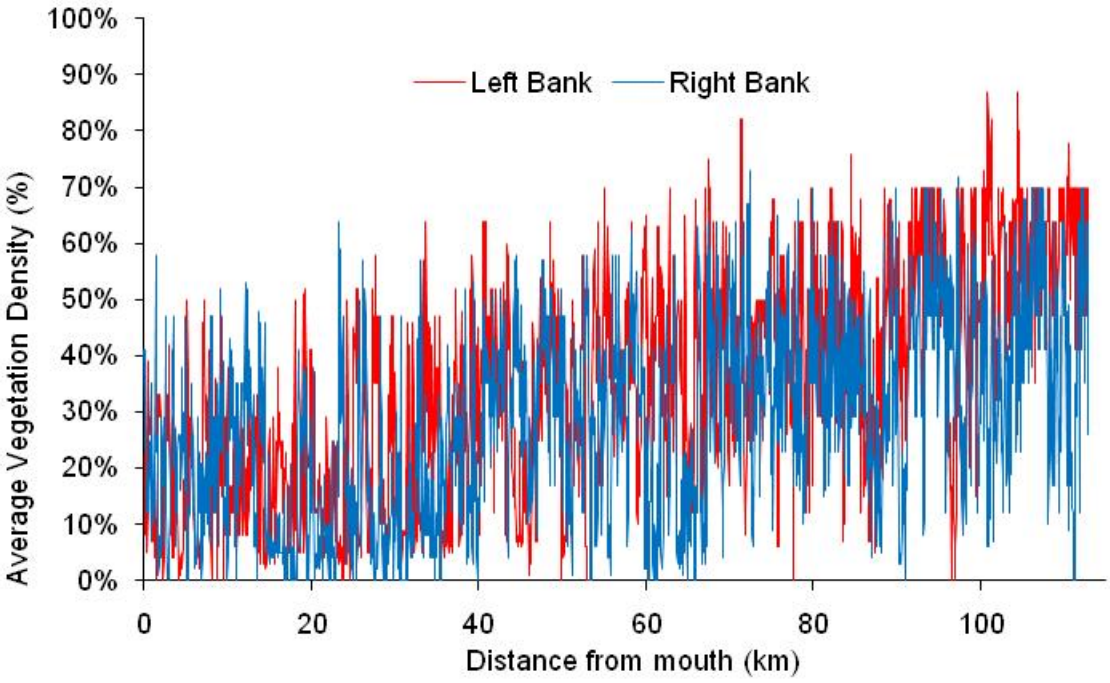

Figure A-94. Predicted shade on Middle Fork John Day River

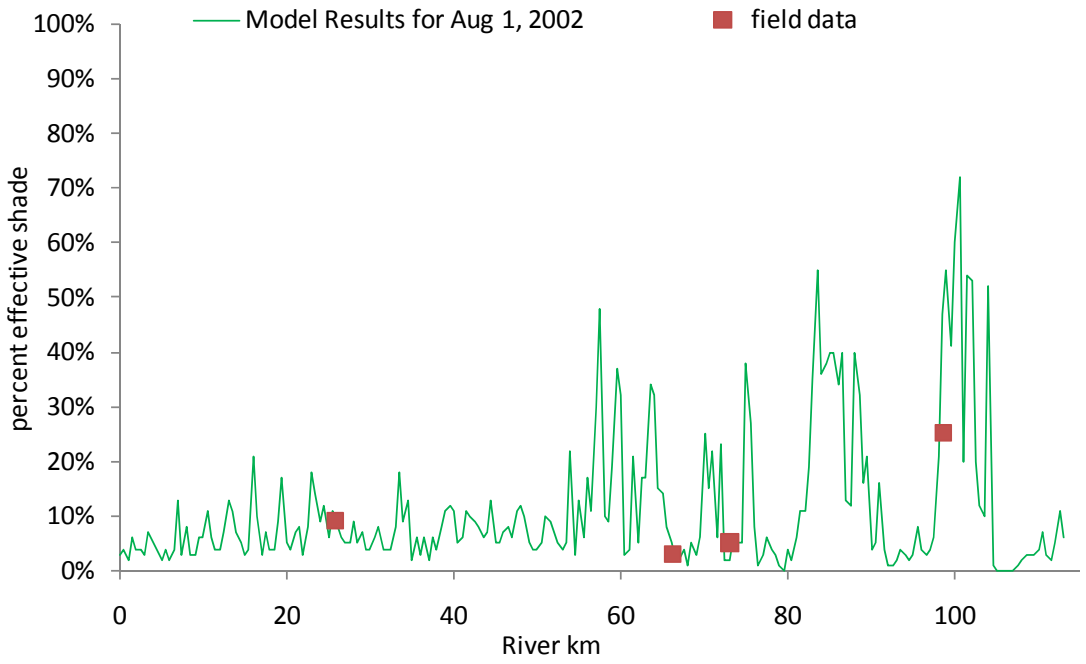

Meteorology

The Middle Fork John Day River model used air temperature, wind speed, relative humidity and solar radiation measurements from the Prairie City meteorological station (**Table A-24**). The air temperature data were adjusted from the Prairie City station to the continuous data node based on elevation and the dry adiabatic lapse rate of 9.8ºC/km, according to the following equation: Adjustment for dry adiabatic lapse rate = 9.8*($Elev_{metstation}$ – $Elev_{contnode}$)/1000, where Elev is elevation in meters (**Table A-25**). Relative humidity from Prairie City was used without any modifications. Wind speed was used from the nearest weather station, although a multiplicative wind sheltering coefficient was applied to the wind speed during calibration (**Table A-25**). Cloudiness was determined by calculating the deviation of measured solar radiation from the theoretical maximum solar radiation on a rolling 24 hour average. The meteorological observations are presented in **Figure A-95, a-d.**

Table A-24. Data inputs for the Middle Fork John Day River model

Site	Source	Elevation (m)	Meteorological Parameters
Prairie City	USBR	1144	cloudiness, wind speed, relative humidity, air temperature

Table A-25. Data inputs by river km

Range (river km)	Adiabatic Adjustment (additive, °C)	Wind sheltering Coefficient (multiplicative)
112.95 - 100.4	-0.6468	1.0
100.4 - 95.9	-0.049	0.75
95.9 - 94.3	0.0294	0.75
94.3 - 91.6	0.1078	0.75
91.6 - 89.5	0.343	0.75
89.5 - 84.2	0.3724	0.75
84.2 - 66.1	0.8526	0.75
66.1 - 36.8	2.1364	0.75
36.8 - 10.2	3.8318	0.75
10.2 - 0.0	4.6844	0.75

Figure A-95. Meteorology inputs for model setup

Figure A-95, a.

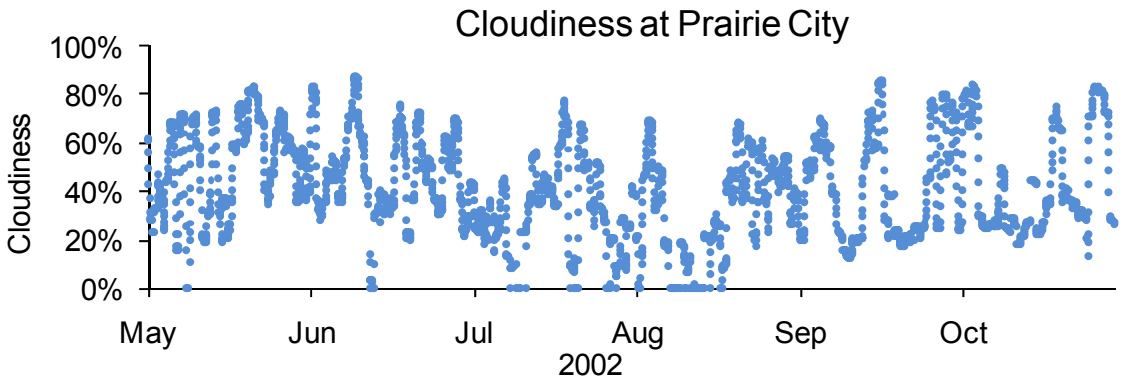

Figure A-95, b.

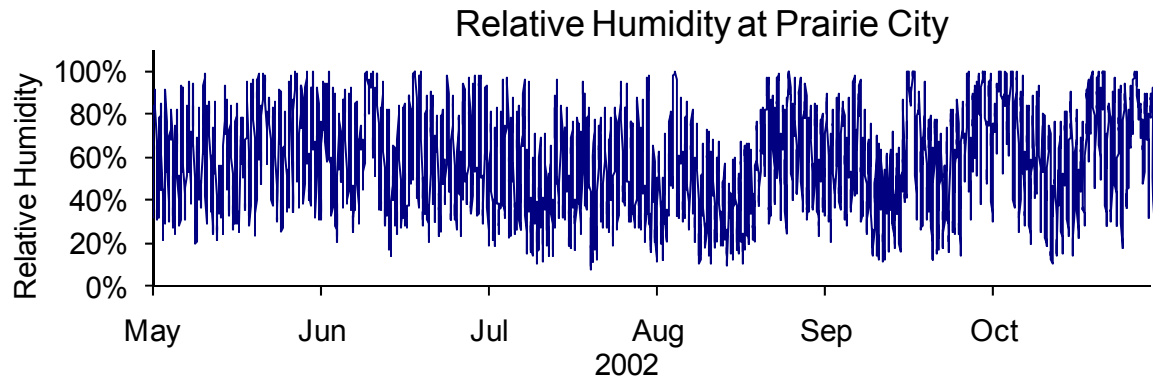

Figure A-95 c.

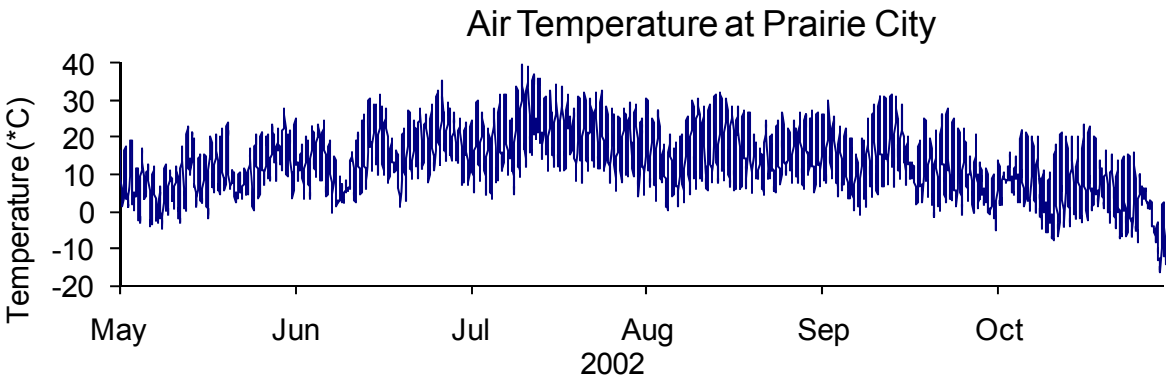

Figure A-95, d.

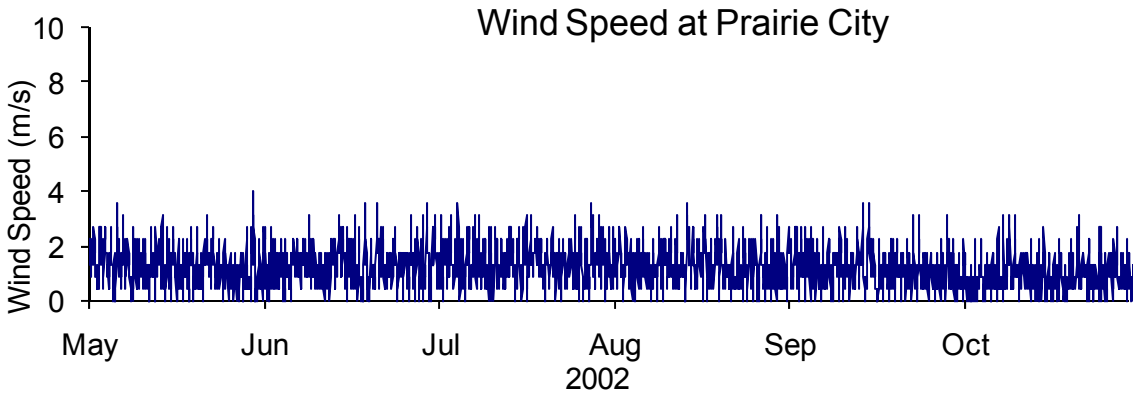

Flow and Temperature of Boundary Condition

The most upstream point of the Middle Fork John Day model was upstream of Clear Creek at river km 112.95. At or near the time frame of the TIR flight, several volumetric flow measurements were taken along the model corridor (**Figure A-5**). One measurement was taken at the model boundary. In addition, current gage data (including 2002) are available for Ritter and historic gage data for Austin (parts of 1924-1926, located near the model upper boundary point). For the model period outside of the day of field measurement (8/10/2002), the flow at the boundary was estimated based on the 2002 Ritter gage record adjusted based on historic information from the Austin station and the 8/10/2002 boundary measurement, in the following steps:

1. Determine the Austin gage mean daily flow for the period of record (Note that the Ritter gage was not operational during the Austin gage period of record).
2. Approximate the relationship between the 2002 Ritter gage and the historic Austin mean gage data from Step 1 (the historic Austin gage data ranges approximately from one-half to one-fifth of the Ritter gage data). Apply this relationship, varying through the year, to the Ritter gage to produce a surrogate record for the boundary that captures the correct year daily fluctuations for the Middle Fork Subbasin, and generally addressed the difference in flow between the Ritter and Austin areas.
3. Further adjust the modified Ritter gage record based on the 8/10/2002 measurement, so that the surrogate boundary record reflects both the current year daily fluctuations (Ritter) and the measurement taken at the boundary. The additional adjustment ranges from a factor of 0.4 (Aug 10, 2002 boundary measurement divided by same day Ritter gage data) to 1.0, where the latter is

assumed for the higher flows, and the former for low flows. Intermediate flows are adjusted via an interpolation of these values.

4. To prevent underestimation during low flow, the aggregate adjustment was limited such that all daily boundary flow estimates are greater than or equal to 1/7th of the Ritter flow.

Figure A-96 portrays the temporal flow array at the boundary for the model period. The temperature monitor placed at the upper boundary was not recovered at the end of the monitoring season. Fortunately, however, there were other monitoring points nearby. The temperature inputs at the boundary (**Figure A-97**) were estimated based on an instream temperature data logger located three kilometers upstream, TIR and the generic temperature profile discussed previously (**Figure A-80**, applicable in both the North and Middle Fork Subbasins – refer to **Temperature Input Section** for the North Fork in this Appendix). The steps taken in deriving the boundary temperature are as follows:

1. The core data was obtained from MSWCD-28, which had been deployed by the Monument Soil and Water Conservation District with the support of the DEQ voluntary monitoring program and TMDL staff. This recorder was deployed at river kilometer 116.
2. Data from MSWCD-28 was adjusted by adding 0.7 ºC for each hour throughout the record. This adjustment is the equal to the difference in summer afternoon temperature between the two sites, based on the 1998 TIR flight.
3. The measurement period for MSWCD-28 did not span the entire model period. The temperature data logger was deployed from 6/19/2002 to 10/10/2002 whereas the model period is 5/1/2002 to 10/31/2002 (noted in the beginning of this section). To estimate temperatures outside of the measurement time frame, the generic temperature array was applied. Both the beginning and end gaps were filled by adjusting the generic array uniformly until the entire record was seamless.

Figure A-96. Volumetric flow of the boundary condition of the Middle Fork John Day River model

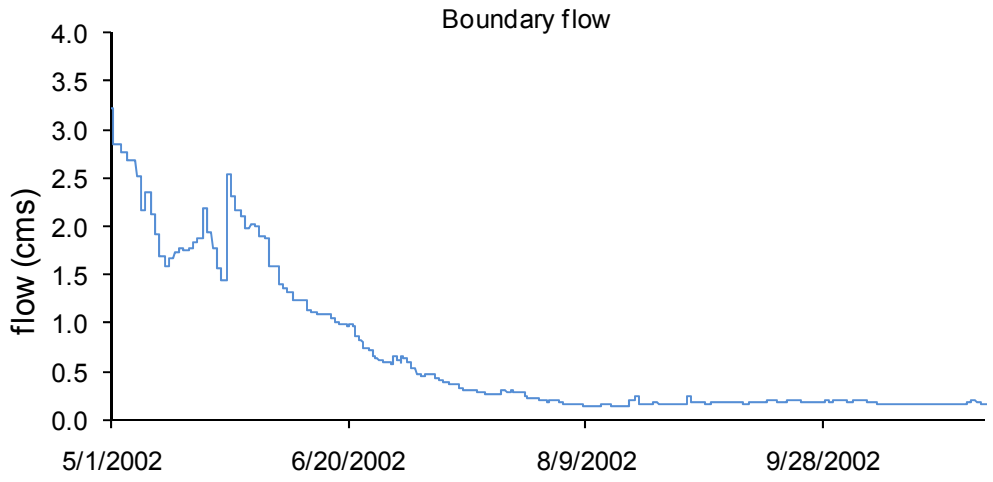

Figure A-97. Temperature of boundary condition of the Middle Fork John Day River model

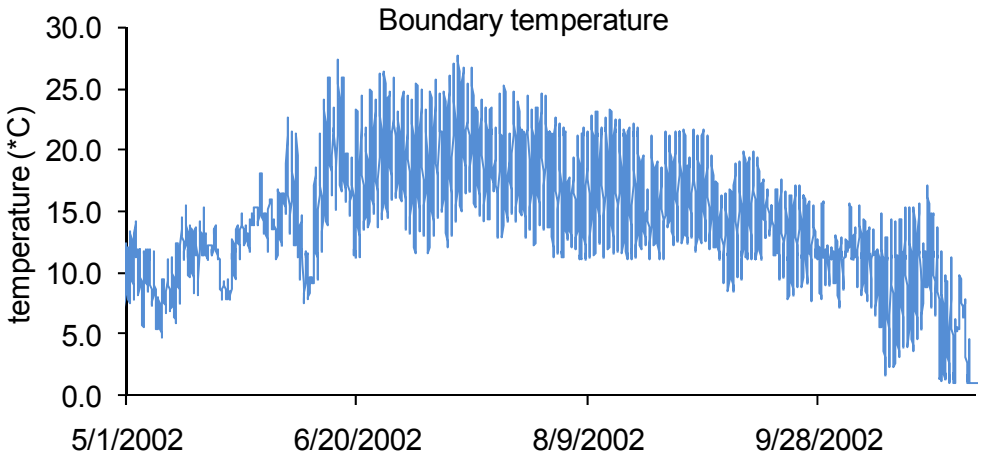

Flow Input

A total of forty-two tributaries were represented as water inputs to the Middle Fork John Day River model (**Table A-26**). All of the flow inputs were based on the 2002 continuous flow data set collected on the Middle Fork John Day River at Ritter (**Figure A-98**). Continuous flow data were not available for any of the tributaries. The measurements from the Middle Fork at Ritter were proportioned to each tributary, based on the drainage area ratio by approximating the area with a ruler on an OWRD map. For tributaries with a distinguishable signal during the TIR flight, flow was based on temperature balance calculations derived from TIR data and proportioned from the Middle Fork at Ritter measurements. Accretion flows were added directly to the model for the entire time period (**Figure A99**), as well as temporally varying additional flow as tributary "calibration flows" (**Figure A-100**). Water withdrawals were based on OWRD's water rights data and represented as out-flowing tributaries (**Figure A-101**) or constant gradual withdrawals (
Figure A-102).

Table A-26. Flow inputs and rates for the Middle Fork John Day River model

Stream km	Location name	Based on	Flow factor
111.50	Clear Creek	TIR temperature balance	0.1042
110.70	Bridge (Bates pond)	Watershed area	0.0380
109.35	Davis Creek	Watershed area	0.0100
108.65	Vinegar Creek	TIR temperature balance	0.0662
107.55	Vincent Creek	Watershed area	0.0100
107.45	Dead Cow Creek	Watershed area	0.0030
103.60	TIR pool	TIR temperature balance	
102.60	Deerhorn Creek	Watershed area	0.0050
101.85	Little Boulder Creek	Watershed area	0.0050
99.75	Little Butte Creek	Watershed area	0.0050
99.30	Hunt Gulch	Watershed area	0.0010
95.25	Butte Ck	TIR temperature balance	0.0344
93.55	Granite Boulder Ck	TIR temperature balance	0.1494
92.20	Ruby Creek	Watershed area	0.0090
92.15	Beaver Creek	Watershed area	0.0070
91.88	Ragged Creek	Watershed area	0.0030
88.90	Dry Creek	Watershed area	0.0020

87.40	Big Boulder Ck	TIR temperature balance	0.1712
83.60	Dunston Creek	Watershed area	0.0020
79.25	Camp Creek	TIR temperature balance	0.0318
77.95	Gibbs Creek	Watershed area	0.0020
76.35	Quartz Gulch	Watershed area	0.0030
74.50	Deep Creek	Watershed area	0.0020
69.30	Armstrong Creek	Watershed area	0.0020
64.25	Big Creek	Watershed area	0.0510
62.15	Huckleberry Creek	Watershed area	0.0100
61.15	Cross Hollow	Watershed area	0.0050
58.35	Indian Creek	Watershed area	0.0240
53.70	Slide Creek	Watershed area	0.0350
45.00	Hansen Canyon Creek (RB)	Watershed area	0.0350
44.35	Lick Creek	Watershed area	0.0100
41.80	Granite Creek	Watershed area	0.0150
41.30	Flowers Gulch	Watershed area	0.0020
30.35	Spring (LB)	Watershed area	0.0001
24.45	Upper Ritter H.S.	Historic Account	
22.85	Ritter Hot Springs	Historic Account	
9.25	Long Creek	Historic gage data	0.0769
3.80	Spring Complex (LB)	Watershed area	0.0001
93.35	Calibration flows	Calibration	
76.00	Calibration flows	Calibration	
61.70	Calibration flows	Calibration	
9.95	Calibration flows	Calibration	

Figure A-98. Measured flow at Middle Fork John Day River at Ritter used as basis for derived tributary flows

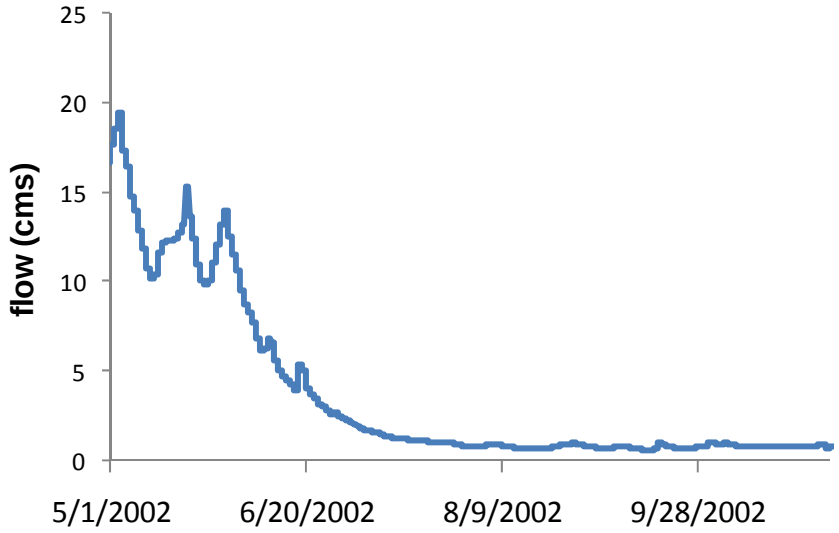

Figure A99. Constant flows into the Middle Fork John Day River model

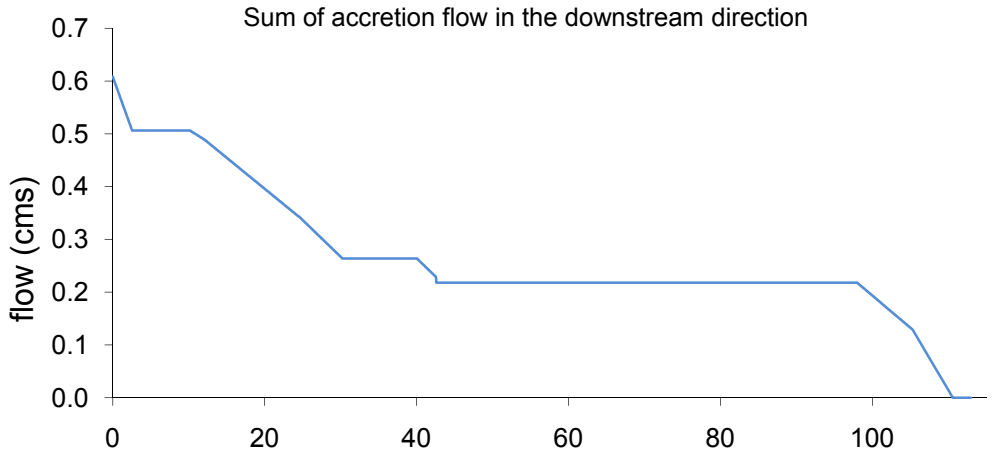

Figure A-100. Calibration flow to the Middle Fork John Day River model

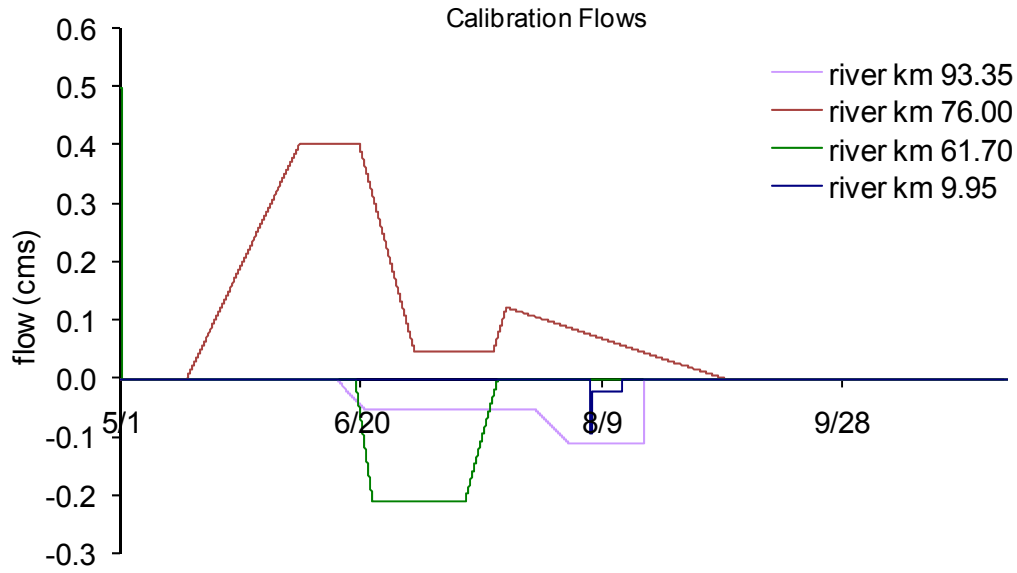

Figure A-101. Time variable water withdrawals from the Middle Fork John Day River model

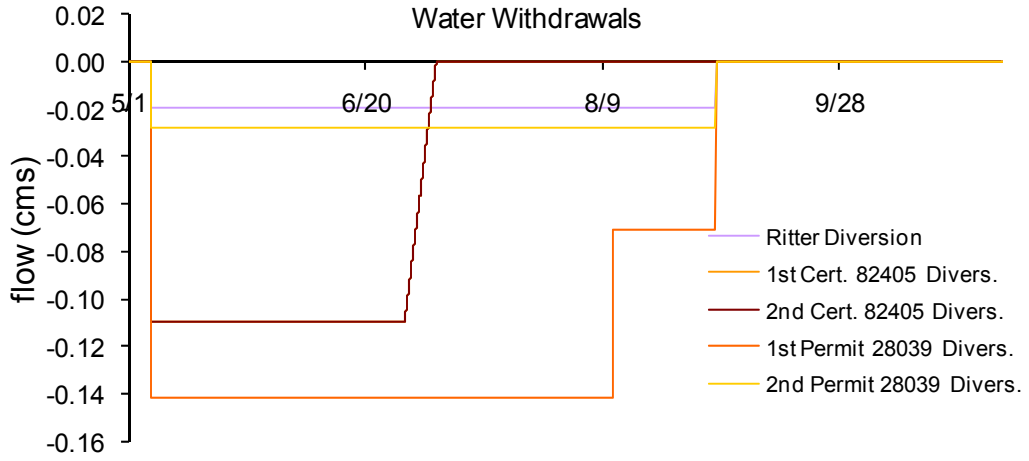

Figure A-102. Constant withdrawals from the Middle Fork John Day River model

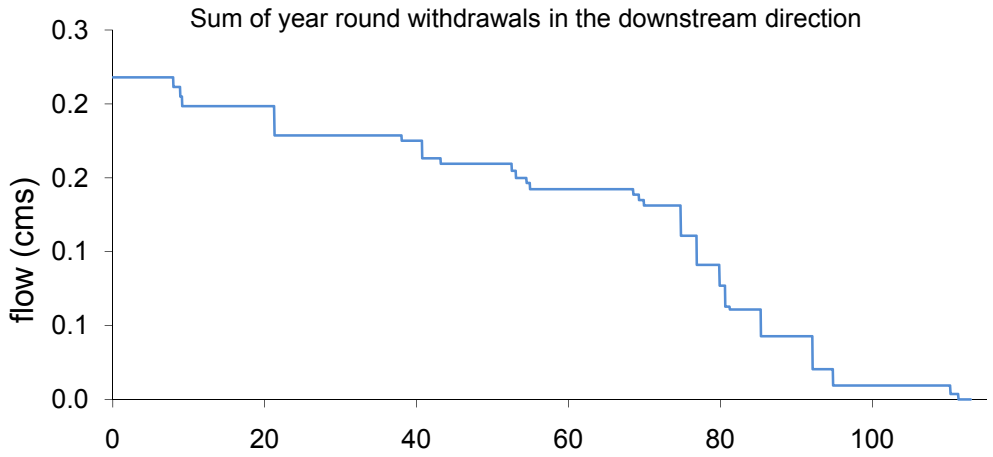

Flow Calibration

Using the above flow inputs, several characteristics estimated by the Middle Fork John Day model were compared to field measurements taken on August 10, 2002. The flow measurements from the Middle Fork John Day River at Ritter were compared to the model flow predictions at the same place. Early in the model period, at higher flows, the model underestimated the volumetric flow in the river. At flow below 2 cms, during the warmest part of the model period, the model reasonably predicted the volumetric flow (**Figure A-103, a**). The longitudinal profile shows the model results with measured river characteristics at several locations. Model results are represented by lines and measurements by points (**Figure A-103, a-d)**. **Figure A-103, d** compares the channel wetted widths predicted by the model to field measurements taken on August 10, 2002. The wetted widths derived from the GIS exercise based on LiDAR data (see **Section 2.2** for discussion) are presented for comparison. The LiDAR data were collected in 2006. Assuming that bankfull width is consistent and there were no large storm flow events that significantly altered channel morphology, the channel wetted width measurements are valid during the model period when volumetric flows are similar. Small morphological changes were assumed to be averaged over the reach.

Figure A-103, a-d. Longitudinal profile of model results with measured river characteristics. Model results are represented by lines and measurements by points

Figure A-103, a

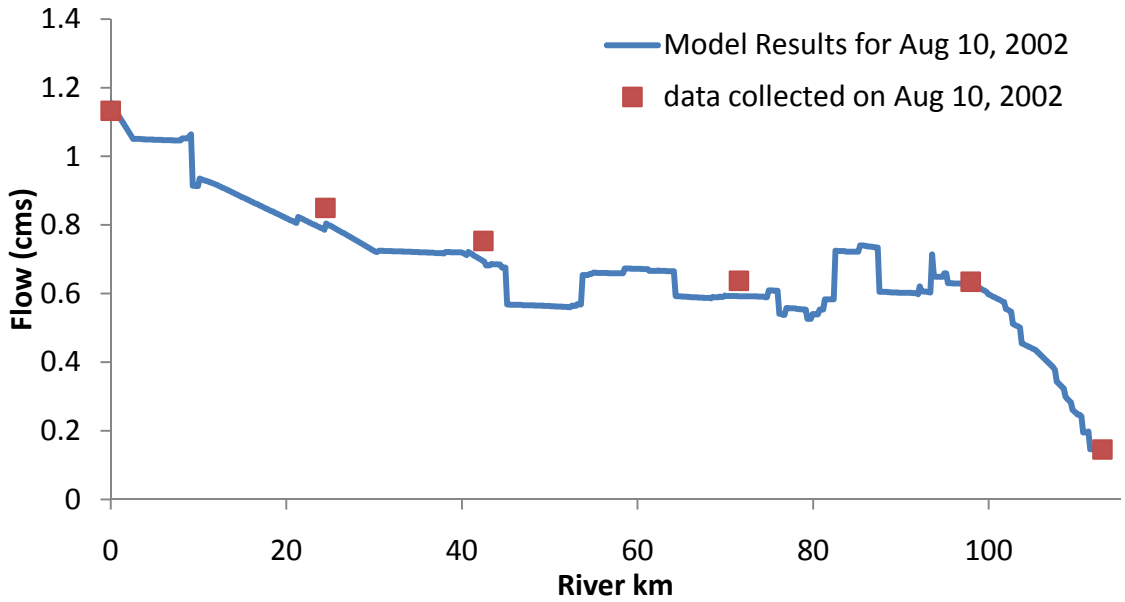

Figure A-103, b

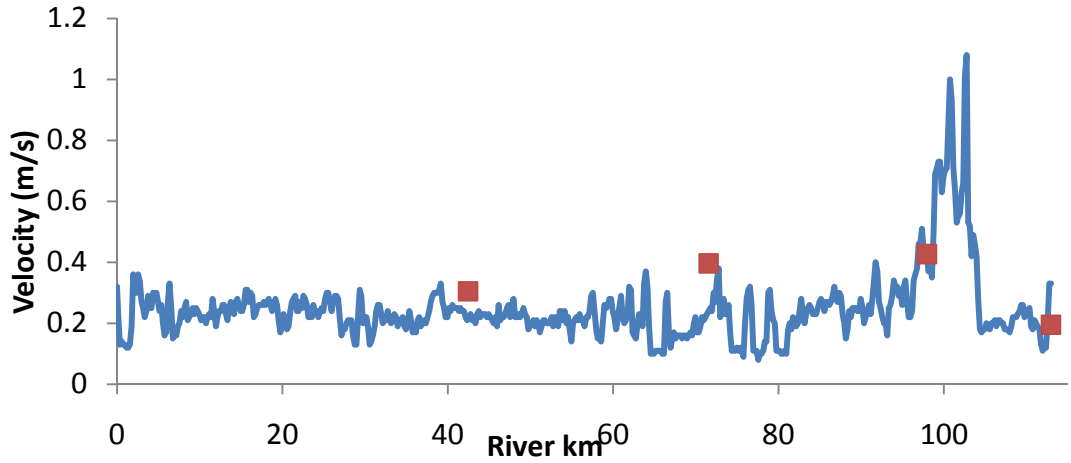

Figure A-103, c

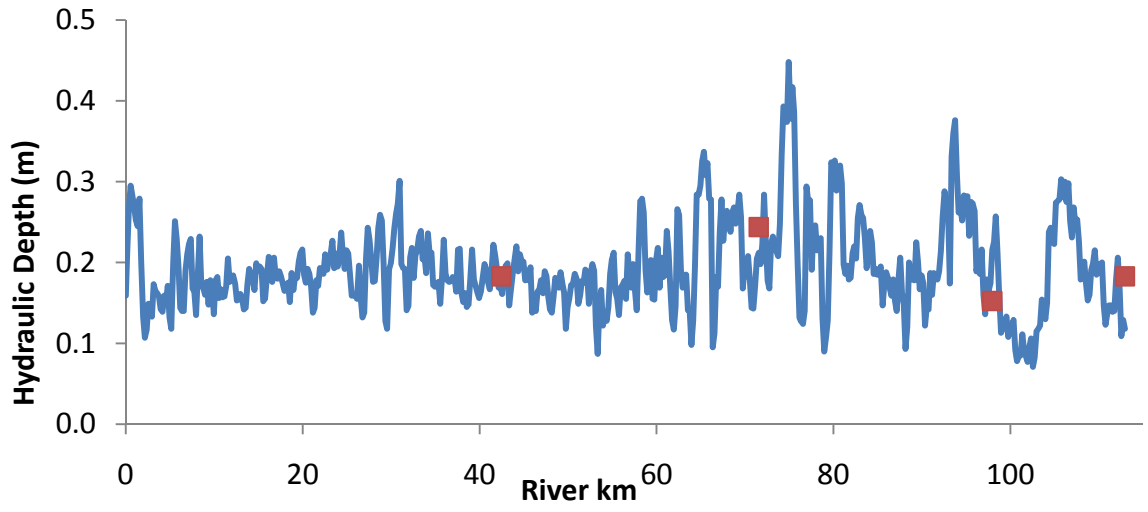

Figure A-103, d

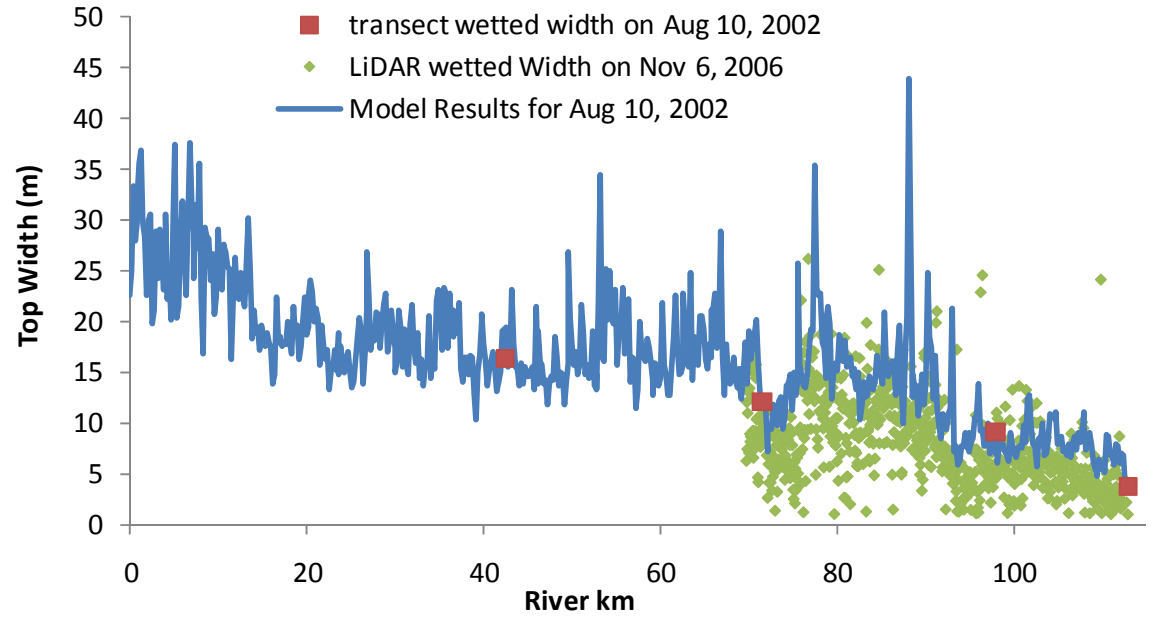

Temperature Input

There were six discontinuous temperature data sets collected on tributaries during some part of the model period (**Figure A-104, Figure A-105,** and **Figure A-106**). In order to fill these data gaps, the generic 2002 data set prepared for the North and Middle Forks, is employed. The data set is discussed in the **Temperature Input Section** for the North Fork in this **Appendix**. To complete the discontinuous data sets, the generic data array was adjusted to align with data at the edges of the gaps, creating a "seamless" array, as described for the North Fork under **Temperature Input.** Ritter Hot Springs were assigned a constant temperature value of 43.4°C (110°F), based on historical notes (Southworth 1972). "Calibration flows" were assigned a temperature profile modified by a simple adding factor to fit within the mid-range of measured values from the generic data set (**Figure A-107**). Likewise, accretion flow added directly to the model was assigned estimated groundwater temperatures (**Figure A-108**). For remaining tributaries where an instantaneous TIR temperature measurement was available, the ratio between the TIR measurement and generic datum at that time was applied to the entire time period (**Table A-27**).

Figure A-104. Discontinuous inflow temperature data sets

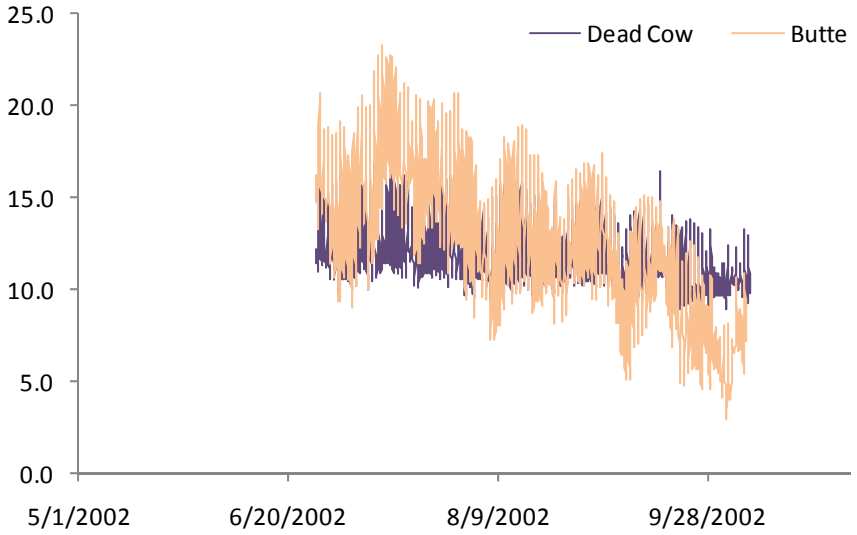

Figure A-105. Discontinuous inflow temperature data sets

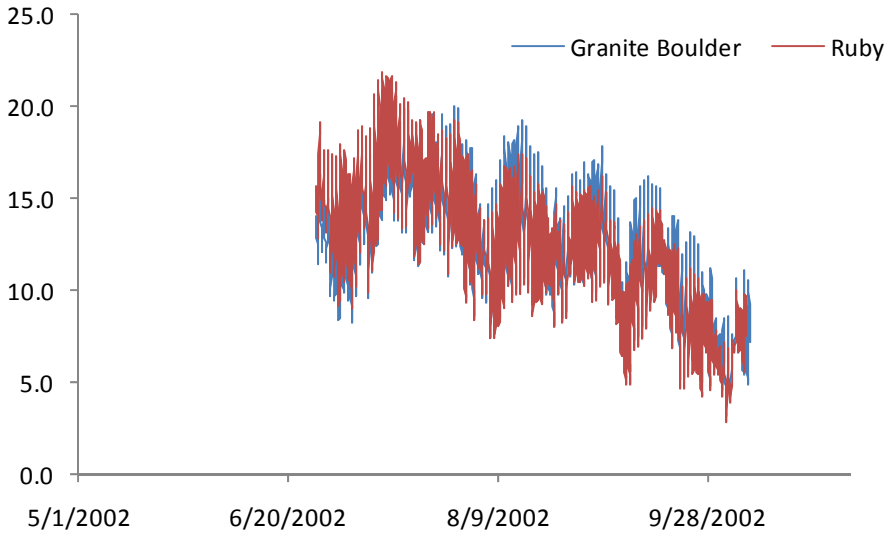

Figure A-106. Discontinuous inflow temperature data sets

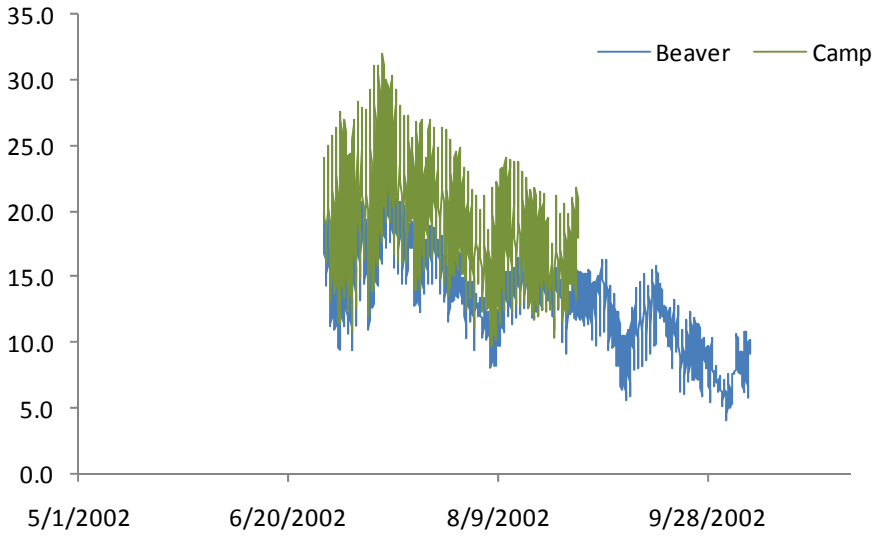

Figure A-107. Temperature of calibration flows to the Middle Fork John Day River model

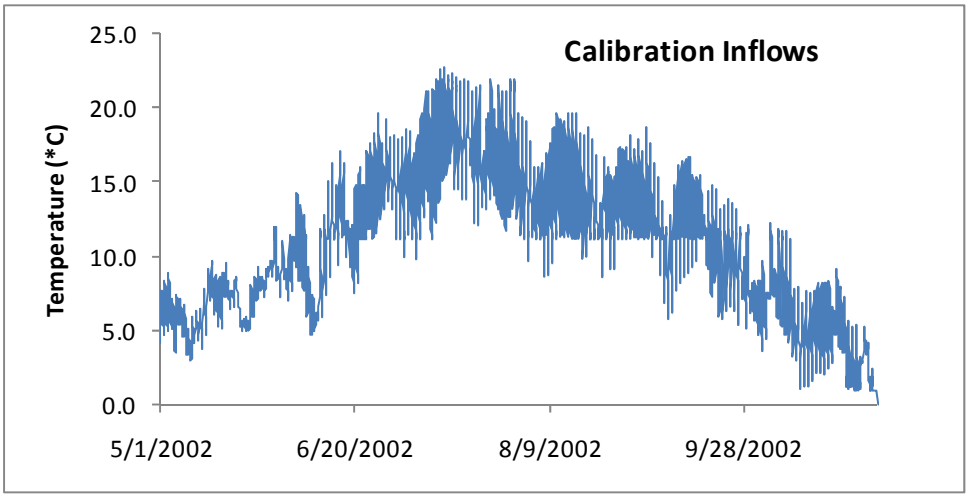

Figure A-108. Temperature of constant inflows to the Middle Fork John Day River model

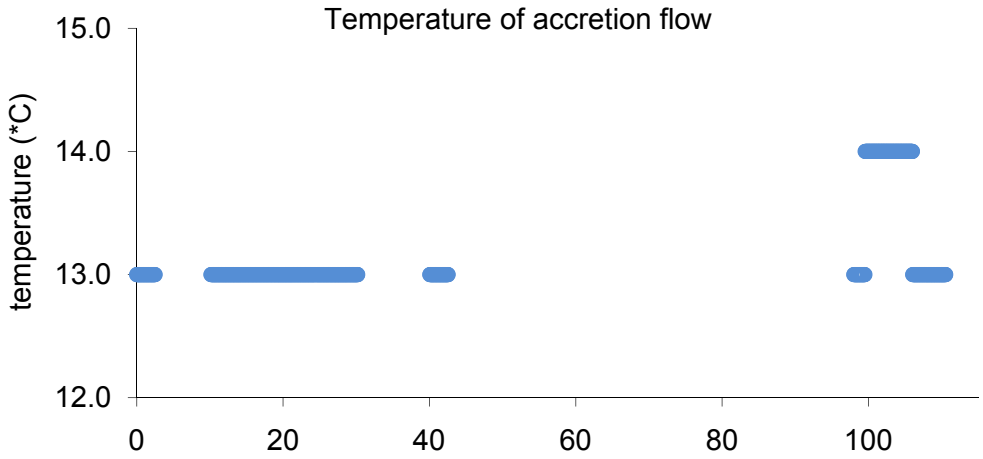

Table A-27. Temperature inputs for the Middle Fork John Day River model

Stream km	Location name	Based on	Temperature factor
111.50	Clear Creek	TIR 1998	0.95
110.70	Bridge (Bates pond)	TIR 1998	1.06
109.35	Davis Creek	TIR 1998	1.00
108.65	Vinegar Creek	TIR 1998	1.08
107.55	Vincent Creek	TIR 1998	0.93
107.45	Dead Cow Creek	Discontinuous data set	0.63
103.60	TIR pool	TIR 1998	
102.60	Deerhorn Creek	TIR 1998	1.09
101.85	Little Boulder Creek	TIR 1998	1.00
99.75	Little Butte Creek	TIR 1998	0.91
99.30	Hunt Gulch	TIR 1998	1.01
95.25	Butte Ck	Discontinuous data set	0.83
93.55	Granite Boulder Ck	Discontinuous data set	0.72
92.20	Ruby Creek	Discontinuous data set	0.81
92.15	Beaver Creek	Discontinuous data set	1.00
91.88	Ragged Creek	TIR 1998	0.96
88.90	Dry Creek	TIR 1998	0.99
87.40	Big Boulder Ck	Generic	0.85
83.60	Dunston Creek	TIR 1998	1.03
79.25	Camp Creek	Discontinuous data set	1.18
77.95	Gibbs Creek	TIR 1998	1.05
76.35	Quartz Gulch	TIR 1998	0.84
74.50	Deep Creek	TIR 1998	0.81
69.30	Armstrong Creek	TIR 1998	1.08
64.25	Big Creek	TIR 1998	0.96
62.15	Huckleberry Creek	TIR 1998	0.97
61.15	Cross Hollow	TIR 1998	1.03
58.35	Indian Creek	TIR 1998	1.09

53.70	Slide Creek	Generic	0.85
45.00	Hansen Canyon Creek (RB)	TIR 1998	1.16
44.35	Lick Creek	TIR 1998	1.09
41.80	Granite Creek	TIR 1998	1.09
41.30	Flowers Gulch	TIR 1998	1.01
30.35	Spring (LB)	TIR 2002	1.04
24.45	Upper Ritter H.S.		
22.85	Ritter Hot Springs	Historic notes	
9.25	Long Creek	Generic	
3.80	Spring Complex (LB)	TIR 2002	1.03

Temperature Calibration

DEQ and Umatilla National Forest provided continuous temperature data for calibration in the Middle Fork John Day River at 11 locations. TIR data were collected in two separate model years, but spatially overlapped by 26.7 km. One location was not used, because it collected temperature data outside of the model period. From river km 0 to 67.05, the TIR data was collected during the model period. The non-overlapping TIR data from 1998, upstream of river km 67.05, were adjusted by subtracting 1.9°C (the average difference through the overlapping section) from each median value to approximate 2002 values. Since these are estimated values, the TIR error statistics only represent the values downstream of river km 67.05 (**Table A-28**). The model's ability to reproduce temporal varying temperature measurements is represented below (**Figure A-109** and **Table A-29**). The model predicts temperatures greater than measured temperatures consistently at continuous monitoring sites (**Figure A-110**). The model captured the diel patterns recoded by the data loggers, although it did not reproduce the TIR profile well. Adjustments to percent hyporheic exchange and Manning's n, in order to better match the TIR profile, resulted in the most downstream site's diel pattern to diverge. In this iteration, the better diel match was preserved. See previous statistics discussion in **Section 3.1** for definitions.

Table A-28. TIR error statistics

Error type	Value
Mean	-0.27
Absolute mean	0.94
Root mean square	1.82
Nash-Sutcliffe	-5.29

Figure A-109. Longitudinal profile of measured temperatures using Thermal Infrared Radiometry and model results

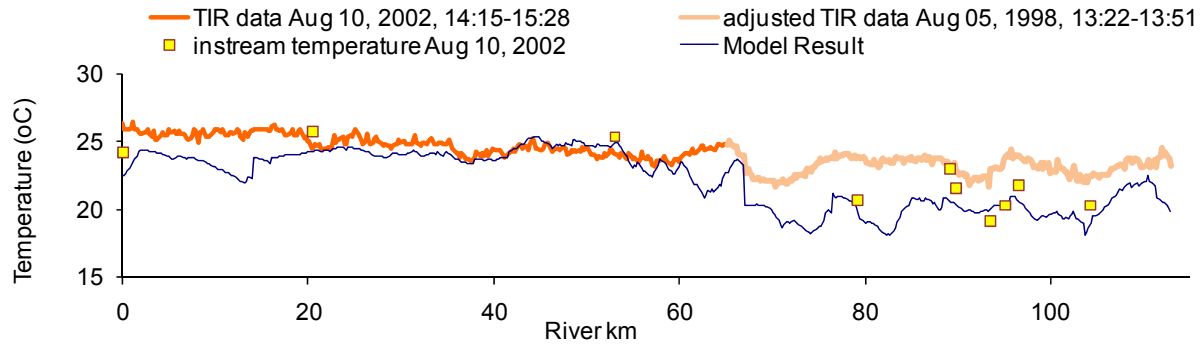

Table A-29. Continuous monitoring error statistics

Site Name	Source of temperature data	Ref	rKM	All data				
				n	Mean Error	Abs Mean Error	RMSE	Nash-Sutcliffe
Middle Fork John Day River at Caribou Cr	CTWSIR	A	104.30	2476	0.70	1.16	1.47	0.89
Middle Fork John Day River upstream of Butte Cr	CTWSIR	B	96.55	2500	0.17	0.92	1.16	0.94
Middle Fork John Day River at Butte Cr	CTWSIR	C	95.15	2500	0.67	0.98	1.25	0.93
Middle Fork John Day River at Riverside R	CTWSIR	D	93.45	2452	0.67	1.07	1.36	0.89
Middle Fork John Day River upstream of Sunshine Cr	CTWSIR	E	89.75	2956	0.87	1.21	1.50	0.93
Sunshine Ranger Station (Sunshine MNF)	ODEQ	F	89.20	3553	1.08	1.69	2.06	0.87
Middle Fork John Day River at Camp Cr	CTWSIR	G	79.20	2463	0.07	1.17	1.43	0.90
Middle Fork John Day River at Burn Canyon	MSWCD	H	53.05	2736	0.18	1.07	1.35	0.93
Middle Fork John Day River upstream of Eightmile Cr	ODEQ	I	20.45	3587	0.58	1.95	2.35	0.87
Middle Fork John Day River at mouth	CTWSIR	J	0.001	1522	0.33	1.11	1.42	0.89
				Average	0.53	1.23	1.54	0.90

Figure A-110. Measured steam temperature versus model results

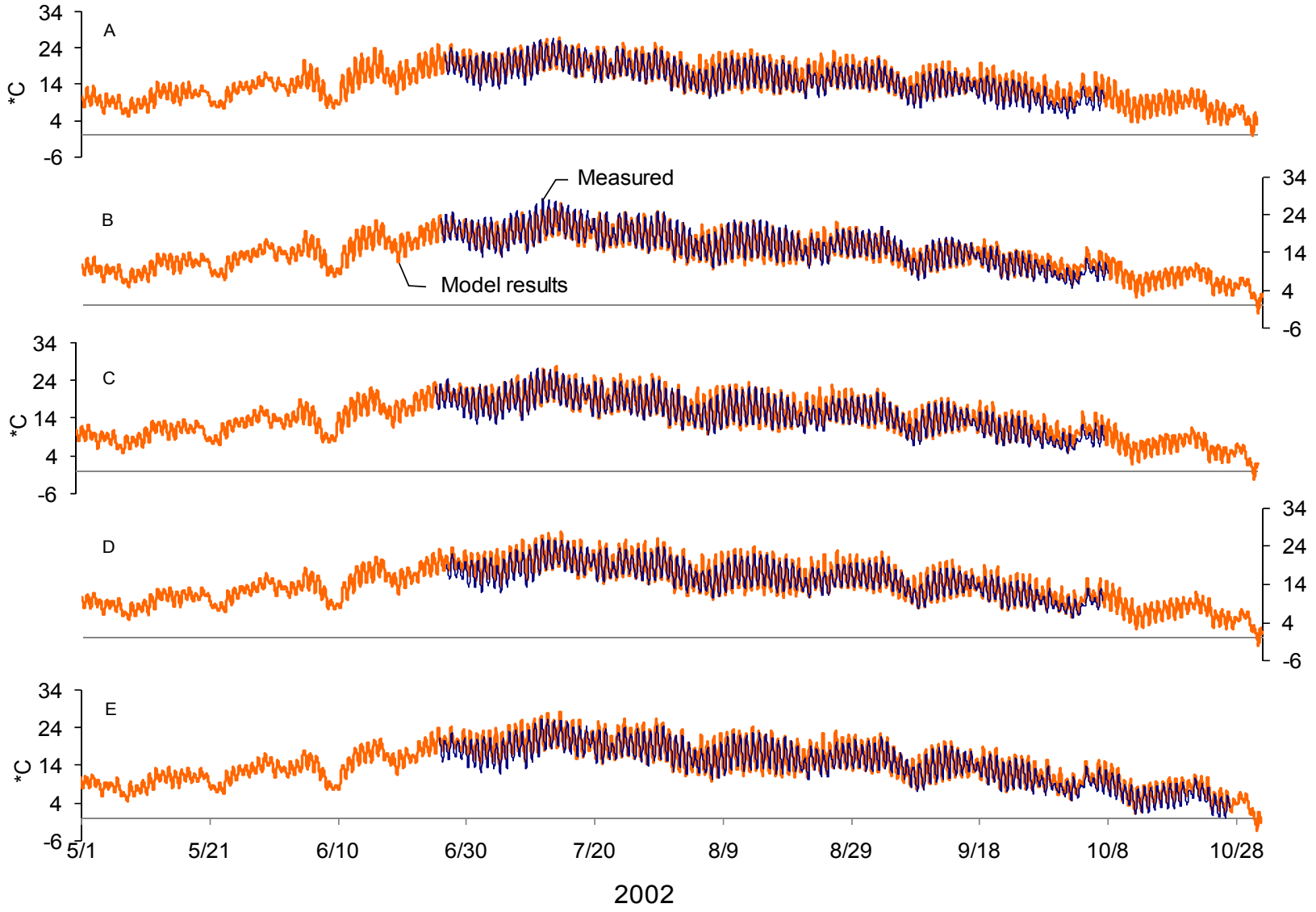

4. REFERENCES

Beschta, R. L., Bilby, R. E., Brown, G. W., Holtby, L. B., and Hofstra, T. D. (1987). Stream temperature and aquatic habitat: Fisheries and forestry interactions. *Streamside Management: Forestry and Fishery Interactions*. University of Washington, Institute of Forest Resources, Seattle, USA. 191-232 [in E. O. Salo and T. W. Cundy, eds.]

Boyd, M. & Kasper B. (2003a). *Analytical Methods for Dynamic Open Channel Heat and Mass Transfer: Methodology for the Heat Source Model Version 7.0,* for Oregon Department of Environmental Quality.

Boyd, M. & Kasper, B. (2003b). Improvements in stream temperature assessment. *Hydrological Science and Technology*, 19(1-4), 149-169.

Castro, Janine M. and Jackson, Philip L. (2001). *Bankfull Discharge Recurrence Intervals and Regional Hydraulic Geometry Relationships: Patterns in the Pacific Northwest, USA*. Journal of the American Water Resources Association, American Water Resources Association, Oct 2001, p. 1249-1262.

Dunne, T. & Leopold, L. (1978). Water in Environmental Planning. *Freeman*, New York.

Dury, G.H. , Hails, J. R., & Robbie, H.B. (1963). Bankfull Discharge and the Magnitude Frequency Series. *Australian Journal of Science*, 26:123-124.

Hicken, E.J. (1968). Channel Morphology, Bankfull Stage and Bankfull Discharge of Stream Near Sydney. *Australian Journal of Science*, 30:274-275.

Leopold, L. B., Miller, J. P., and Wolman, M. G. (1964). Fluvial Processes in Geomorphology. *Freeman*, San Francisco, California. 522 pp.

Leopold, L. B., (1994). A View of the River. Harvard University Press, Cambridge, MA. 298 pp.

Oregon Water Resources Department (2009). *Water Availability Report System*. http://apps2.wrd.state.or.us/apps/wars/wars_display_wa_tables/.

Rosgen, D. (1996). Applied River Morphology. *Wildland Hydrology.* Pagosa Springs, Colorado. Southworth, Jo. 1972.

United States Department of Agriculture (2005). *National Agriculture Imagery Program.* http://www.fsa.usda.gov/FSA/apfoapp?area=home&subject=prog&topic=nai.

Watershed Sciences (1998). *Description of Aerial Surveys in the Upper John Day River Basin, Thermal Infrared and Color Videography,* for Oregon Department of Environmental Quality.

Watershed Sciences (2002). *Surveys in the John Day River Basin, Thermal Infrared and Color Videography*, for Oregon Department of Environmental Quality.

Watershed Sciences (2004). *Aerial Surveys of John Day, OR, Thermal Infrared and Color Videography,* for Oregon Department of Environmental Quality.

Watershed Sciences (2006). *LiDAR Remote Sensing Data Collection: Desolation Creek, Middle Fork John Day River, & John Day River, Oregon*

Wolman, M.G. (1954). A method of sampling coarse river-bed material. *Transaction of American Geophysical Union* 35: 951-956.